Development of Fibrinolytic Platelet Systems for the Reduction of Cancer Metastasis and *in vitro* Feasibility of Targeting Thrombosis

by Brian Schnoor

B.S. in Bioengineering, May 2019, George Mason University

A Dissertation submitted to

The Faculty of
The School of Engineering and Applied Science
of The George Washington University
in partial fulfillment of the requirements
for the degree of Doctor of Biomedical Engineering

May 19, 2024

Dissertation directed by

Anne-Laure Papa
Assistant Professor of Biomedical Engineering

The School of Engineering and Applied Sciences of The George Washington University certifies that Brian Schnoor has passed the Final Examination for the degree of Doctor of Philosophy as of April 2nd 2024. This is the final and approved form of the dissertation.

Development of Fibrinolytic Platelet Systems for the Reduction of Cancer Metastasis and *in vitro* Feasibility of Targeting Thrombosis

Brian Schnoor

Dissertation Research Committee:

Anne-Laure Papa, Assistant Professor, Dissertation Director

Vesna Zderic, Department Chair and Professor, Committee Member

Emilia Entcheva, Professor, Committee Member

Matthew W. Kay, Professor, Committee Member

Mathumai Kanapathipillai, Associate Professor, Committee Member

© Copyright 2024 by Brian Schnoor
All rights reserved

Acknowledgements

I wish to first acknowledge and thank Dr. Anne-Laure Papa, my dissertation director, for all of her mentorship and guidance. Without her expertise, support, and dedication to her students, this would not have been possible.

I would also like to thank my dissertation research committee, Dr. Entcheva, Dr. Kanapathipillai, Dr. Kay, and Dr. Zderic, for their advice and direction.

I would also like to thank the staff at the George Washington University animal facility and the George Washington Nanofabrication and Imaging Center for their technical expertise and support.

Thank you also to the George Washington University and the Department of Defense Breast Cancer Research Program Expansion Award (W81XWH-19-1-0667) for supporting this work, and to the Department of Biomedical Engineering for their support.

I would like to thank my colleagues and friends, especially Kenise Morris and Regina Kottana, for always being willing to help and encourage me. Finally, I would like to thank my friends and family who have been so patient, encouraging, and supportive throughout this process. Thank you all.

Abstract of Dissertation

Development of Fibrinolytic Platelet Systems for the Reduction of Cancer Metastasis and *in vitro* Feasibility of Targeting Thrombosis

The objective of this dissertation is to develop a fibrinolytic platelet system capable of disassociating circulating tumor cell clusters and enhancing the lysis of thrombi by leveraging platelet interactions for targeted delivery. Platelets play a key role in the metastasis of circulating tumor cell (CTC) clusters and the formation of thrombi largely through receptor mediated interactions. As such, a platelet-based carrier approach provides a promising opportunity to address these critical medical challenges.

To explore this fibrinolytic platelet approach, we first characterized lyophilized platelets (LPs) and their effect on unaltered platelet function. The LPs have an inhibitory effect on platelet aggregation but promote platelet adhesion, which could be leveraged in promising drug delivery applications. These LPs also maintain some of the critical surface receptors necessary to interact with CTC clusters or thrombi.

We then developed a platelet-based system to target circulating tumor cell (CTC) clusters and deliver a fibrinolytic agent to dissociate the fibrin bound clusters into single cells with lower metastatic potential. We characterized the tPA loading onto platelet-decoy and LPs carriers and assessed the enhanced fibrinolytic activity of the system. We then demonstrated that the fibrinolytic platelets can effectively disassociate tumor cell clusters *in vitro* and assessed the efficacy of this system for reducing cancer metastasis *in vivo*.

Finally, we applied a modified fibrinolytic platelet approach to the need for an effective method of delivering tPA to thrombi, which can increase the efficacy of smaller fibrinolytic doses and reduce the risk of severe complications such hemorrhage. Using

partially activated platelet decoys, we demonstrated that the system can adhere on a thrombogenic surface and can effectively lyse fibrin *in vitro*.

Through these analyses this dissertation demonstrates the viability and efficacy of a fibrinolytic platelet approach for the reduction of cancer metastasis and the lysis of thrombi.

Table of Contents

Acknowledgements……iv

Abstract of Dissertation Proposal……...……..v

List of Figures……..…….viii

List of Tables……x

Chapter 1: Introduction - Leveraging Platelet Interactions with Cancer for Targeted Drug Delivery……...……1

Chapter 2: Background - Platelet Functions and Fibrinolysis……...6

Chapter 3: Lyophilized platelets inhibit platelet aggregation with simultaneous paradoxical promotion of platelet adhesion……14

Chapter 4: Development of a Fibrinolytic Platelet Systems to Reduce Cancer Metastasis by Dissociating Circulating Tumor Cell Clusters……..……...…43

Chapter 5: Development and *in vitro* Assessment of Fibrinolytic Platelet Carriers for Thrombosis …….....…….....……77

Chapter 6: Conclusions…….…….97

References….……...…….99

Appendix I: List of Manuscripts, Conference Proceedings and Local Presentations.…109

Appendix II: Permissions……...…..112

List of Figures

Fig. 1: Overview of Platelet Activation ……..7

Fig. 2: Overview of Platelet Aggregation……...…..9

Fig. 3: Illustration of Platelet Adhesion onto Collagen ……..10

Fig. 4: Schematic of Fibrinolysis……12

Fig. 5: Characterization of Key Receptor Surface Expression on Lyophilized and Fresh Human Platelets by Flow Cytometry……..……..27

Fig. 6: Characterization of Phosphatidylserine Exposure and Fibrinogen Binding on Lyophilized and Fresh Human Platelets……...…….29

Fig. 7: Aggregation of Platelets in the presence of LPs at Different Concentrations and Ratios…..…….31

Fig. 8: Aggregation of PRP compared to Diluted PRP…….……...33

Fig. 9: Adhesion of Platelets Mixed with Lyophilized Platelets on a Collagen Surface.....34

Fig. 10: Micrographs of Fresh and Lyophilized Platelets……...37

Fig. 11: Characterization of tPA Loading on the Platelet Carriers, tPA Loading Efficiency, and Identification of the tPA Receptor …….....58

Fig. 12: Fibrinolytic Activity Assay for Fibrinolytic Platelets compared to Free tPA…..……..…..61

Fig. 13: Flow Cytometry Analysis of Cancer Cell Interactions with Fibrinolytic Platelet Systems ……...……..62

Fig. 14: Effect of the Fibrinolytic Platelet Systems on Angiogenesis Determined using a HUVEC Tube Formation Assay…….....64

Fig. 15: Characterization of Cancer Cell Disassociation Curves obtained by Light Transmission Aggregometry after Fibrinolytic Platelet Treatment……..…...66

Fig. 16: *In Vivo* Assessment of Fibrinolytic Platelets Efficiency in Reducing Metastatic Dissemination..……...……..68

Fig. 17: Characterization of tPA-Loading on aDecoys compared to Decoys……87

Fig. 18: Flow Cytometry Analysis for Receptors on aDecoys and tPA-aDecoys…….....…..88

Fig. 19: Preliminary Data: Adhesion of tPA-aDecoys, aDecoys, and Decoys to a Thrombogenic Surface under Flow……...…….....…...89

Fig. 20: Effectiveness of tPA-aDecoys in Lysing Adhered Fibrin *in vitro* ……90

List of Tables

Table. 1: Detailed Platelet and LP Concentrations used for Each Mixing Experiment for Chapter 3…….24

Chapter 1: Introduction - Leveraging Platelet Interactions with Cancer Cells for Targeted Drug Delivery

Parts of this text is published (cited below) and is included in this chapter with author/journal's permission:

K. Morris*, B. Schnoor*, A.L. Papa, Platelet cancer cell interplay as a new therapeutic target. *Biochimica et Biophysica Acta (BBA) - Reviews on Cancer, 1877*(5), 188770 (2022). *co-first authors

The relentless cycle initiated by cancer metastasis with both direct and indirect effects on patient lifespan, morbidity and quality of life remain a challenge in the clinic. Furthermore, clusters of CTCs have a 23 to 50-fold increased metastatic potential as compared to single circulating tumor cells (Aceto et al., 2014). CTC clusters are detected in approximately 35% of patients with advanced breast cancer and their presence at multiple measurements is associated with a significantly shorter time to disease progression (Aceto et al., 2014). There is a definite unmet need of developing novel therapies to address hematogenous seeding to distant organs and the formation of new metastasis by these CTC clusters. However, many drug delivery methods for cancer treatment depend on the conditions of the tumor microenvironment and would thus be ineffective in targeting circulating tumor cell clusters (Dang and Guan, 2020; Manzari et al., 2021). Given the serious off-target effects of anti-cancer therapies (Young and Simmons, 2017), new methods must be developed to target CTC clusters and deliver therapeutics to disperse them. As such, there is a critical need for new carrier technologies to deliver therapeutic agents to the targeted cells and tissues, improving efficacy, modulating bioavailability and decreasing off target effects of the treatment.

One promising approach to address these drug delivery challenges is the use of

platelet-based carrier systems. The strong interaction between platelets and cancer cells has been repeatedly demonstrated to be an important factor in the growth and metastasis of cancer. The characterization of these interactions has revealed mechanisms by which platelets can protect cancerous cells in the blood, facilitate metastasis, and even promote tumor growth. Despite the challenges posed by these platelet-cancer interactions, these mechanisms also present a therapeutic opportunity. Some of the interactions such as those involving platelet surface receptors result in the direct adhesion of the platelets to the cancer cells. Thus, these mechanisms present a possible method for targeting cancerous cells by loading or modifying a platelet with a therapeutic agent. Different systems based on this approach have been developed with promising results.

One such avenue of research is the use of platelet-based delivery systems to target hematological malignancies. Many of the cell types most commonly affected by these malignancies interact extensively with platelet microparticles or platelets, demonstrating the viability of this approach (Ohana et al., 2015; Takagi et al., 2018). For example, it has been demonstrated that platelets release microparticles that interact with leukocytes (Kailashiya et al., 2019). Therefore, microparticles have been explored to deliver doxorubicin to leukemia cells (Kailashiya et al., 2019). In addition, strategies have used the delivery of doxorubicin with modified platelets themselves (Xu et al., 2017). In some studies targeting lymphoma cells, the platelets were modified using an anti-CD22 antibody conjugated to their membrane (Xu et al., 2017). Both of these approaches have demonstrated success increasing cancer cell uptake of doxorubicin and thus improving the cytotoxic effect. Additionally, these studies indicated a lower uptake of doxorubicin by non-target cells resulting in lower off-target effects (Xu et al., 2017). The combination of

these two trends demonstrates that this loading system is able to successfully target circulating tumor cells while remaining in the bloodstream for an extended period. This is a key advantage over the systemic delivery of traditional chemotherapeutics and provides a promising basis for continuing research.

Tang *et al.* used a similar modified platelet carrier approach and incorporated an active motion generating component (Tang et al., 2020). This was achieved by modifying platelets with an asymmetrical distribution of immobilized urease enzymes on their surface (Tang et al., 2020). This Janus structure results in a chemo-phoretic propulsive force on the modified platelet, allowing for active movement in the presence of a urea concentration (Tang et al., 2020). The data demonstrates that this induced carrier motion results in increased binding of the doxorubicin loaded Janus platelet carriers with cancer cells (Tang et al., 2020). Although authors acknowledge that further research is needed to design a system that is capable of complex roles in dynamic biological environments, these results demonstrate the potential of these active carrier systems (Tang et al., 2020).

Another potential target of platelet-based drug delivery systems is disseminating tumor cells. These CTCs are a key component of the metastatic cascade, and the ability to target and treat them in the bloodstream would severely inhibit the progression of the disease. **Currently there are only a few platelet-based drug delivery systems being developed to target CTCs, however they are showing promising preclinical results.** One such study examines the use of platelets to deliver the PD-L1 antibodies to the circulating tumor cells to prevent T-cell PD-1 and cancer cell PD-L1 binding, thus inhibiting programmed cell death of T-cells and ensuring a robust T-cell-mediated anti-cancer effect (Wang et al., 2017b). Since this ligand is also found in healthy cells, it is

important that the delivery system preferentially targets the cancerous cells. Similar to systems developed for use with solid tumors, the PD-L1 antibody for this approach was conjugated onto the surface membrane of the platelet to create the targeted delivery system (Wang et al., 2017b). The results of this study showed a significant decrease in the formation of secondary, metastatic tumors (Wang et al., 2017b).

Platelets have also been used to deliver TRAIL (tumor necrosis factor (TNF)-related apoptosis-inducing ligand) with similar success (Li et al., 2016; Ortiz-Otero et al., 2020). The delivery of TRAIL to circulating tumor cells has been explored using multiple methods. In one study by Li *et al.*, the platelets were genetically modified to express the TRAIL ligand on the cell surface (Li et al., 2016). Another experiment by Ortiz-Otero *et al.*, loaded the platelets by conjugating TRAIL carrying liposomes to platelets (Ortiz-Otero et al., 2020). This conjugation was accomplished by functionalizing the liposomes with von Willebrand Factor A_1 domain which binds to the GPIb-IX-V receptor complex on the platelet surface (Ortiz-Otero et al., 2020). Both of these approaches have yielded promising results for the efficient targeting and killing of CTCs *in vivo* (Li et al., 2016) and in collected blood samples of metastatic patients (Ortiz-Otero et al., 2020). Finally, drug free 'platelet decoys', that are detergent treated and inert platelets, display a dominant negative antiplatelet effect on both the metastatic dissemination and thrombosis *in vivo* (Papa et al., 2019). This approach capitalizes on the fact that CTCs cannot survive well in circulation without the support of platelets. Through the antiplatelet effect, the decoys inhibit platelet support in regard to CTCs and thus delay metastasis.

Based on these examples, the development of platelet-based carrier systems represents an innovative and effective approach to targeted drug-delivery for reducing

cancer metastasis. Therefore, the focus of our research is the development of fibrinolytic platelet systems that can be used to reduce cancer cell metastasis, and then be leveraged into further applications addressing key medical challenges. To accomplish this goal, we first explored the effect of lyophilized platelets, one potential platelet-based carrier system, on unaltered platelets (Chapter 3). In order to effectively leverage a carrier system, it is important to understand its effects on aggregation and adhesion of the native platelets, both to anticipate possible complications and determine possible beneficial effects. We then developed a fibrinolytic platelet system to target tumor circulating tumor cell clusters (Chapter 4). This system was robustly analyzed for efficacy *in vitro* and *in vivo* using a mouse model. Next, we explored the efficacy of this same fibrinolytic system for thrombus targeting *in vitro* (Chapter 5).

Due to the maintenance of key targeting receptors on our carriers, this fibrinolytic platelet system we developed could be leveraged for a variety of conditions that involve platelet interactions. In particular efficient drug delivery *via* fibrinolytic platelet system could be useful for the extremely time-sensitive treatment of pulmonary embolisms or stroke. Thus, this work robustly explores the development of a promising fibrinolytic platelet approach through the analysis of a potential platelet-based carrier system, the development of a fibrinolytic platelet system for reducing metastasis, and the application of this fibrinolytic platelet system in the treatment of thrombosis.

Chapter 2: Background - Platelet Functions and Fibrinolysis

Platelets are a critical component for maintaining hemostasis through hemostatic plug formation (thrombus), as well as triggering and assisting some steps of the coagulation cascade. Platelets achieve this function through three mechanisms: activation, aggregation, and adhesion. Platelets activate through receptor signaling to become pro-coagulant. Once activated platelets can then aggregate together through receptors interacting with bridge proteins allowing for thrombus formation when combined with fibrin. Furthermore, platelets will adhere to a thrombogenic surface, allowing for them to localize to the damaged area vessel and begin thrombus formation (also called platelet plug). After the hemorrhage has successfully been stemmed and the vessel repaired, then fibrinolysis, which is also regulated in part by platelets, can occur to dissociate the excess thrombus to maintain appropriate flow. Each of these aspects of platelet functions is not only critical for maintaining hemostasis, but also determines platelet interactions with cancer cells and thrombogenic microenvironments. As such, understanding these mechanisms is critical to develop platelet-based carriers for the effective delivery of fibrinolytic agents to circulating tumor cell clusters and thrombi.

2.1 Platelet Activation

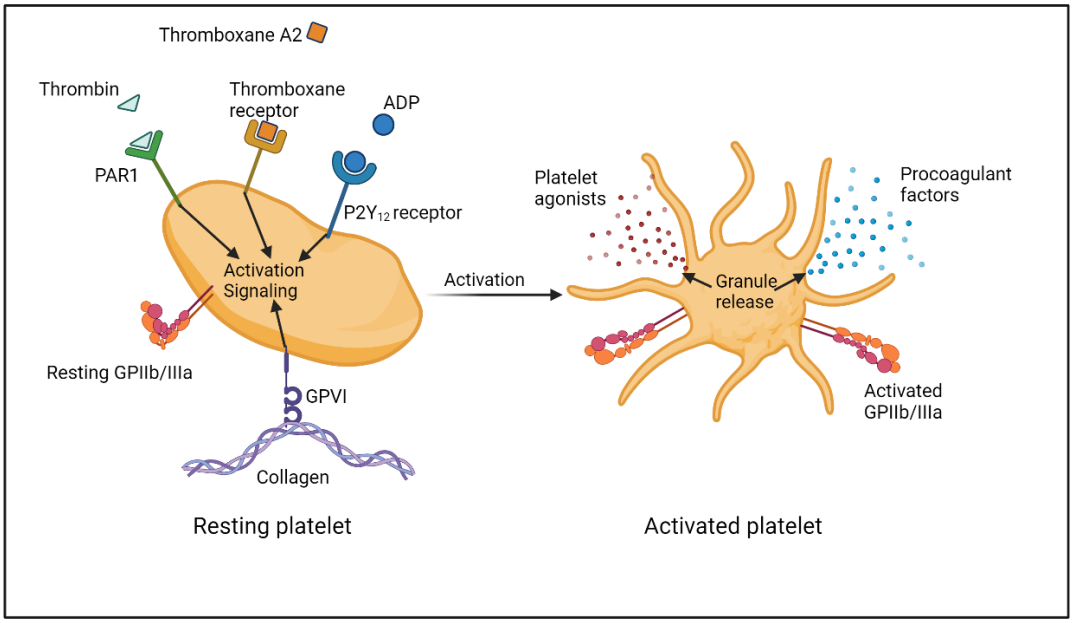

Figure 1: *Overview of Platelet Activation.* Stimulation of platelet receptors by agonists such as collagen, adenosine diphosphate (ADP), thrombin, or thromboxane A2, initiate signaling cascades that transform platelets from a resting to active state. These responses include a change in platelet shape, the release of pro-coagulative factors and platelet agonists, and the conformation change of key receptors such as GPIIb/IIIa. Created using Biorender.

In order to fulfil their primary role, platelets must change to an activated state which allows the platelets to promote coagulation and aggregate together into thrombi along with fibrin (Michelson, 2013). In this activated state, the platelets will also adhere more firmly to thrombogenic surfaces, which allows for the thrombus to affix to the damaged area of the vessel to reduce hemorrhage (Varga-Szabo et al., 2008). When a vessel is damaged, collagen is exposed to the platelets in the bloodstream. Collagen acts as an agonist to the GPVI receptor on platelets, which signals platelet activation *via* an immunoreceptor tyrosine–based activation motif (ITAM) sequence (Michelson, 2013; Yun et al., 2016; Rayes et al., 2019). In short, the activation of GPVI induces the kinase-dependent

phosphorylation of the tyrosine in the ITAM, and initiating a signaling cascade involving the PI3K/Akt pathway and secondary messengers eventually leading to the mobilization of intracellular calcium and the activation of protein kinase C (Michelson, 2013; Rayes et al., 2019). The CLEC-2 (C-type lectin-like type II) receptor can also induce platelet activation *via* a similar ITAM signaling pathway (Yun et al., 2016; Rayes et al., 2019). As illustrated in figure 1, this activation signaling cascade induces several key changes such as the release of granules (dense and α-granules), the activation of the GPIIb/IIIa receptors, and changes to the shape of the platelets (Fig. 1) (Roberts et al., 2004; Michelson, 2013; Eriksson et al., 2019). The granules contain platelet agonists, such as ADP (adenosine diphosphate), to induce more platelet activation, along with additional key receptors and pro-coagulant factors (Harrison and Cramer, 1993; McNicol and Israels, 1999). The conformational change in GPIIb/IIIa is an important aspect of platelet activation as it greatly increases the binding affinity for bridging proteins such as von Willebrand factor (vWF) and fibrinogen, which will allow for platelet aggregation (Michelson, 2013; Yun et al., 2016). As such, antibodies that interact specifically with activated GPIIb/IIIa receptors (PAC-1) are used as markers for platelet activation (Shattil et al., 1985; Chung et al., 2007). In contrast to the GPVI signaling pathway, platelet activation from ADP, along with most other readily soluble agonists including thrombin and thromboxane A2, functions *via* G protein-coupled receptors (GPCR) (Yun et al., 2016). When ADP interacts with the $P2Y_{12}$ receptor, the coupled Gi protein dissociates into 2 subcomponents (Li et al., 2023). The first of these subcomponents inhibits adenylate cyclase, resulting in a decrease of cAMP concentration and the decrease in activation inhibitors regulated by cAMP (Li et al., 2023). The second subcomponent (Gβγ) activates the PI3K/Akt signaling pathway leading to the activation of

the platelet (Li et al., 2023). Activated platelets also release coagulations factors such as FV and FVIII which are important for the coagulation cascade and promotes fibrin formation (Rendu and Brohard-Bohn, 2001; Al-Amer, 2022). There is also evidence that platelets can release tissue factor, another key component for the formation of thrombin during coagulation (Siddiqui et al., 2002).

2.2 Platelet Aggregation

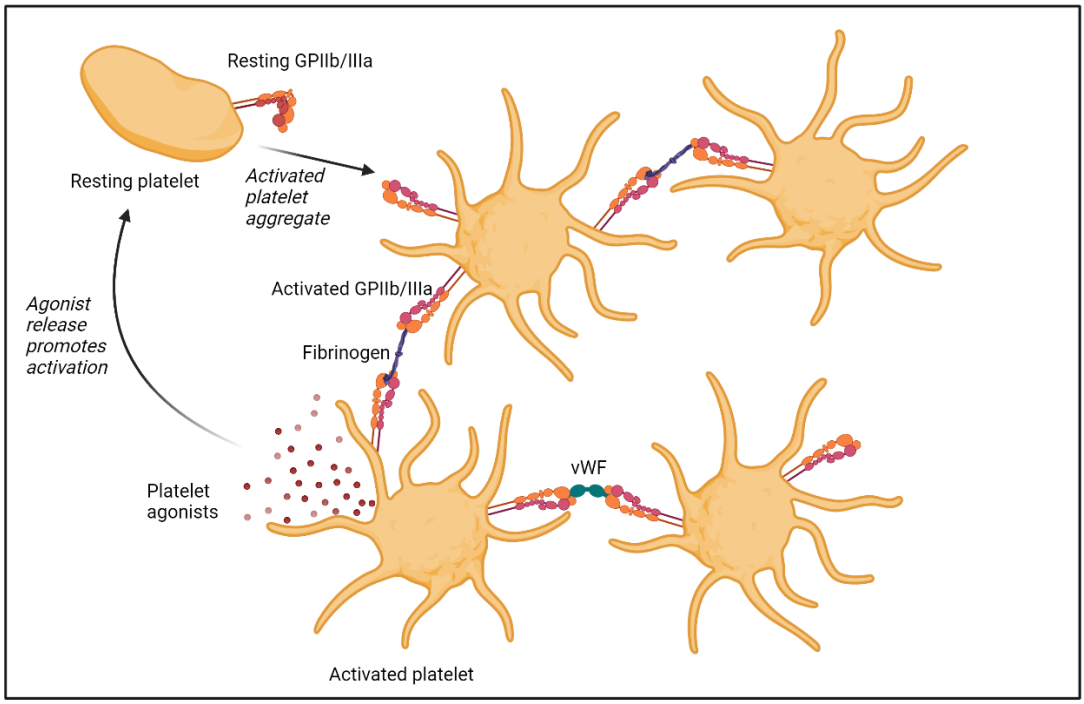

Figure 2: *Overview of Platelet Aggregation.* Activated platelets will aggregate *via* the interactions of active conformation GPIIb/IIIa receptors and the bridging proteins fibrinogen and von Willebrand factor (vWF). Activated platelets will also release additional platelet agonists to activate additional platelets that can then aggregate. Figure generated using Biorender.

The primary receptor involved in the aggregation of platelets is the activated GPIIb/IIIa receptor (Rumbaut and Thiagarajan, 2010). The GPIIb/IIIa receptor is able to

interact with fibrinogen with a high affinity, allowing the plasma protein to act as a bridging molecule between activated platelets (Varga-Szabo et al., 2008; Rumbaut and Thiagarajan, 2010). Similarly, vWF can act as this bridging protein, especially under high shear conditions (Rumbaut and Thiagarajan, 2010). Through this mechanism, the activated platelets are able to interact with each other, forming a growing aggregate (Fig. 2). During this process, the activated platelets are releasing agonists for platelet activation such as ADP and thromboxane A2 to promote further platelet activation (FitzGerald, 1991; McNicol and Israels, 1999), as well as procoagulant factor that promote fibrin formation (McNicol and Israels, 1999; Rendu and Brohard-Bohn, 2001; Al-Amer, 2022). Thus, the thrombus grows by the activated platelets aggregating together along with fibrin formed due to the coagulation cascade while the platelets continue to release more factors that promote additional platelet activation and coagulation.

2.3 Platelet Adhesion

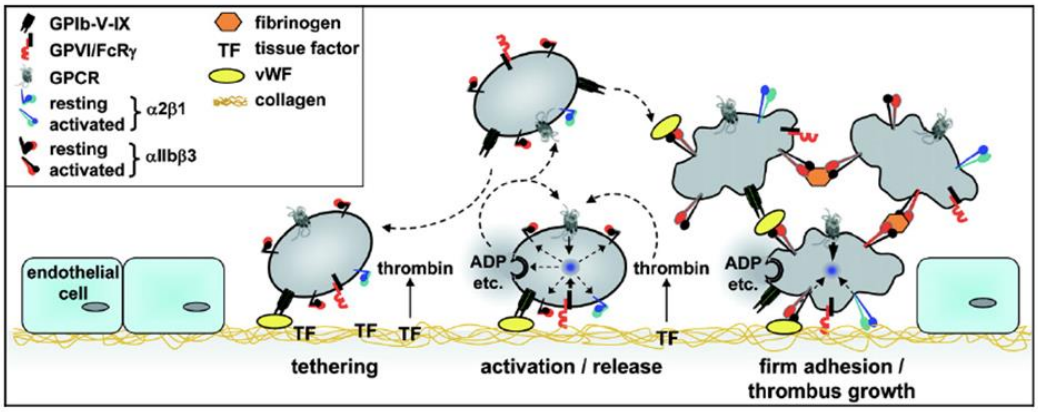

Figure 3: *Illustration of Platelet Adhesion onto Collagen.* Initially platelet tethering is driven by weak interactions between GPIb and vWF immobilized in the collagen. Subsequently GPVI receptors on platelets are able to bind to collagen, allowing for increased adhesion and initiating platelet activation. Taken from (Varga-Szabo et al., 2008) with permission.

Another key component of platelet function is the ability of platelets to adhere to a thrombogenic surface such as collagen. As depicted in figure 3, when platelets come into contact with the collagen the initial tethering of the platelets is driven by the interactions of GPIb (of the GPIb-IX-V complex) with vWF immobilized in the collagen (Fig. 3) (Varga-Szabo et al., 2008; Michelson, 2013). Specifically, GPIb is able to rapidly form bonds with the exposed A1 domain of vWF, however these weak bonds have a short duration, and thus cannot support firm adhesion of the platelets (Varga-Szabo et al., 2008; Michelson, 2013). Due to these weak bonds, the movement of the platelets is slowed and transformed into a "rolling" motion that allows GPVI receptors to interact with the collagen layer (Savage et al., 1998). Although GPVI receptors have a relatively lower affinity and do not form bonds with the collagen as rapidly as GPIb interacts with vWF, the GPVI-collagen interactions are stronger and have a more robust duration (Varga-Szabo et al., 2008). Moreover, the GPVI interaction with collagen also signals platelet activation through the mechanisms previously discussed (section 2.1). Activation induces a conformational change in the α2β1 receptor which will then bind to the collagen, allowing for firm adhesion of the platelet to the surface (Jung and Moroi, 2000). Activated GPIIb/IIIa receptors can also interact with the vWF immobilized in the collagen layer, further enhancing the firm adhesion of the platelet (Michelson, 2013). Other high affinity integrins such as α5β1 and α6β1 can bind to additional proteins such as fibronectin and laminin found in the extracellular matrix to further support firm adhesion (Varga-Szabo et al., 2008). Through platelet aggregation, these adhered platelets will interact with other activated platelets, growing the thrombus at the site of the damaged vessel wall. Additionally, thrombus formation is supported by tissue factor (TF), which is exposed at

the site of damage along with collagen and promotes thrombin formation through the coagulation cascade (Varga-Szabo et al., 2008). Thrombin is not only a potent platelet agonist, but also converts fibrinogen to the fibrin critical for coagulation and thrombus formation (Al-Amer, 2022). Activated platelets also release factors to promote coagulation, further promoting fibrin formation and the growth of the thrombus.

2.4 Fibrinolysis

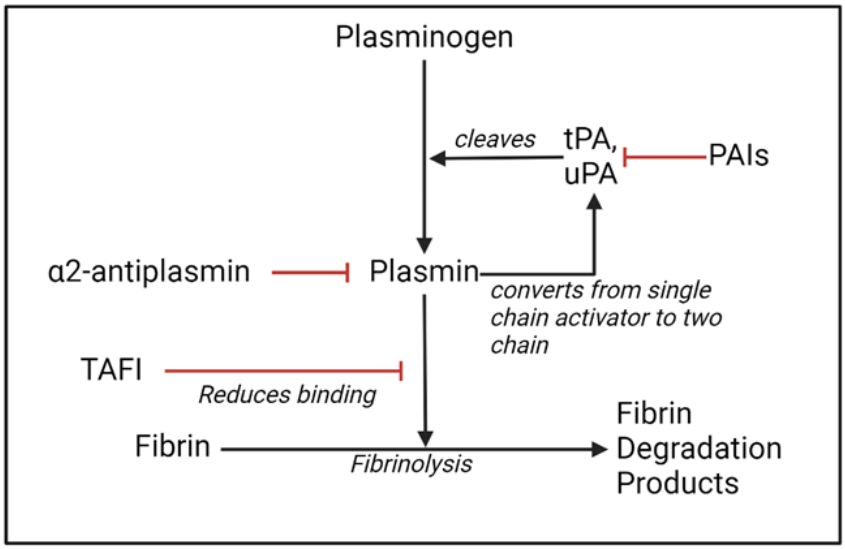

Figure 4: *Schematic of Fibrinolysis.* The lysis of fibrin into soluble products is driven by plasmin which is cleaved from plasminogen by tissue plasminogen activator (tPA) and urokinase plasminogen activator (uPA). This process is regulated by inhibitors including plasminogen activator inhibitors (PAIs) which inhibit tPA and uPA, α2-antiplasmin which inhibits plasmin, and thrombin activated fibrinolysis inhibitor (TAFI) which reduces plasmin binding to fibrin. Created using Biorender.

Thrombi are dispersed and removed *via* the process of fibrinolysis (Fig. 4), which is primarily driven by the protein plasmin (Cesarman-Maus and Hajjar, 2005; Chapin and Hajjar, 2015). Plasmin is generated from plasminogen, which is activated by tPA (tissue

plasminogen activator), or less commonly by uPA (urokinase plasminogen activator) (Cesarman-Maus and Hajjar, 2005). Secreted by vascular endothelial cells, tPA is a serine protease that cleaves plasminogen at the Arg561-Val562 peptide bond (Collen, 1987; Kooistra et al., 1994). For efficient generation of plasmin, this interaction requires a substrate cofactor, typically fibrin, to colocalize the tPA and plasminogen (Michelson, 2013). Once cleaved from the plasminogen, plasmin can then lyse fibrin into soluble fragments referred to as fibrin degradation products (Chapin and Hajjar, 2015). The plasmin can also convert single chain tPA into a higher activity two chain tPA, proving a positive feedback mechanism to promote fibrinolysis (Cesarman-Maus and Hajjar, 2005; Michelson, 2013). This fibrinolytic process is regulated by plasminogen activator inhibitors (PAIs), which inhibit plasmin generation by tPA, and by α2-antiplasmin, which directly inhibits plasmin (Cesarman-Maus and Hajjar, 2005). Moreover, fibrinolysis can be regulated in part by platelets, which can promote fibrinolysis by providing a surface for colocalization of tPA and plasminogen (Miles and Plow, 1985; Michelson, 2013). Platelets can also release thrombin activatable fibrinolysis inhibitor (TAFI) during activation, which can locally attenuate fibrinolysis during the short half-life of the inhibitor by reducing plasminogen binding sites on fibrin (Michelson, 2013; Chapin and Hajjar, 2015). Through these mechanisms tPA can induce the lysis of fibrin found in thrombi or in circulating tumor cell clusters.

Chapter 3: Lyophilized Platelets Inhibit Platelet Aggregation with Simultaneous Paradoxical Promotion of Platelet Adhesion

This text is published (cited below) and is included in this chapter with author/journal's permission:

B. Schnoor, A.L. Papa, Lyophilized platelets inhibit platelet aggregation with simultaneous paradoxical promotion of platelet adhesion. *Frontiers in Bioengineering and Biotechnology,* 10:941817 (2022).

Lyophilized platelets have been explored as a potential hemostatic agent due to their long-term ambient storage capabilities that make them readily available in various scenarios. Additionally, their high biocompatibility and the key role of platelet interactions in various clinical conditions make them a promising platform for drug delivery. To explore these applications and for wider clinical deployment, the interactions between lyophilized platelets and fresh platelets must be examined. This project characterized receptor expression on the lyophilized platelet surface and their ability to bind fibrinogen using flow cytometry. The effect of lyophilized platelets on aggregation of unaltered platelets was assessed using light transmission aggregometry while the effect on adhesion was evaluated using static and microfluidic assays. Lyophilized platelets maintained significant levels of GPIIb and GPVI receptors on their surface, though the expression was reduced from fresh platelets. Additionally, lyophilized platelets maintained GPIb expression similar to fresh platelets. Furthermore, 15.8% of the lyophilized platelets exhibited the active conformation of the GPIIb/IIIa receptor, indicating a significant increase over fresh platelets. Lyophilized platelets also exhibited an increase in exposed phosphatidylserine and fibrinogen binding. Despite the effect of lyophilized platelets in

promoting the adhesion of fresh platelets on a collagen-coated surface, their net effect was inhibitory on platelet aggregation. This study demonstrates that lyophilized platelets can have paradoxical effects on platelet adhesion and aggregation, which could have an impact for clinical applications. Detailed characterization and engineering of these effects will be important for their continued development as a drug delivery platform.

3.1. Introduction

Lyophilized platelet (LP) formulations represent a promising platform for the development of a variety of therapeutic approaches. Most research to date has focused on LPs as a potential therapy for treating hemorrhage (Alemany et al., 1997; Bode et al., 1999; Fischer et al., 2002; Barroso et al., 2018; Bynum et al., 2019), because they present several potential advantages over traditional platelet transfusion. Fresh platelet transfusions are currently a widely used and essential therapy for preventing and treating hemorrhage (Stroncek and Rebulla, 2007). The effectiveness of this treatment method has long been recognized and existing clinical criteria are used to determine optimal use of platelet transfusions (Kumar et al., 2015; Stolla et al., 2015). However, there are some key weaknesses of current fresh platelet transfusions that LPs may be able to overcome. Under current methods, platelets can only be stored for 5 days prior to transfusion (Food and Drug Administration, 2020). Additionally, these platelet units must be kept under constant agitation at 20-24°C (Food and Drug Administration, 2020). In contrast, LPs can be stored for extended periods of time at room temperature and without the need for agitation. Since the LPs are stored in dry form, they are less susceptible to bacterial contamination during the storage phase. Additionally, the profound blood shortage noted in the ongoing COVID-19 pandemic have emphasized the critical need for the development of storable blood

products (Al Mahmasani et al., 2021). These advantages of LPs could vastly increase the availability and utility of platelets for any number of treatments including hemostatic or drug delivery applications, and for wide capability deployment including resource limited conditions. A special emphasis has also been on the study of their circulation time and biodistribution in relevant models (Jackson et al., 1959; Fischer et al., 2001; Macko et al., 2016). This research has shown that LPs are rapidly cleared by the splenic macrophages (Fischer et al., 2001), possibly leading to their short circulation time and limited hemostatic effects in some models (Jackson et al., 1959; Macko et al., 2016). Thus, the LP approach may not be best suited for an application requiring extended circulation, but these LP carriers may be ideal for applications where the effect is intended for a more acute timescale.

The properties of these LPs also potentially create opportunities for drug delivery beyond hemorrhage and trauma. If LPs can be incorporated into a growing clot, they could potentially be leveraged as a fibrinolytic delivery platform to target thrombosis while mitigating the side effects of the loaded therapeutic drug, *via* a targeting effect. Furthermore, platelets have been shown to extensively interact with cancer cells (Gay and Felding-Habermann, 2011a; Papa et al., 2019). LPs could use this bioaffinity to target the cancer cells or inhibit the cancer cell-platelet interactions *via* drug delivery/release.

Studies examining LP systems have covered many different formulations designed to maximize effectiveness. The most common formulations included platelets fixed with paraformaldehyde and then lyophilized in a solution of serum albumin (Jackson et al., 1959; Bode et al., 1999; Fischer et al., 2002; Valeri et al., 2004). Other formulations have used trehalose as a cryoprotectant (Bynum et al., 2019), or lyophilized the platelets without

a cryoprotectant (Alemany et al., 1997; Fischer et al., 2001). These studies have assessed the effectiveness of the LPs for adhering to a thrombogenic surface and reducing bleeding in thrombocytopenic models. This foundational research has even led to clinical trials such as the ones developed by Cellphire (Cellphire Therapeutics, Inc., 2017, 2019, 2020, 2021, 2022). This research included a safety evaluation that showed no serious adverse effects after infusion of autologous LPs in healthy patients (NCT02223117 phase I) (Cellphire Therapeutics, Inc., 2017). Other trials currently underway are evaluating the safety and efficacy of allogenic LP formulations in thrombocytopenic (NCT03394755 phase I, NCT04631211 phase II) (Cellphire Therapeutics, Inc., 2019, 2021), and bleeding patients (NCT04631211 phase II, NCT04619108 Expanded Access) (Cellphire Therapeutics, Inc., 2020, 2021). Lastly, LP formulations are being evaluated to control bleeding during cardiopulmonary bypass surgery compared to platelets (NCT04709705 phase II) (Cellphire Therapeutics, Inc., 2022).

In order to develop these LPs into drug delivery systems though, the interactions between LPs and fresh platelets must be further characterized to best leverage this platform. Current research has explored many aspects of how LPs react independently of native platelets or under thrombocytopenic conditions. However, this study aims to bring new insight into how these LPs interact with and affect fresh platelet function. Additionally, understanding these interactions will help determine the best suited therapeutic applications for the LPs. Depending on the interactions, LPs can be further biofunctionalized and engineered to be used therapeutically to promote or inhibit specific platelet functions. However, all these applications depend on a robust understanding of how LPs impact the functioning of untreated native platelets.

The characterization of LPs in comparison to unaltered platelets was conducted by analyzing key receptors involved with platelet interactions. Then LPs were examined for the exposure of phosphatidylserine on the platelet surface, as well as the ability to bind fibrinogen. Subsequently, the analysis of the interaction of lyophilized and fresh human platelets *ex vivo* was assessed through the aggregation and adhesion of human platelets incubated with LPs. These experiments expand current understanding on how LPs interact with unaltered platelets. In brief, flow cytometry analysis demonstrates that LPs maintained significant levels of the key adhesion receptors GPIIb, GPVI, and GPIb. Additionally, a significant portion of LPs also expressed an activated form of the GPIIb/IIIa receptor, as well as increased phosphatidylserine exposure and fibrinogen binding. Finally, LPs demonstrated contrary effects on platelet function by inhibiting platelet aggregation but promoting platelet adhesion.

3.2. Materials and Methods

3.2.1 Materials

The adenosine diphosphate (ADP) used for aggregation analysis was purchased from Chrono Log (cat# 384). The reagents for the lactate dehydrogenase (LDH) assay were obtained from Promega (cat# J2380). The dye-conjugated antibodies were purchased from BD Biosciences: APC mouse anti-human CD41a (cat# 559777), APC mouse IgG, κ isotype control (cat# 555751), FITC mouse anti-human PAC-1 (cat# 340507), FITC mouse IgM, κ isotype control (cat# 551448), FITC mouse anti-human CD42b (cat# 555472), FITC mouse IgG1, k isotype control (cat# 555748), PE mouse anti-human platelet GPVI (cat# 565241), and PE mouse IgG1, k isotype control (cat# 554680). Additionally, APC-labeled

annexin V was obtained from Biolegend (cat# 640932). Alexa Fluor 647-conjugated fibrinogen was obtained from Thermo-Fisher Scientific (cat# F35200). Calcein AM was purchased from ThermoFisher (cat# C3099).

3.2.2 Lyophilized Platelets and Blood Sources

LPs were purchased from Chrono-Log (cat# 299-2). The LPs are fixed with paraformaldehyde before lyophilization. The human whole blood was purchased from BioIVT, following approval from the Institutional Biosafety Committee at the George Washington University, and drawn with 3.8% sodium citrate. Commercial blood was collected as late as possible in the day and shipped overnight before being processed in our experiments. The untreated platelets were obtained in platelet rich plasma (PRP) *via* centrifugation at 150 g from the whole blood from healthy donors. Platelet poor plasma (PPP) was obtained *via* centrifugation of the remaining blood fraction after the PRP had been removed. If more PPP was required than could be obtained with this method, addition PPP was produced by centrifuging a portion of PRP at 2,000 g.

3.2.3 Flow Cytometry for Receptor Characterization

In order to characterize the receptor availability, the lyophilized and untreated platelets were analyzed *via* flow cytometry. In brief, the platelets, lyophilized and untreated, were each stained for APC-CD41a (GPIIb), FITC-PAC-1 (specific to the activated GPIIb/IIIa complex), FITC-CD42b (GPIb), and PE-anti-GPVI. The staining for all receptors was conducted using 500,000 platelets or LPs in 50uL of Tyrode solution and incubated for 20 min. The CD41a, PAC-1, and CD42b antibodies were added at a 1:50

dilution from stock, while the GPVI antibody was added at a 2:25 dilution. Following the staining, the platelets were analyzed with the Novocyte flow cytometer (Agilent) with the 488 nm and 640 nm lasers activated and the appropriate detection filters. The platelets were then gated according to FSC (forward scatter) and SSC (side scatter). Then the median fluorescence and the percentage of stained platelets could be determined. Fluorescently conjugated IgG or IgM isotypes were used as controls.

3.2.4 Flow Cytometry for Phosphatidylserine Exposure and Fibrinogen Binding

The exposure of phosphatidylserine on the surface of the lyophilized and fresh platelets was evaluated using flow cytometry. The lyophilized and fresh platelets were stained using APC-labeled annexin-V and analyzed with the Novocyte flow cytometer. The staining was conducted with 500,000 platelets or LPs in 100uL of Tyrode and incubated for 20 min. The annexin-V was added at a 1:25 dilution from the stock concentration. To assess their fibrinogen binding, 500,000 of the lyophilized and fresh platelets were also separately incubated with 100 μg/mL Alexa Fluor 647-conjugated fibrinogen (2 μg total) for 20 min in 20 μL of Tyrode. The samples were then fixed with 1% paraformaldehyde and analyzed with the Novocyte flow cytometer. For both experiments the 640nm laser was used and the platelets were gated according to FSC and SSC. The median fluorescence and the percentage of the platelets stained were determined.

3.2.5 Light Transmission Aggregometry

The aggregation of the lyophilized and untreated platelets was assessed using light transmission aggregometry (LTA) with a Model 490 4+4 instrument from Chrono-Log. Untreated platelet concentrations of 200,000; 150,000; 100,000; and 75,000 platelets/uL were prepared in plasma to represent a range of healthy and thrombocytopenic conditions. The aggregation of each suspension was measured in the presence of ADP as an agonist in concentrations of 20uM and 50uM. The 20uM ADP concentration was selected based on previous work by Valeri *et al.* and Fitzpatrick *et al.* analyzing LP aggregation (Valeri et al., 2004; Fitzpatrick et al., 2013). The 50uM ADP concentration was selected to assess the robustness of the antiplatelet effect in supra-physiological conditions. The experiments were repeated with a 5:0, 5:1, and 5:2 ratio of untreated platelets to LPs for each of the above concentrations (Table 1). These ratios were selected to approximate the ratios achieved with one and two units of standard platelet transfusion. The volume of the mixture was 250uL for each condition. The same concentration of LPs in PPP was used to produce an accurate reference sample. An additional trial with only LPs was conducted at each concentration as a control to verify that LPs do not undergo aggregation when exposed to ADP.

3.2.6 Platelet Static Adhesion Assay

A procedure based around a LDH assay was developed to assess the adhesion of mixed lyophilized and untreated platelets on collagen. First a 1mg/mL fibrillar collagen solution (Chrono-Log, cat# 385) was diluted with phosphate buffered saline (PBS) to 0.1mg/mL and incubated in each well in 96-well plates for 1 hour to form a collagen layer

to which platelets could adhere. The wells were then gently rinsed with PBS to remove excess collagen. Then each mixture of lyophilized and untreated platelets was incubated in the wells for 2 hours to allow adhesion to occur. Samples at 200,000 platelets/uL and 75,000 platelets/uL in plasma were used to represent healthy and thrombocytopenic conditions, respectively. For each respective condition an untreated platelets only, a LP only, a 5:1 platelet to LP, and a 5:2 platelet to LP trial was performed (Table 1). After the incubation time, the suspension was removed, and the well was rinsed with PBS again. Then the well was treated with 50uL of 10% Triton solution to permeabilize platelets adhering to the collagen layer. After a 20 min incubation the sample was diluted 1,000 x with PBS and then incubated for 30 min with the LDH detection solution from the Promega assay kit. The fluorescence of each sample was then determined, and the concentration calculated from a standard curve of a known concentration of permeabilized platelets. The fluorescence detected from the LDH 'released' by the LPs alone was also measured and deducted from each sample so only the adherence of fresh platelets was measured.

3.2.7 Platelet Adhesion Under Flow Assay

A procedure for assessing the adhesion of platelets to a collagen surface under flow conditions was developed using calcein AM live cell stain (ThermoFisher cat# C3099). First a 0.1 mg/mL fibrillar collagen solution (Chrono-Log, cat# 385) was incubated in a fluidic glass bottom channel (Ibidi, cat# 80167) for 1 hour to deposit a collagen layer on which platelets could adhere. Then the microfluidic channel was gently rinsed with PBS to remove any excess collagen. Separately the platelets obtained in PRP were stained using a calcein AM live-cell stain. This live-cell stain was selected because it does not stain the

LPs which cannot undergo a metabolic process. Experimental samples were created using the calcein-stained fresh platelets at 200,000 plt/uL and 75,000 plt/uL to simulate normal and thrombocytopenic platelet count conditions, respectively. For each condition a sample was made with no added LPs and with LPs added at ratios of 5:1, and 5:2 platelets to LPs. A control sample was also made with an LP concentration of 200,000 and 75,000 LPs/uL, respectively, but without fresh platelets. The lyophilized platelets used in the control were incubated with calcein AM to confirm that they did not generate fluorescent signal. All conditions incorporated 40% hematocrit to simulate physiological conditions and corn trypsin inhibitor (Prolytix, cat# CTI-01) was also added at 50 μg/mL to inhibit the contact pathway of coagulation. Using a syringe pump (Cole-Parmer, cat# 78-0200C) the samples were then steadily pumped through the microfluidic channel at a rate of 1,800 μL/min for 4 min to produce a shear stress of 20.16 dynes/cm^2, selected to simulate physiological shear in arteries (Malek et al., 1999). The microfluidic channels were then all rinsed with Tyrode at a rate of 1,800 μL/min for 4 min to remove any platelets that had not adhered to the collagen. A second rinse of 250 μL of Tyrode was conducted *via* pipetting to remove any additional excess cells. Then the channel was incubated with 100 U/mL collagenase in Tyrode for 1 hour at 37°C to break down the collagen layer and release the adhered platelets. Each channel was thoroughly rinsed with 250 μL of Tyrode and the fluorescence of each collected sample was then measured (Ex/Em 494 nm / 517 nm) and normalized. Fresh platelet and LP counts for all conditions in the LTA, static adhesion, and adhesion under flow assays are listed for reference (Table 1).

Aggregation Assay						
200,000 PLT/uL condition	PLT Concentration PLT/uL	LP Concentration LP/uL	Total Volume uL	Total PLT Count	Total LP Count	Total PLT + LP
5:0; PLT:LP	200,000	0	250	50,000,000	0	50,000,000
5:1; PLT:LP	200,000	40,000	250	50,000,000	10,000,000	60,000,000
5:2; PLT:LP	200,000	80,000	250	50,000,000	20,000,000	70,000,000
LP control	0	200,000	250	0	50,000,000	50,000,000
150,000 PLT/uL condition	PLT Concentration PLT/uL	LP Concentration LP/uL	Total Volume uL	Total PLT Count	Total LP Count	Total PLT + LP
5:0; PLT:LP	150,000	0	250	37,500,000	0	37,500,000
5:1; PLT:LP	150,000	30,000	250	37,500,000	7,500,000	45,000,000
5:2; PLT:LP	150,000	60,000	250	37,500,000	15,000,000	52,500,000
LP control	0	150,000	250	0	37,500,000	37,500,000
100,000 PLT/uL condition	PLT Concentration PLT/uL	LP Concentration LP/uL	Total Volume uL	Total PLT Count	Total LP Count	Total PLT + LP
5:0; PLT:LP	100,000	0	250	25,000,000	0	25,000,000
5:1; PLT:LP	100,000	20,000	250	25,000,000	5,000,000	30,000,000
5:2; PLT:LP	100,000	40,000	250	25,000,000	10,000,000	35,000,000
0:5 PLT:LP	0	100,000	250	0	25,000,000	25,000,000
75,000 PLT/uL condition	PLT Concentration PLT/uL	LP Concentration LP/uL	Total Volume uL	Total PLT Count	Total LP Count	Total PLT + LP
5:0; PLT:LP	75,000	0	250	18,750,000	0	18,750,000
5:1; PLT:LP	75,000	15,000	250	18,750,000	3,750,000	22,500,000
5:2; PLT:LP	75,000	30,000	250	18,750,000	7,500,000	26,250,000
0:5 PLT:LP	0	75,000	250	0	18,750,000	18,750,000
Static Adhesion Assay						
200,000 PLT/uL condition	PLT Concentration PLT/uL	LP Concentration LP/uL	Total Volume uL	Total PLT Count	Total LP Count	Total PLT + LP
5:0; PLT:LP	200,000	0	100	20,000,000	0	20,000,000
5:1; PLT:LP	200,000	40,000	100	20,000,000	4,000,000	24,000,000
5:2; PLT:LP	200,000	80,000	100	20,000,000	8,000,000	28,000,000

0:5 PLT:LP	0	200,000	100	0	20,000,000	20,000,000
LP control (5:2)	0	80,000	100	0	8,000,000	8,000,000
LP control (5:1)	0	40,000	100	0	4,000,000	4,000,000
75,000 PLT/uL condition	PLT Concentration PLT/uL	LP Concentration LP/uL	Total Volume uL	Total PLT Count	Total LP Count	Total PLT + LP
5:0; PLT:LP	75,000	0	100	7,500,000	0	7,500,000
5:1; PLT:LP	75,000	15,000	100	7,500,000	1,500,000	9,000,000
5:2; PLT:LP	75,000	30,000	100	7,500,000	3,000,000	10,500,000
0:5 PLT:LP	0	75,000	100	0	7,500,000	7,500,000
LP control (5:2)	0	30,000	100	0	3,000,000	3,000,000
LP control (5:1)	0	15,000	100	0	1,500,000	1,500,000
Adhesion Under Flow Assay						
200,000 PLT/uL condition	PLT Concentration PLT/uL	LP Concentration LP/uL	Total Volume uL	Total PLT Count	Total LP Count	Total PLT + LP
5:0; PLT:LP	200,000	0	7200	1,440,000,000	0	1,440,000,000
5:1; PLT:LP	200,000	40,000	7200	1,440,000,000	288,000,000	1,728,000,000
5:2; PLT:LP	200,000	80,000	7200	1,440,000,000	576,000,000	2,016,000,000
0:5 PLT:LP	0	200,000	7200	0	1,440,000,000	1,440,000,000
75,000 PLT/uL condition	PLT Concentration PLT/uL	LP Concentration LP/uL	Total Volume uL	Total PLT Count	Total LP Count	Total PLT + LP
5:0; PLT:LP	75,000	0	7200	540,000,000	0	540,000,000
5:1; PLT:LP	75,000	15,000	7200	540,000,000	108,000,000	648,000,000
5:2; PLT:LP	75,000	30,000	7200	540,000,000	216,000,000	756,000,000
0:5 PLT:LP	0	75,000	7200	0	540,000,000	540,000,000

Table 1: *Detailed Platelet and LP Concentrations used for Each Mixing Experiment for Chapter 3.* To clarify the procedure used for experiment involving mixing untreated platelets and LPs in different ratios, this table includes the untreated platelet and LP concentration and total cell number added to each respective sample for both normal and thrombocytopenic conditions.

3.2.8 Scanning Electron Microscopy

A silicon wafer (Ted Pella, cat# 16006) was prepared by rinsing the wafer in ethanol and then PBS. Then a 0.1 mg/mL collagen solution (Chrono-Log, cat# 385) was incubated with the silicon wafer for 1 hour to form a collagen layer. Then the excess collagen was removed and the samples, fresh platelets and LPs respectively, were incubated with the silicon wafer for 2 hours before centrifuging the samples at 150 g for 5 min. The samples were subsequently fixed with a 2.5% glutaraldehyde and 1% paraformaldehyde in a 0.12 M sodium cacodylate buffer. The samples were then washed with 0.12 M sodium cacodylate buffer and fixed with 1% osmium tetroxide in a 0.12 M sodium cacodylate buffer. The samples were afterwards dehydrated with increasing EtOH concentrations and dried with hexamethyldisilane. The samples were imaged with a FEI Teneo Scanning Electron Microscope (SEM) using a low vacuum detector. The images were taken in low vacuum (10 Pa) at 5 kV voltage and 50pA current settings.

3.2.9 Statistical Analysis

All graphical representations and statistical analyses of the data were developed using the Prism software from GraphPad. Statistical significance between experimental groups in the receptor characterization, light transmittance aggregometry, and adherence assay trials was determined using an analysis of variance (ANOVA) method. A Tukey's multiple comparison test was used for the *post hoc* analysis.

3.3. Results

3.3.1 Analysis of Surface Receptor Expression on Lyophilized Platelets

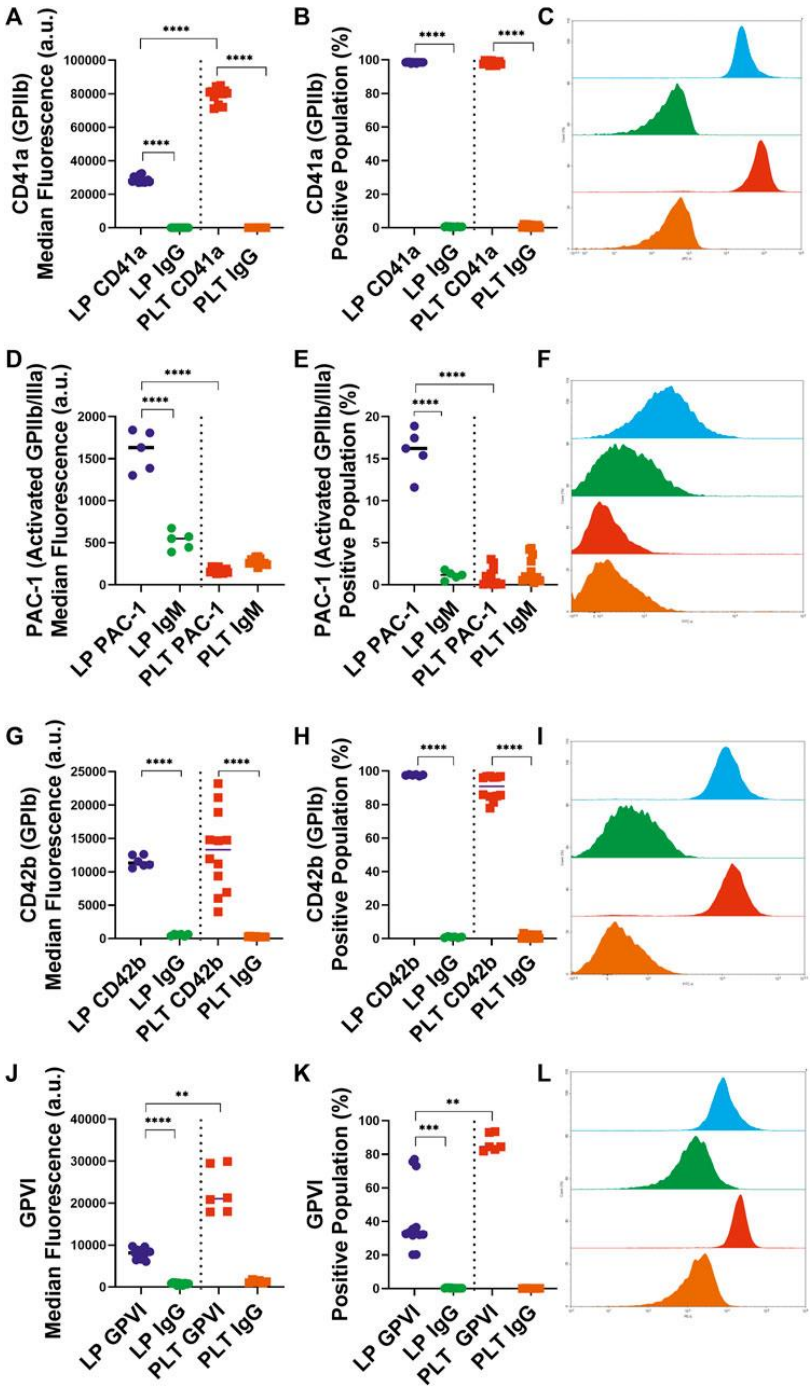

Figure 5*: Characterization of Key Receptor Surface Expression on Lyophilized and Fresh Human Platelets by Flow Cytometry.* Quantification of expression level (left), percent positive events (middle), and representative curves (right), for (A,B,C) GPIIb [LP: n=14,

PLT: donor = 5, n=12], (D,E,F) active GPIIb/IIIa [LP: n=6, PLT: donor = 4, n=12], (G,H,I) GPIb [LP: n=6, PLT: donor = 5, n=12], (J,K,L) GPVI [LP: n=13, PLT: donor = 3, n=6].

To assess the interactions of the LPs with untreated native platelets, the availability of key receptors was characterized. Almost all (98.4%) LPs retained approximately one-third of GPIIb (CD41a) at their surface compared to platelets with median fluorescence values of 28,348 versus 80,556 a.u. ($P<0.0001$), respectively (Fig. 5A-C). Next, we determined the fraction of activated GPIIb/IIIa receptors using a PAC-1 antibody. 15.8% of the LP population exhibited the active conformation of the GPIIb/IIIa receptor (Fig. 5D-F). Thus, the activated receptor that is critical to the platelet aggregation process and the late stages of adhesion on thrombogenic surfaces is available on some of the LP carriers. After analyzing the GPIIb receptor availability, the presence of the GPIb (CD42b) receptor essential for surface adhesion was characterized. In contrast with GPIIb, LPs retained the majority of GPIb receptors compared to platelets (Fig. 5G-I). Additionally, a significant portion of the LPs, (41.0%, Fig. 5K) maintained expression of the GPVI receptor ($P=0.0042$). Though this expression was reduced from platelets in terms of both percentage of the positive population and median fluorescence (Fig. 5J-L; $P=0.0042$ and $P=0.0062$, respectively).

3.3.2 Analysis of Phosphatidylserine Exposure and Fibrinogen Binding to Lyophilized Platelets

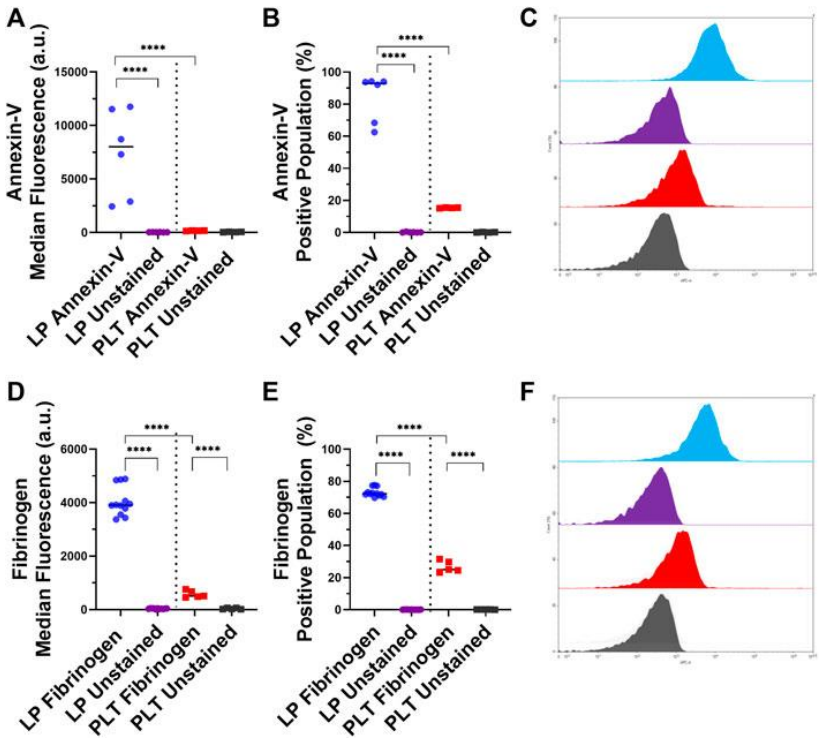

***Figure 6**: Characterization of Phosphatidylserine Exposure and Fibrinogen Binding on Lyophilized and Fresh Human Platelets.* Quantification of expression level (left), percent positive events (middle), and representative curves (right), for (A,B,C) phosphatidylserine [LP: n=6, PLT: donor = 2, n=4], and (D,E,F) fibrinogen binding [LP: n=12, PLT: donor = 2, n=5].

After analyzing the key platelet receptors on the lyophilized and control platelets, we subsequently characterized the pro-coagulant characteristics of the LPs. One of the most important markers for pro-coagulant platelets is the presence of exposed phosphatidylserine on activated platelets, which is involved in the regulation of fibrin formation during thrombosis (Reddy and Rand, 2020). A large majority of LPs (84.2%) displayed significantly more exposed phosphatidylserine compared the control platelets (Fig. 6 A-C; $P<0.0001$).

Next, the binding of fibrinogen to the surface of the LPs was assessed due to the central role of fibrinogen in platelet aggregation and thrombogenesis. The flow cytometry results demonstrated that the LPs had 7.7 times more binding of fibrinogen compared to the control platelets (Fig. 6D; $P<0.0001$). The percentage of fibrinogen binding in these two populations was also significantly different: 73.1% and 26.8% for LPs and platelets, respectively (Fig. 6E; $P<0.0001$).

3.3.3 Aggregation of Platelets with Different Ratios of Lyophilized Platelets

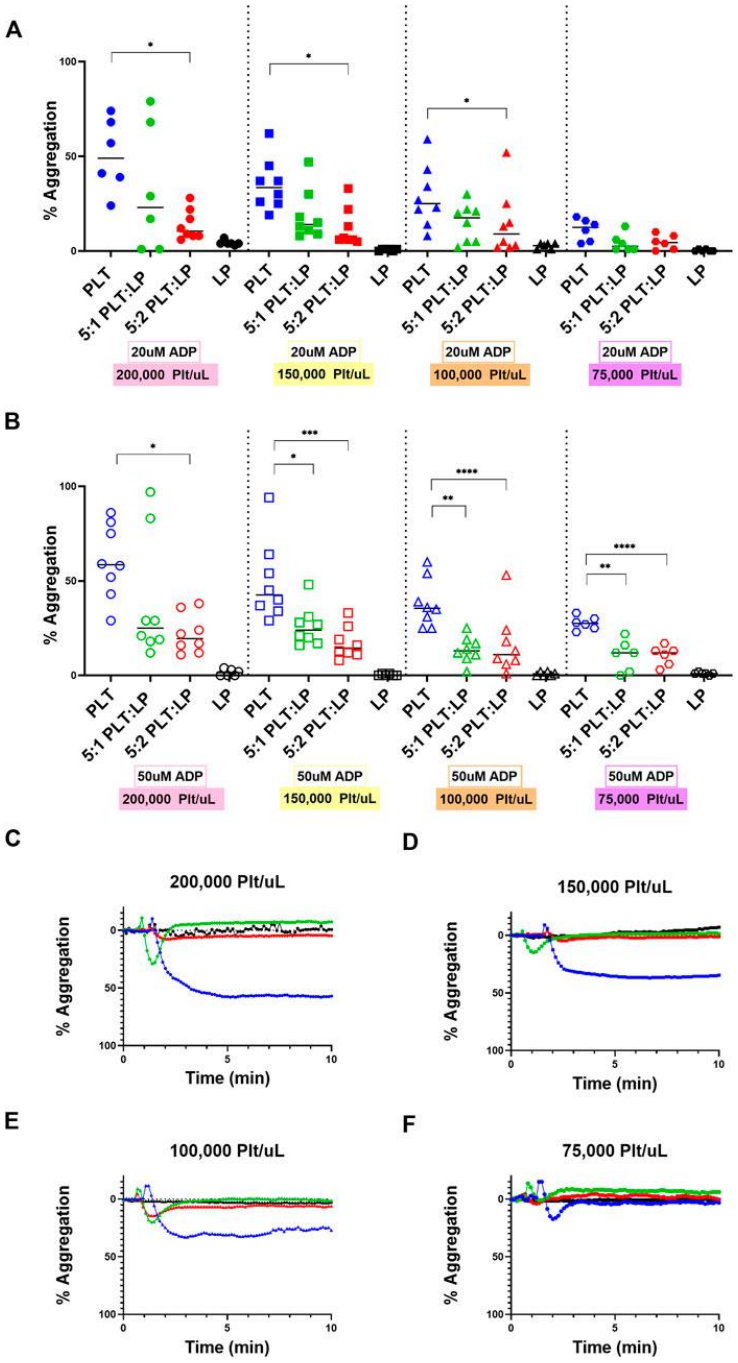

Figure 7*: Aggregation of Platelets in the presence of LPs at Different Concentrations and Ratios.* Quantification (A,B) and representative LTA curves (C-F) for the aggregation of platelets compared to platelets mixed with LPs at ratios of 5:1 and 5:2 platelets to LPs using ADP agonist at concentrations of 20uM (A; shown in representative figures C-F) and 50uM (B) using healthy platelet levels of (C) 200,000 platelets/uL [donor = 4, n=8] and (D) 150,000 platelets/uL [donor = 4, n=8], as well as thrombocytopenic platelet levels of (E)

100,000 platelets/uL [donor = 4, n=8] and (F) 75,000 platelets/uL [donor = 3, n=6] for all ratios. LP alone conditions are included for each platelet condition as a control.

With the most significant platelet interaction receptors characterized, the effect of LPs on platelet aggregation was analyzed using LTA. This analysis was conducted with a ratio of 5:1 and 5:2 platelets to LPs in order to approximate the ratios achieved with one and two standard platelet transfusions and compare to the 5:0 platelet control. These experiments were also tested at different platelet count conditions ranging from thrombocytopenic scenarios (75,000 and 100,000 platelets/uL) to normal healthy counts (150,000 and 200,000 platelets/uL). ADP was used as a platelet agonist. In each condition, there was a significant decrease in platelet maximum aggregation between the fresh platelets alone and the fresh platelets mixed with LPs. The trend was consistent across all platelet concentrations and with two different concentrations of platelet agonists (Fig. 7A-F). Specifically, at the normal platelet concentration of 200,000 Plt/uL, there was a significant decrease in platelet maximum aggregation with the 5:2 platelet:LP ratio for both ADP concentrations (Fig. 7A-C; *vs.* 20uM: P=0.0426, *vs.* 50uM: P=0.0158). This effect was also observed with the alternative normal platelet concentration of 150,000 Plt/uL with the 5:2 ratio at both ADP agonist concentrations (Fig. 7A,B,D; *vs.* 20uM: P=0.0180, *vs.* 50uM: P=0.0003). Under thrombocytopenic conditions there was a significant decrease in maximum aggregation for both agonist concentrations when 100,000 Plt/uL were mixed with LPs at a 5:2 ratio (Fig. 7A,B,E; *vs.* 20uM: P=0.0444, *vs.* 50uM: P=0.0002), but this same trend only appears at the 50uM ADP agonist concentration for the 5:2 ratio sample in the 75,000 Plt/uL condition (Fig. 7B,F; P<0.0001). Furthermore, a significant inhibitory effect was seen at the higher agonist condition and 5:1 ratio for 150,000 Plt/uL, 100,000

Plt/uL, and 75,000 Plt/uL conditions (Fig. 7B; P=0.0133, P=0.003, and P=0.0001, respectively). This trend was also visible in most conditions, but it was only statistically significant at the high agonist concentration. There also appears to be a dose dependent effect with the higher dose of LPs resulting in lower aggregation, but this was not statistically significant.

Additionally, further aggregation studies were conducted with platelets in undiluted PRP compared to platelets diluted to 200,000 platelets/uL with PPP and with Tyrode to ensure that the dilution did not significantly affect the aggregation of platelets. The data demonstrates that there is no significant difference in platelet aggregation between undiluted PRP, and platelet aggregation diluted with centrifuged PPP or Tyrode (Fig. 8)

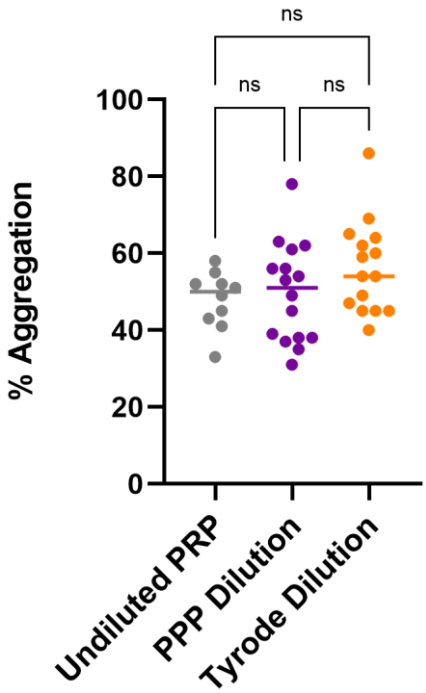

Figure 8: *Aggregation of PRP compared to Diluted PRP.* A LTA analysis of platelet aggregation comparing the aggregation of platelets in undiluted PRP (250,000 platelet/uL and 370,000 platelet/uL) (left, 2 donors, n=10 replicates) with the aggregation of platelets in PRP diluted to 200,000 platelets/uL with PPP obtained *via* centrifugation (middle, 2 donors, n=16 replicates) with Tyrode buffer (right, 2 donors, n=15 replicates).

3.3.4 Adhesion of Platelets in Mixtures with Lyophilized Platelets

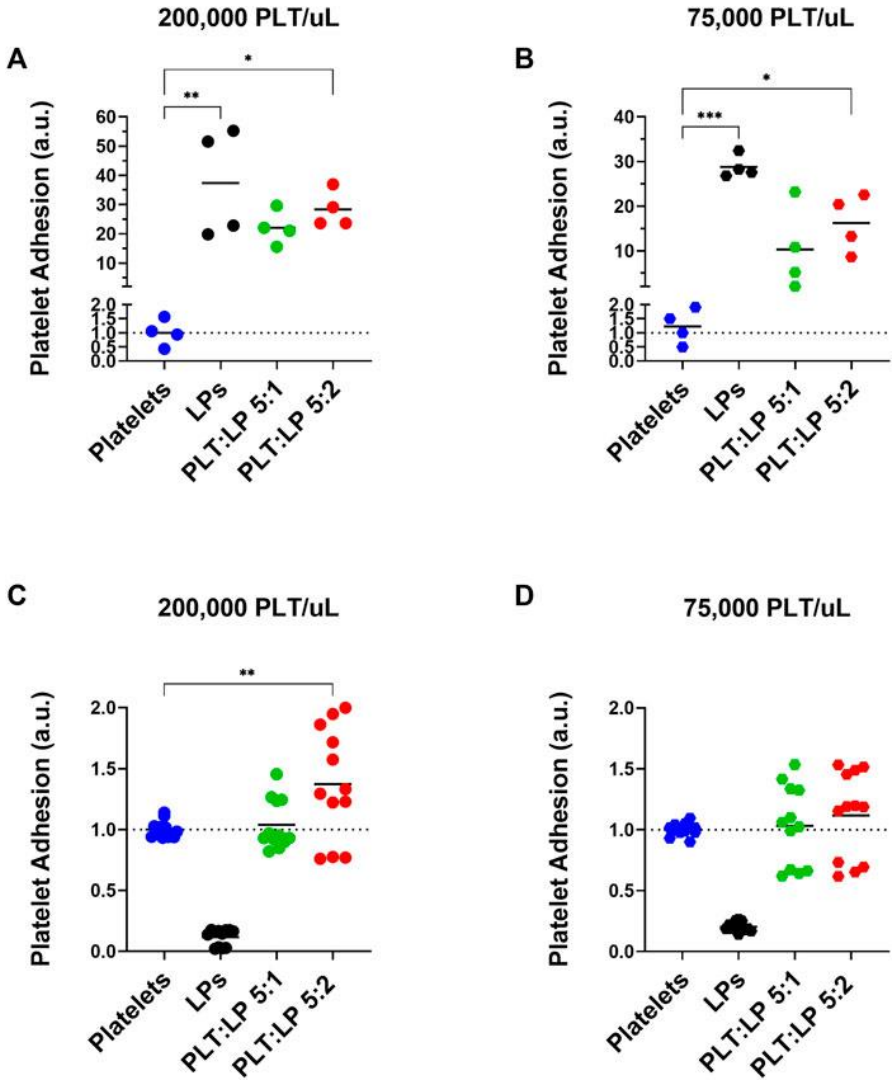

***Figure 9**: Adhesion of Platelets Mixed with Lyophilized Platelets on a Collagen Surface.* Normalized quantification of the adhesion of platelets in comparison to platelets mixed with LPs (at ratios of 5:1 and 5:2 platelets to LPs) in static conditions using and LDH assay (A,B) and under flow using calcein AM live-cell staining (C,D). Both assays were conducted at a (A,C) normal platelet concentration of 200,000 platelets/uL [Static: donor = 2, n=4, Flow: donor = 3, n=12], and a (B,D) thrombocytopenic platelet concentration of 75,000 platelets/uL [Static: donor = 2, n=4, Flow: donor = 3, n=12]. Note that the calcein AM live-cell staining (C,D) does not stain the inert LPs and thus the LP only condition does not represent their adhesion and is used as a control to ensure that there is no off target staining.

The other aspect of platelet function that needed to be examined was the adhesion of the platelets to a thrombogenic surface. During clot formation, platelets adhere to exposed collagen at an injury site and become activated. This initiates the formation of a platelet plug and is an essential aspect of hemostasis. To assess the effect of LPs on this key platelet function, the adhesion of the platelets to a collagen-coated surface while in a mixture with LPs was assessed under static and flow conditions. The adhered platelets under static conditions were measured through a LDH fluorescence assay. Appropriate controls were also conducted to account for the contributions of LPs to the measured fluorescence. This was repeated under healthy and thrombocytopenic conditions to simulate different scenarios where LPs could interact with native platelets. LPs adhered significantly more to the collagen surface compared to platelets in both normal (Fig. 9A, 37.4-time more, P=0.0015) and thrombocytopenic scenarios (Fig. 9B, 28.8-time more, P=0.0001). The results also showed a significant increase in platelet adhesion when mixed with LPs at both healthy (Fig. 9A, 28.3-time increase, P=0.0123) and thrombocytopenic conditions (Fig. 9B, 16.2-time increase, P=0.0153) at a 5:2 ratio. This indicates that the LPs interact with untreated platelets to promote surface adhesion. There appears to be a slight but not statistically significant dose effect for the 5:1 and 5:2 platelet to LP ratios as well.

The adhesion of the platelets was also assessed under flow using calcein AM-stained platelets in a microfluidic channel. The calcein AM live-cell stain was chosen because it does not stain the metabolically inactive LPs, and thus there is no LP component to the detected fluorescence (Fig. 9C,D). The adherence was measured using a platelet control as well as platelets mixed with LPs at a ratio of 5:1 and 5:2 platelets to LPs for both

normal and thrombocytopenic conditions. Compared to the fresh platelet control, there was a significant increase in the adherence of platelets under flow for those mixed with LPs at a 5:2 ratio with normal platelet counts (Fig. 9C, 1.4-time more, P=0.0042). A similar trend was seen for the 5:2 platelet to LP ratio under thrombocytopenic conditions, though the difference was not significant (Fig. 9D, 1.1-times more, P=0.6384). This indicates that the LPs promote surface adhesion of fresh platelets even under shear stress from flow conditions. Though, the pro-adhesion effect is small under flow compared to static conditions.

3.4. Discussion

The objective of this study was to characterize the interactions between LPs and untreated platelets. The scanning electron microscopy observation of platelets *versus* LPs on a collagen surface showed that LPs have much less pseudopodia than the adhered platelets (Fig. 10A,B), which is consistent with the fact that LPs are fixed and unable to undergo further morphological changes.

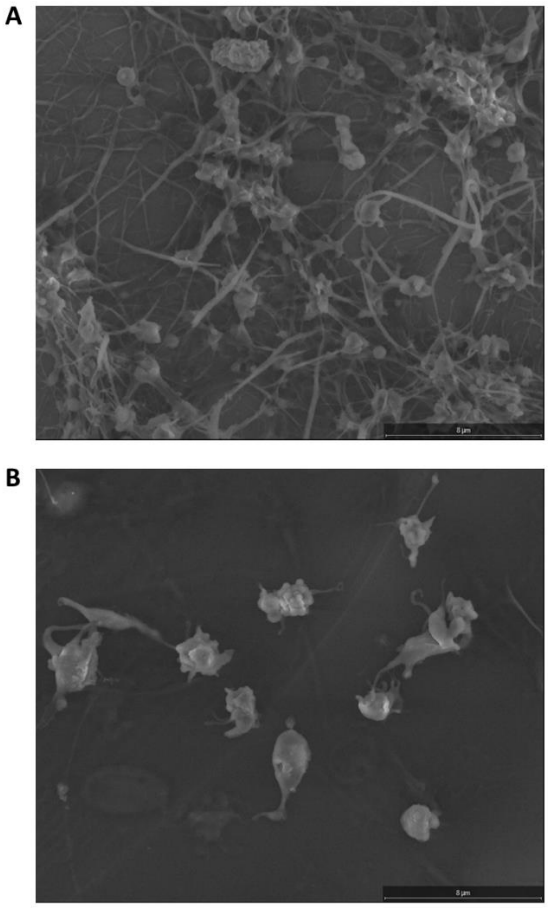

Figure 10: *Micrographs of Fresh and Lyophilized Platelets.* Scanning Electron Microscopy images of (A) fresh platelets and (B) LPs on a silicon wafer with a collagen surface. The images were taken in low vacuum (10 Pa) at 5 kV voltage and 50pA current settings.

Though these images provide some interesting insight into the possible morphological changes, quantitative analyses of the platelet receptors and functions is needed to understand differences between LPs and fresh platelets. The first aspect of this analysis was the characterization of the receptors available on the surface of the LPs. The presented data demonstrates that almost all the LPs do maintain two critical receptors for platelet interactions and adhesion, GPIIb and GPIb. The GPIIb/IIIa receptor is essential for the aggregation of platelets through binding to fibrinogen and von Willebrand Factor. The conservation of this receptor on the LPs (Fig. 5A-C) is a strong indicator that these

lyophilized platelets can, at least weakly, interact with untreated platelets or any GPIIb/IIIa ligands. Furthermore, a significant percentage, 15.8%, of these LPs have GPIIb/IIIa receptors in the active conformation (Fig. 5D-F). The activation of these LPs is likely due to the temperature decrease in the lyophilization process since cold exposure is known to cause platelet activation (Gousset et al., 2004). This activated GPIIb/IIIa receptor increases the ability of the LPs to interact with its ligands (e.g. fibrinogen) *via* enhanced affinity (Michelson, 2013). Additionally, the primary receptor for platelet adhesion, GPIb, is also significantly maintained on the LP surface (Fig. 5G-I). A significant portion of the LPs also retain the GPVI receptor important for collagen binding (Fig. 5J-L). Thus, the LPs can be expected to interact with thrombogenic surfaces (Fig. 9A-D). This characterization of the surface receptors present in the LPs provides strong evidence that the LPs can interact with native platelets and affect their performance in aggregation and adhesion.

This initial receptor data was then reinforced by assessing the exposure of phosphatidylserine on the LPs, as well as the fibrinogen binding to the LPs. The exposed phosphatidylserine on platelets has been shown to regulate fibrin binding and thrombogenesis and thus serves as a marker to identify pro-coagulant platelets (Reddy and Rand, 2020). As seen in figure 6, the LPs have a significant annexin-V staining which indicates significantly more exposed phosphatidylserine compared to unaltered platelets (Fig. 6A-C). Additionally, the fibrinogen binding to the LPs is shown to be significantly increased compared to the unaltered platelets (Fig. 6D-F). This correlates with the expression of activated GPIIb/IIIa receptors detected on the surface of the LPs since these activated receptors are known to have an increased affinity for fibrinogen (Michelson, 2013). Given the key role of fibrinogen in platelet interaction and thrombosis, the increased

fibrinogen binding also indicates that these LPs will significantly interact with unaltered platelets and may have a pro-hemostatic effect.

The effects of LPs on the aggregation and adhesion of untreated platelets were then assessed through the LTA, LDH, and calcein AM assays. The evidence clearly demonstrates that these LPs do interact with the untreated platelets and have a significant impact on their function. However, it is interesting to note that interactions have contrary effects for aggregation *versus* adhesion. The LPs have a robust anti-platelet effect in terms of aggregation, as we demonstrated that this effect is seen at extremely high ADP concentrations (including 50 uM). Indeed, there were significant decreases in platelet aggregation when LPs were mixed with the untreated platelets. This was a consistent trend across platelet counts as well. Additionally, our data (Fig. 8) indicates that there are no factors in the centrifuged PPP that could account for the observed anti-platelet effect. Thus, the data demonstrates that LPs inhibit the aggregation function of untreated platelets. In addition, Bynum *et al.* observed that the maximum clot firmness is significantly reduced in presence of LPs (Bynum et al., 2019). Our observation of the antiplatelet effect on fresh platelet aggregation (Fig. 7) could potentially explain this reduced clot firmness. However, the LPs have an equally significant pro-platelet effect in terms of adhesion. There was an increase in the adherence of platelets to a collagen surface under static conditions when untreated platelets were mixed with LPs. This phenomenon offers an interesting contrast to the effect of LPs on aggregation. The evidence shows that the LPs improve the ability of platelets to interact and adhere with a surface while interfering with the ability of platelets to aggregate. In addition, our data corroborate the findings by J.A. Bynum *et al.* and G. M. Fitzpatrick *et al.* demonstrating that LPs adhere to collagen thrombogenic

surface (Bynum et al., 2019), despite a reduction in GPIb expression after they undergo freeze drying (Fitzpatrick et al., 2013). Moreover, LPs adhere to collagen surfaces despite them being unable to undergo firm adhesion, subsequent to a lack of signaling convergence toward the recruitment of receptors beyond GPIb/V/IX. The low GPIIb and GPVI expression might be overcome by the priming of a fraction of these platelets into an activated state by induction of GPIIb/IIIa active conformation during lyophilization. Activated GPIIb/IIIa has a high binding affinity for von Willibrand factor, which interacts with collagen, thus facilitating the consolidation of platelet adhesion by active GPIIb/IIIa receptors in support of GPIb initial tethering. Indeed, PAC-1 antibody, that specifically targets the active conformation of GPIIb/IIIa, binds LPs significantly more than untreated platelets (Fig. 5D-F). Additionally, other receptors, such as $\alpha 2\beta 1$ are also involved in the consolidation step of platelet adhesion on a collagen surface (Varga-Szabo et al., 2008), and might also compensate for the decreased expression of GPVI and GPIIb in LPs. Indeed, we observed promotion of platelet adhesion on thrombogenic surface in static conditions and in the presence of LPs both in normal (Fig. 9A) and thrombocytopenic samples (Fig. 9B). Moreover, this pro-platelet effect on adhesion was also observed under shear stress in a microfluidic channel for the 5:2 ratio of platelets to LPs at a normal platelet concentration (Fig. 9C). Though the effect was greatly reduced compared to the static conditions. There was also a pro-platelet adhesion trend in the thrombocytopenic condition under flow at this ratio (Fig. 9D), but it was not significant in our experimental settings. This is in contrast with the study by Bynum *et al.* that observed this effect solely in thrombocytopenic condition (Bynum et al., 2019). This could be explained by the difference in formulation between the fixed LPs used in our study and their trehalose stabilized LPs. Our results

under flow conditions demonstrate that the LPs have a robust effect promoting fresh platelet adhesion, even though there is a reduction in effect compared to static adhesion.

These contrary effects for different aspects of platelet functions highlight the need for further research into the underlying mechanisms. Understanding these mechanisms could provide insight into platelet function and allow for more targeted treatments of platelet disorders and pathologies involving platelet cooperation.

The characterization of these interactions provides for interesting opportunities in therapeutics and drug delivery. The contrary effect indicates that the LPs may be used as a therapeutic that inhibits improper platelet aggregation in circulation, without hindering platelet adhesion at an injury site. For example, the LPs could be developed into a therapeutic that reduces platelet interactions with cancer cells or inhibits Tumor Cell Induced Platelet Aggregation (TCIPA) without disrupting other key platelet functions. Alternatively, the tendency of the LPs to adhere to collagen surfaces and promote platelet adhesion could be used to deliver a therapeutic to an injury site while mitigating the possibility of such an agent inducing platelet aggregation systemically.

It is possible that the activated LPs may increase the risk of thrombosis. However, in an early phase I clinical trial, there has been no sign of thrombotic complication reported to date (Ohanian et al., 2022). The antiplatelet effect of LPs on platelet aggregation observed in our study could be a possible explanation for the lack of thrombotic side effects in spite of its ability to act as hemostatic agent.

Further understanding the effects of LPs on untreated platelets would form a foundation for creating a LP therapeutic or drug delivery product. Regardless of the targeted application, an in-depth characterization of their efficiency along with limitations

and potential side effects (e.g. adverse events such as thrombotic complication and dose-limiting toxicities) will be required in the context of each pathological scenario to assess risks *versus* benefits.

Chapter 4: Development of a Fibrinolytic Platelet Systems to Reduce Cancer Metastasis by Dissociating Circulating Tumor Cell Clusters

This text/article is under revision with a journal and is included in this chapter with author's permission:

Schnoor, B., Morris, K., Kottana R. K., and Papa, A.-L. (in revisions). Fibrinolytic Platelet Decoys Reduce Cancer Metastasis by Dissociating Circulating Tumor Cell Clusters.

Circulating tumor cell (CTC) clusters play a significant role in cancer metastasis. During metastasis, CTCs can travel in the bloodstream as individual cells or as clusters associated with fibrin and platelets (Karpatkin and Pearlstein, 1981; Palumbo et al., 2005). The CTC clusters have a higher metastatic potential than individual tumor cells (Aceto et al., 2014) due to their ability to better withstand shear stress together compared to single cells, as well as the increased chance of large clusters arresting in small vessels. As such, there is a need to develop methods to disperse CTC clusters. Previous work with the fibrinolytic urokinase-type plasminogen activator has shown initial success in reducing metastasis by dissociating cancer cell clusters (Choi et al., 2015). However, fibrinolytics are potent drugs that are associated with bleeding side effects and thus improving the plasminogen activator targeting while decreasing the drug associated side effects is critical for addressing this challenge. In addition, another key component of metastasis is the interaction of CTCs with platelets. Platelets bind to the CTC surface which protects the CTC clusters from shear stress and immune detection, increasing their metastatic potential (Morris et al., 2022). While these interactions represent a challenge as they support CTC dissemination, they also provide a window of opportunity to target CTC clusters. As such,

the objective of this project is to develop a fibrinolytic platelet system to dissociate CTC clusters while also potentially disrupting CTC-platelet interactions. For this approach, tissue plasminogen activator (tPA) was loaded onto two modified platelet systems: platelet decoys (Papa et al., 2019) and lyophilized platelets (Schnoor and Papa, 2022). Each tPA-loaded system was assessed to determine the surface receptor characteristics, drug loading, and interaction with tumor cells *in vitro*. The fibrinolytic activity of the systems was also characterized using a FRET-based assay and the angiogenic effects of the systems were measured using a HUVEC tube formation assay. Furthermore, the ability of the system to dissociate cancer cell clusters *in vitro* was assessed using light transmission aggregometry using a protocol developed by our group (Kottana et al., 2024). The results demonstrate that the tPA was successfully loaded onto both platelet decoys and lyophilized platelets while maintaining tPA's fibrinolytic activity. Furthermore, a high percentage of cancer cells interact with the tPA-loaded carriers, which corresponds to the relative maintenance of key surface receptors such as GPIIb/IIIa (Schnoor and Papa, 2022). The data also demonstrates that the fibrinolytic platelet systems can successfully dissociate cancer cell clusters *in vitro*. Finally, the fibrinolytic platelet decoys were able to successfully reduce the metastatic dissemination of the cancer *in vivo* by targeting and dispersing tumor cell clusters. Based on these results, this fibrinolytic platelet approach is a promising method to leverage platelet-CTC interactions to disperse CTC clusters and reduce metastasis.

4.1 Introduction

Circulating tumor cell (CTC) clusters present a critical challenge with cancer metastasis. For example, breast cancer patient mortality in more than 90% of patients is

related to cancer metastasis and accompanying complications such as an increased incidence of cancer-associated thrombosis (Cummings et al., 2014; Chen et al., 2018). During metastasis, CTCs can travel in the bloodstream as individual cells or as clusters associated with fibrin and platelets (Karpatkin and Pearlstein, 1981; Palumbo et al., 2005). Clusters of CTCs have a 23 to 50-fold increased metastatic potential as compared to single circulating tumor cells (Aceto et al., 2014), due to their ability to better withstand shear stress together compared to single cells, as well as the increased chance of large clusters arresting in small vessels (Aceto, 2023). Moreover, CTC clusters are detected in approximately 35% of patients with advanced breast cancer and their presence is associated with a significantly shorter time to disease progression (Aceto et al., 2014). As such, there is a need to develop methods to disperse CTC clusters in order to reduce their metastatic potential.

These challenges with CTC clusters are further complicated by the interaction between platelets and CTC clusters. Platelets coat the surface of CTCs, which helps CTCs navigate the harsh environment of the bloodstream where they experience shear stress and immune cell detection (Bambace and Holmes, 2011; Gay and Felding-Habermann, 2011b; Morris et al., 2022). Platelets also support tumor cell metastasis by assisting CTC arrest in the vasculature, by facilitating their extravasation, and by providing pro-angiogenic and pro-oncogenic factors (Labelle et al., 2011; Morris et al., 2022). Furthermore, platelet-CTC interactions activate signaling pathways to trigger the epithelial-mesenchymal transition in CTCs, resulting in increased migratory and invasive capabilities for the tumor cells (Labelle et al., 2011; Pearson, 2019; Morris et al., 2022). The importance of these platelet-CTC interactions are supported by the association of high platelet count and poor prognosis

in cancer patients (Sierko and Wojtukiewicz, 2004), as well as the significant reduction in cancer metastasis observed in platelet-depleted animal models (Stone et al., 2012).

However, these platelet-CTC interactions also present an opportunity along with the challenges. Since platelets interact with CTCs through several receptor interactions (Morris et al., 2022), platelet-based drug delivery systems can utilize these interactions to target the CTCs while they are in transit in the bloodstream. One approach to leverage these interactions is to use platelet Decoys obtained *via* a detergent-extraction process (Papa et al., 2019). These platelet Decoys have been shown to interact with CTCs and delay metastasis in a mouse model (Papa et al., 2019). There are also alternative modified platelet systems based on lyophilized platelets (LPs), which have been explored *in vitro* and *in vivo* for their potential as hemostatic agents (Cellphire Therapeutics, Inc., 2021, 2022) and their effect on normal platelet function (Cellphire Therapeutics, Inc., 2019, 2021; Schnoor and Papa, 2022). Both of these platelet-based carriers present key advantages for targeting CTC clusters. Platelet Decoys and LPs substantially preserve surface receptors such as GPIIb/IIIa that are involved in platelet-CTC interactions (Papa et al., 2019; Schnoor and Papa, 2022), and can thus be leveraged for CTC targeting. Furthermore, both platelet Decoys and LPs are inert in terms of their intrinsic signaling pathways. Platelet Decoys do not activate in the presence of various platelet agonists such as adenosine diphosphate (ADP) (Papa et al., 2019). Similarly, LPs do not aggregate, and significantly inhibit platelet aggregation, when treated with ADP (Schnoor and Papa, 2022). Since signaling pathways are not preserved in the platelet-based carriers, they do not support tumor cells through the active release of pro-oncogenic or pro-angiogenic factors.

In order to develop these systems, we loaded an FDA approved fibrinolytic drug, tissue plasminogen activator (tPA), on the surface of platelet Decoys and LPs to disassemble these CTC clusters and disrupt their metastatic potential. Our hypothesis is that platelet Decoys or LPs would target CTC clusters and deliver tPA that would then lyse fibrin holding these tumor cells together, thus releasing individual CTCs. Fibrinolytics can efficiently dissociate CTC clusters (Choi et al., 2015) and platelets have a natural strong binding affinity to fibrinolytics, including tPA (Park et al., 1989; Vaughan et al., 1989). Thus, cellular therapeutic platelet platforms such as platelet Decoys - that already deploy an antiplatelet effect on thrombosis and the metastatic cascade (Papa et al., 2019) - are an attractive drug delivery system to explore for targeting and breaking apart these highly aggressive and invasive CTC clusters. As for LPs, they possess more receptors on their surface compared to platelet Decoys and could potentially enable more tPA loading per platelet (Schnoor and Papa, 2022).

The role of the plasminogen activator system in cancer dissemination is being increasingly investigated. Plasminogen activators, such as tPA, are fibrinolytic drugs used in the treatment of stroke or pulmonary embolism. Their fibrinolytic action disrupts already formed blood clots and they are part of the body's endogenous mechanisms to prevent excessive clotting. Moreover, tPA infusion, as a component of an angiostatic cocktail, has shown no dose limiting toxicity in a phase I trial studying patients with metastatic cancer (Soff et al., 2005). We chose tPA as our candidate fibrinolytic agent for targeted delivery to CTC clusters, based on these favorable characteristics and its known long track record for its current FDA-approved indications in acute ischemic strokes and pulmonary embolism.

4.2. Materials and Methods

4.2.1 Materials

Human whole blood drawn with 3.8% sodium citrate was procured from BioIVT LLC, following approval from the Institutional Biosafety Committee at the George Washington University. Platelet apheresis with anticoagulant citrate dextrose solution A (ACD-A) was obtained from Charles River (cat# PLTS-5577) and lyophilized platelets were procured from Chrono-Log (cat# 299-2).

Tissue plasminogen activator conjugated with fluorescein isothiocyanate (tPA-FITC) was obtained from Cell Sciences (cat# CRT172B). The clinical grade tissue plasminogen activator, Alteplase, was procured *via* a material transfer agreement with Genentech.

Sodium chloride (cat# S7653), magnesium chloride (cat# M8266), sucrose (cat# S7903), HEPES (cat# H3537), potassium chloride (cat# P9333), and glucose (cat # D9434) were obtained from Sigma-Aldrich. Sodium citrate (cat# 7228-16) was obtained from Ricca Chemical. Triton X-100 solution (CAS# 9002-93-1) was purchased from ACROS Organics and the protease inhibitor cocktail tablets (cat# 04 693 116 001) were purchased from Roche. Alprostadil (PGE-1) (cat# 1620) was obtained from Tocris. CellMask™ plasma membrane stains (cat# C10046) and Hoechst (cat# H3570) were procured from Invitrogen. The fluorometric AMC tPA activity assay kit (cat# AS-72160) was purchased from Anaspec. The Human Umbilical Vein Endothelial Cells (HUVEC) (cat# C2519AS) were procured from Lonza and the Cultrex basement membrane gel matrix (cat# 3445-001-01) was obtained from Trevigen.

Immunocompromised BALB/c nude mouse model (CAnN.Cg-Foxn1nu/Crl, strain code: 194) was obtained from Charles River Laboratories. Additional supplies included luciferin sodium salt (Abcam, cat# ab145164), 28G insulin syringe (Covetrus, cat# 74075), 0.9% Saline (Hospira, NDC 0409-4888-06), alcohol wipes (Becton Dickinson, cat#326895), optixcare eye cream (Aventix, cat# OPX-4242), and isoflurane (Covetrus, NDC 11695-6777-2).

4.2.2. Cell Culture

MDA-MB-231 breast cancer cells (ATCC, cat# HTB-26) and MDA-MB-231-LUC-D3H2LN breast cancer cells were cultured in 75 cm^2 Falcon tissue culture flasks in Dulbecco's Modified Eagle's Medium (DMEM) with 4.5 g/L D-glucose, L-glutamine, 110 mg/L sodium pyruvate (Gibco, cat# 11995-065) supplemented with 10% Fetal Bovine Serum (FBS, Gibco, cat# 26140-079) and 1% Pen Strep (penicillin streptomycin, Gibco, cat# 15140-122). The cells were collected using cell scrapers (Falcon, cat# 353089) and centrifuged at 1,200 rpm for 3 min. The cells were then resuspended in Tyrode buffer (136 mM NaCl, 12 mM $NaHCO_3$, 2.9 mM KCl, 0.34 mM $Na_2H_2PO_4$, 1 mM $MgCl_2$, and 10 mM HEPES, pH 7.5). Cells cultured for *in vivo* experiments were collected using 0.25% Trypsin – EDTA (Gibco, cat# 25200-056) instead of cell scraping. The cells were then resuspended in 0.9% saline after neutralizing the trypsin and centrifuging. The cell concentration was determined with a LUNA-II^{TM} cell counter (Logos Biosystems Inc., South Korea) and a trypan blue viability stain.

4.2.3. Decoy Platelet Preparation

Human whole blood samples were centrifuged at 290 g for 20 min with no braking deceleration to collect platelet rich plasma (PRP). Alprostadil (PGE_1) was then added to the PRP at 50 ng/mL and incubated for 15 min before centrifuging again at 1,000 g to pellet the platelets. The platelets were then resuspended in 2 mL of platelet poor plasma (PPP). Decoys prepared for the *in vivo* metastasis model were resuspended in 1.2 mL of PPP and 0.8 mL of 25x concentration of complete protease inhibitor and incubated for 30 min. Then, for all preparations, 2.5 mL of extraction buffer (0.01 M HEPES, 0.05 M NaCl, 2.5 mM $MgCl_2$, and 0.3 M sucrose) was added along with 0.5 mL of 1% Triton X-100. The sample was gently mixed by inversion twice and then centrifuged at 1,000 g for 10 min. The Decoys were then resuspended in the wash buffer (140 mM NaCl, 5 mM KCl, 12 mM sodium citrate, and 10 mM glucose) and centrifuged again. This wash step was repeated before the Decoys were resuspended in Tyrode buffer. When these Decoys were stored, they were frozen in a 10% sucrose solution.

4.2.4. tPA-Loading on Platelet Carriers

In order to load the tPA onto the fibrinolytic system, the LPs or Decoys were resuspended in Tyrode buffer at a concentration of 250,000 carriers/uL. For the Decoy formulation, 20 ug/mL of tPA was added to the suspension. For the LP formulation, only 10 ug/mL was added to the sample. Each sample was then incubated under mixing for 1 hour at 4 °C. Subsequently, the sample was centrifuged at 1,000 g for 1 hour to pellet the tPA-loaded Decoys and LPs. In order to assess the percent decoration and the loading efficiency, this procedure was performed using FITC-conjugated tPA. The Novocyte 3000

flow cytometer was used to measure the percent of the carriers successfully loaded with FITC-tPA. The fluorescence of the samples was then measured using a Spectramax ID5 fluorescent plate reader at an excitation of 488 nm and an emission of 528/45 nm to determine the amount of drug loaded and the loading efficiency. The loading efficiency is determined by comparing the measured amount of tPA loaded on to the system to the amount of tPA incubated with the carriers in the loading procedure. For subsequent experiments, clinical grade tPA, Alteplase, was used instead of the fluorescent tPA.

4.2.5 Determination of the tPA Receptor on Platelets by Flow Cytometry

The receptor involved in tPA binding was identified using flow cytometry. First, the involvement of the NDMA receptor was assessed by incubating 12.5 million LPs with either the mouse anti-human NDMA 1 antibody (Biolegend, cat# 818601) or an IgG control (Biolegend, cat# 401402) at a concentration of 0.1 mg/mL in 50 uL of Tyrode buffer for 20 min. Then the fluorescent tPA was added to the suspension at the same concentration and using the same procedure as above (section 4.2.4). The fluorescence of the tPA-LPs treated with anti-NMDA 1 antibodies and respective IgGs were compared to tPA-LPs prepared without antibodies. Then, the involvement of the GPIIb/IIIa receptor was analyzed by incubating 500,000 LPs with APC-conjugated mouse anti-human CD41a antibodies (BD Pharminogen, cat# 559777) or APC-IgGs (BD Pharminogen, cat# 555751) respectively at a concentration of 0.5 ug/mL in 50 uL of Tyrode for 20 min. This procedure was repeated using tPA-LPs prepared using the method above (section 4.2.4) at the same concentration and duration. Finally, a control was created using bovine serum albumin (Sigma, cat# A7030-10G), which was selected because it has a similar molecular weight

to tPA, but does not selectively bind to platelets. For this control, bovine serum albumin was incubated with LPs at the same concentration and using the same procedure as for tPA loading. Then the LPs were centrifuged and incubated with APC-CD41a or IgG antibodies as described above. All samples were then assessed using the Novocyte flow cytometer to determine the median fluorescence.

4.2.6. Fibrinolytic Activity Assay

The fibrinolytic activity of the tPA-loaded system was the determined using the Sensolyte AMC tPA activity assay. This assay contains a tPA substrate that becomes fluorescent when broken down, and thus, the rate of fluorescent increase for the assay is determined by the fibrinolytic activity. The Decoys and LPs were loaded with Alteplase using the procedure described in section 4.2.4. Then 0.4 ug/mL tPA in the form of free tPA, tPA-loaded LPs, or tPA-loaded Decoys were added to a 96-well plate and incubated with the tPA substrate solution. Controls for unloaded Decoys and LPs, loaded Decoys and LPs without the tPA substrate, the substrate with/without tPA, and with/without a tPA inhibitor were also added. The fluorescence was then measured every minute over an hour using a Spectramax ID5 fluorescent plate reader with excitation at 354 nm and emission of 442 nm.

4.2.7. *In vitro* Fibrinolytic Platelet-Cancer Cell Interaction Assay

The interaction of the fibrinolytic platelet systems with cancer cells was assessed using flow cytometry. First PRP was obtained by centrifuging human whole blood at 150 g for 20 min with no brake for deceleration. Alprostadil was then added to the PRP at 50

ng/mL and incubated for 15 min before centrifuging again at 1,000 g to pellet the platelets. These platelet pellets were then resuspended in Tyrode solution to produce a concentrated platelet suspension. tPA-Decoys and tPA-LPs were obtained *via* the tPA-loading procedure described above (section 4.2.4). The CellMask red stain was then added at a 1,000x total dilution to each different platelet or tPA-loaded platelet suspension and incubated for an hour at 37 °C. The platelets were washed twice *via* centrifugation at 1,000g for 20 min.

MDA-MB-231 cells were incubated with stained platelets or loaded platelets at a concentration of 2,000 MDA-MB-231 cells/uL and a 200:1 ratio of platelets, tPA-Decoys, or tPA-LPs to cancer cells. This incubation suspension was maintained under gentle tilt plate agitation at 37 °C for 2 hours. After incubation, the cancer cells were then washed twice by centrifugation at 1,200 rpm at 10 min before being resuspended in fresh Tyrode solution. Subsequently, the washed cancer cells were then analyzed *via* flow cytometry to determine if CellMask red stained platelets were interacting with each cancer cell and the results were normalized for each carrier system.

Controls were also added to account for any incidental staining not resulting from direct platelet-cancer cell interactions. For each platelet and fibrinolytic platelet condition, the cell mask red-platelets, -tPA-Decoys, or -tPA-LPs were incubated alone at the same concentration and under the same conditions as the experimental groups, but without cancer cells. Then the samples were centrifuged at 1,000 g to remove the platelets and tPA-loaded fibrinolytic platelets. The supernatant was then incubated with MDA-MB-231 cells at the same concentration and incubation time as with the experimental groups.

4.2.8. HUVEC Angiogenesis Assay

The effect of the fibrinolytic platelet system on angiogenesis was analyzed using a HUVEC tube formation assay. For this assay, a Cultrex basement membrane matrix was plated on an Ibidi µ-plate angiogenesis 96-well plate. Then the HUVEC cells were seeded onto this membrane with Endothelial Growth Medium 2 (EGM-2) and treated with either free tPA, tPA-loaded Decoys, or tPA-loaded LPs. Control groups without any treatment, with unloaded Decoys, and with unloaded LPs were also included. For each sample with tPA, a 0.1 ug/mL concentration of Alteplase was used. This was conducted both with medium including growth factors and with growth factor deprived medium. The plate was then allowed to incubate for 12 h before images were taken at 10x magnification. These images were processed using the ImageJ software incorporating the Angiogenesis Analyzer feature designed by Gilles Carpentier to determine the number of nodes, number of segments, and the length of the segments present in each well (Carpentier et al., 2020).

4.2.9. Dissociation of Tumor Cell Clusters using Light Transmission Aggregometry

In order to assess the effectiveness of our fibrinolytic platelet systems *in vitro*, we developed for the first time a light transmission aggregometry (LTA)-based assay that quantitatively measured the dissociation of tumor cell clusters (Kottana et al., 2024).

The protocol for the light transmission aggregometry was modified to study tumor cell association and dissociation using a model 490 4+4 aggregometer. A control plasma made of a 15 healthy donor pool was warmed at 37 °C for 10 min. The tumor cell suspensions were diluted to 4,000 cells/uL in Tyrode buffer and were mixed with the

warmed control plasma in a 1:1 volume ratio. 250 uL of the plasma-tumor cell mixture was then added, under stirring at 1,200 rpm, to the LTA cuvette which was preloaded with the stir bar and 20 uL of 62.5 mM of $CaCl_2$ for a final concentration of 5 mM $CaCl_2$. The reference cuvette was loaded with the supernatant that was collected from a separate identical clustered cell samples and subsequently filtered through a 0.22 um filter to represent the 100% transmittance reference for our samples. The trace of the sample was then immediately set to baseline and observed for 10 min or until the tumor cell-fibrin clusters formed (i.e. a clot formation over the stir bar) and a stable trace at 90±10% aggregation was observed. At the 10 min timepoint, the respective treatment for each group was added. The tested treatments included free tPA, tPA-Decoys, and tPA-LPs each with a final tPA (Alteplase) concentration of 0.5 ug/mL. Control groups without treatment, as well as with unloaded Decoys or LPs, were also included.

The absorbance over time values were processed by subtracting the initial absorbance after baseline from each point within the replicate. For each curve the dissociation at each timepoint was calculated by the difference between the observed percent disassociation and the disassociation at 10 min. The lag time between the fibrinolytic treatment and the start of tumor cell dissociation was measured as 5% dissociation. The percentage of tumor cell dissociation at 10, 35, and 60 min after the beginning of the measurement period were obtained from each curve (0, 25, and 50 min after addition of fibrinolytic agent). Additionally, the time needed to reach the maximum recorded tumor cell dissociation was measured. An average of the dissociation curves was also created for each of the treatment groups.

4.2.10. Experimental Metastatic Model of Breast Cancer Cell Clusters in Mice

The effectiveness of the fibrinolytic platelet system was assessed *in vivo* using a Balb/c nude mouse model (CAnN.Cg-Foxn1nu/Crl) injected with tumor cell clusters. The study was designed following the NIH Guide for the Care and Use of Laboratory Animals and reviewed and approved by the Institutional Animal Care and Use Committee of The George Washington University, as well as the DOD Animal Care and Use Review Office. Tumor cell clusters are created from cultured MDA-MB-231-luc-D3H2LN cells that have been vortexed for 20 s in saline solution with 5% PPP. Then the cancer cell clusters were incubated under light mixing for 7 min with either free-tPA, tPA-Decoys, unloaded-Decoys, or saline as a control for each treatment group. The tPA-Decoys were chosen as the fibrinolytic platelet system because the tPA-LPs quickly induced sudden animal death in our model shortly after injection, which could be a reflection of the hemostatic nature of the LPs (Fitzpatrick et al., 2013) which in a pro-coagulant cancerous microenvironment could catalyze acute thrombosis. No such observations were made with the tPA-Decoys, which display an antiplatelet effect and are not hemostatic (Papa et al., 2019). After the incubation, 100 uL of the tumor cell clusters and treatment were introduced to the mouse model *via* an intracardiac injection. A total of 50,000 MDA-MB-231-luc-D3H2LN cells were simultaneously injected with the treatment. A tPA dosage of 0.9 mg/kg was used for both the free-tPA and the tPA-Decoy treatment groups based on preliminary data and because this dose is considered standard for tPA bolus injections in humans (Reed et al., 2023). After injection, the mouse was imaged using an IVIS device. In short, each mouse was injected with 100 uL of 0.1 M luciferin sodium salt *via* intraperitoneal injection. This was allowed to diffuse for 15 min as the mouse was aestheticized using 2% aerosolized

isoflurane. Then the luminescent signal produced by the enzymatic processing of the luciferin in the tumor cells was measured. This imaging procedure was repeated twice a week for 7 weeks. Additional treatment injections at 0.9 mg/kg tPA were also administered *via* a 100 uL retro-orbital injection at day 4, 7, and 11.

4.2.11. Statistical Analysis

All graphical representations and statistical analyses of the data were developed using the Prism software from GraphPad. Statistical significance between experimental groups was determined using an analysis of variance (ANOVA) method. Tukey's test for multiple group comparisons and Dunnett's test for comparisons to control were used to determine significances for all *in vitro* experiments. (*$P \leq 0.05$, **$P \leq 0.01$, ***$P \leq 0.001$, and ****$P \leq 0.0001$). Regarding the *in vivo* data analyses, a 2-way ANOVA analysis with comparisons within all groups and within time points (uncorrected Fisher's LSD) was used with a Last Observation Carried Forward (LOCF) method. A logrank test was used to analyze the Kaplan Meyer survival curves. All figures display the mean ± SD for each group.

4.3. Results

4.3.1. Characterization of tPA Loading and Loading Efficiency

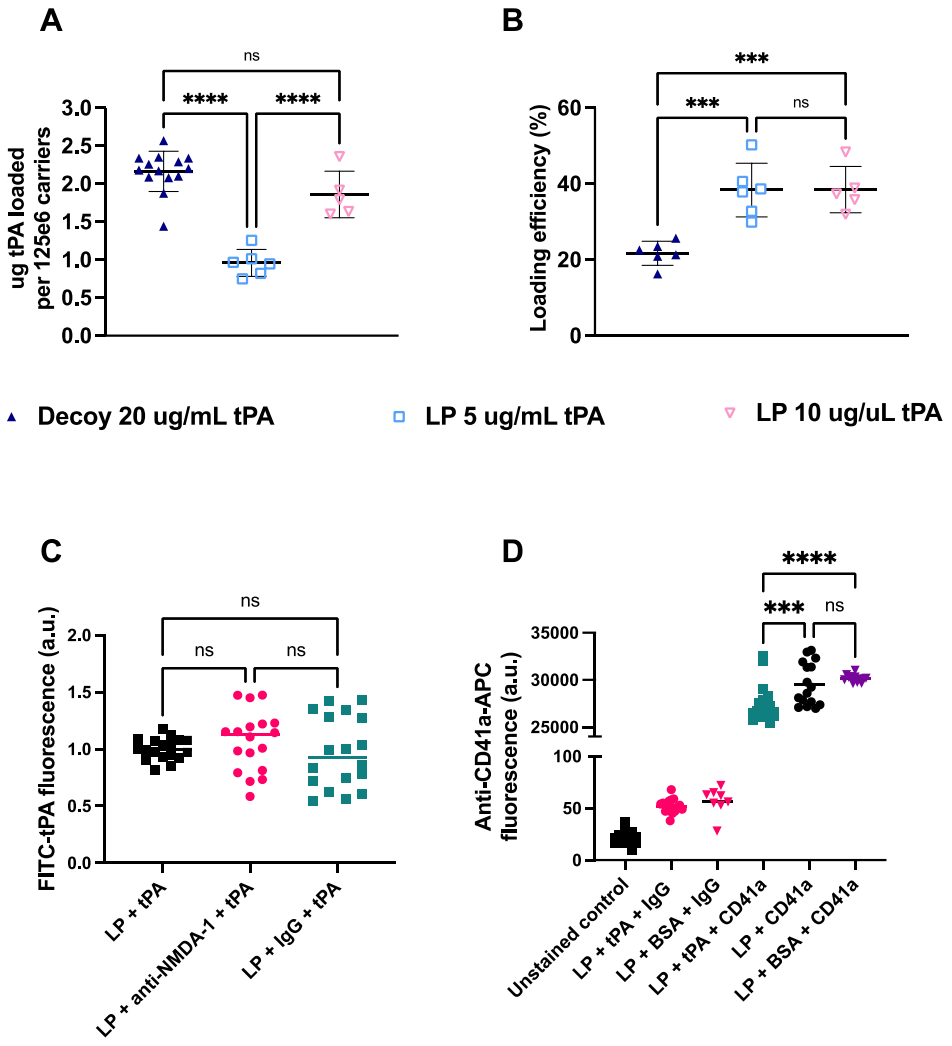

Figure 11: *Characterization of tPA Loading on the Platelet Carriers, tPA Loading Efficiency, and Identification of the tPA Receptor*. Assessment of tPA loaded onto the Decoy or Lyophilized Platelet Carrier using a plate reader to detect FITC-conjugated tPA. (A) tPA loading onto 125 million carriers for 3 optimized carrier and tPA concentration formulations [n=6]. (B) tPA loading efficiency for the 3 optimized carriers [n=6]. Additionally, potential receptors involved in tPA loading were assessed by (C) blocking the NMDA 1 receptor prior to the FITC-tPA loading procedure [n=18] or by (D) assessing the detection of the GPIIb receptor subunit (CD41a) on platelets after tPA (Alteplase) loading [n≥8].

In order to assess and optimize the loading procedure, the loading efficiency and the amount of tPA loaded onto three optimized system formulations were measured using FITC-conjugated tPA. This loading efficiency was determined for systems loaded with various incubation times, carrier concentrations, and tPA concentrations to determine the optimal loading procedure. Our goal was to produce fibrinolytic Decoys and LPs with similar loading to enable direct comparison of the two systems in subsequent experiments. Similar loading (~ 2 ug of tPA per 125e6 platelets) was achieved by using double the concentration of tPA with Decoys compared to LPs (Fig. 11A). Indeed, the loading efficiency was greater for the LPs: 38.3 ± 7.0% versus 21.7 ± 3.2% for platelet Decoys (Fig. 11B, P=0.0005).

The next step was to identify the involved receptor(s) to better characterize this loading process. The NMDA receptor was selected as the first potential candidate interacting with tPA because tPA is known to interact with NMDA receptors in neurons (Lesept et al., 2016), and this receptor is significantly expressed on platelets (Hearn et al., 2022). However, when the LPs were incubated with an anti-NMDA 1 antibody and then loaded with tPA, there was no decrease in the tPA loading when compared with LPs treated with a non-specific antibody control or those without any treatment prior to the loading procedure. (Fig. 11C). As such, blocking the NMDA receptors did not affect tPA loading. However, prior research has shown that the GPIIb/IIIa receptor is involved with the binding of plasminogen to the surface of platelets (Miles and Plow, 1985; Vaughan et al., 1989). Furthermore, plasminogen and tPA can share common binding sites on nucleated cells (Félez et al., 1996). Therefore, the GPIIb/IIIa receptor was investigated as a possible binding site for tPA on platelets. Thus, the involvement of the GPIIb/IIIa receptor was

characterized by determining the availability of the GPIIb subunit (CD41a) before and after tPA loading onto the LP carriers. The availability of the GPIIb/IIIa receptor on LPs loaded with tPA was significantly decreased compared to the availability for unloaded LPs (Fig. 11D, P=0.0002). Moreover, when LPs were incubated with bovine serum albumin, a protein similar in size to tPA that does not bind to GPIIb/IIIa, there was no corresponding decrease in GPIIb availability (Fig. 11D, P = 0.8495). This indicates that the tPA molecules are interacting with the GPIIb receptor subunit, resulting in the decreased availability after loading.

4.3.2. Assessment of Fibrinolytic Activity for tPA-Loaded Systems

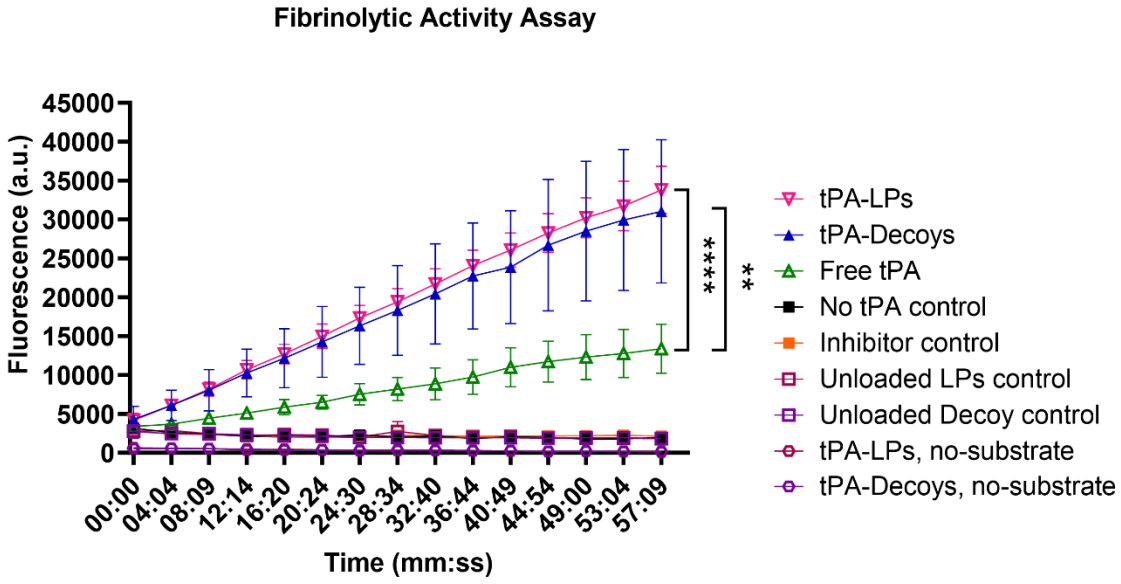

Figure 12: *Fibrinolytic Activity Assay for Fibrinolytic Platelets compared to Free tPA.* Measurements of fluorescence generated over time by the lysis of the tPA substrate in the Anaspec assay. Comparing the rate of fluorescence increase for the different samples allows for the assessment of the fibrinolytic activity. Free tPA, tPA-LPs, and tPA-Decoys were compared to free Alteplase, all at a tPA concentration of 0.4 ug/mL.

The data obtained using the fibrinolytic activity assay indicate that the Alteplase-loaded Decoys and LPs are highly fibrinolytic. All Alteplase experimental conditions demonstrate increasing fluorescence over time, consistent with active fibrinolysis (Fig. 12). However, the Alteplase-loaded LPs and Alteplase-loaded Decoys have similar fibrinolytic activity that are significantly higher than the activity of free Alteplase at the same concentration (Fig. 12, $P<0.0001$, $P=0.001$). Moreover, the unloaded carriers have no change in fluorescence, indicating a lack of fibrinolytic activity.

4.3.3. Evaluation of Fibrinolytic Platelet Interactions with Cancer Cells *in vitro*

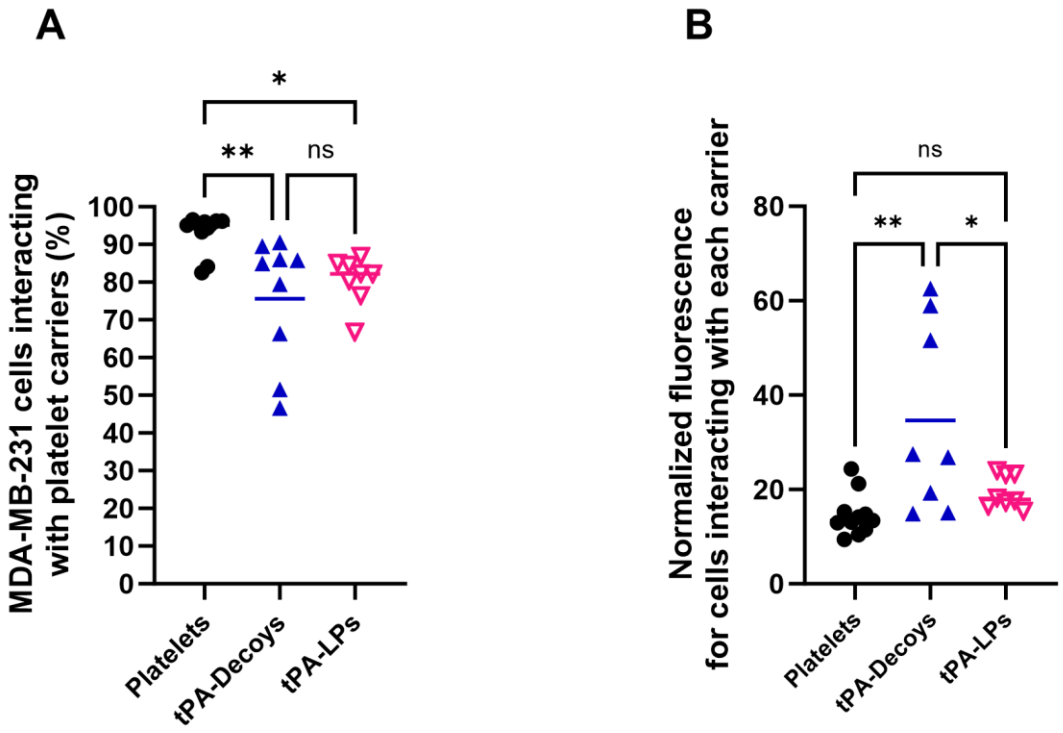

Figure 13: *Flow Cytometry Analysis of Cancer Cell Interactions with Fibrinolytic Platelet Systems.* Measure of the interactions between human MDA-MB-231 breast cancer cells and fluorescently labelled platelets, tPA-LPs or tPA-Decoys. (A) Percentage of MDA-MB-231 cells interacting with platelets or fibrinolytic platelets. (B) Median fluorescence of MDA-MB-231 interacting with each carrier type or control normalized for each carrier [n=9].

After assessing the fibrinolytic activity of the Alteplase-loaded systems, their ability to interact with MDA-MB231 breast cancer cells was assessed *in vitro*. When incubated with platelets, 93.2% of the MDA-MB-231 cells interacted with platelets in control experiments (Fig. 13A). A slightly lower interaction was observed with the fibrinolytic systems, with an average of 75.7% and 80.6% of the MDA-MB-231 cells interacting with tPA-Decoys and tPA-LPs, respectively (Fig. 13A). Although these are statistically significant decreases from the percentage of breast cancer cells interacting with

untreated platelets (P=0.003, and P=0.04), a large majority of cancer cells were successfully targeted by the modified platelet systems. Additionally, the median fluorescence of the cancer cells interacting with the modified platelet systems was equal to or greater than the fluorescence of the cells interacting with platelets after normalizing for the median fluorescence of each modified platelet. The average normalized fluorescence of the cells incubated with tPA-Decoys (34.6) was significantly higher than those incubated with platelets (14.6) (Fig. 13B, P=0.0024). Furthermore, the normalized fluorescence of the cells incubated with tPA-loaded LPs was very similar with 19.6 (Fig. 13B).

4.3.4 Effect of Fibrinolytic Platelets on Angiogenesis

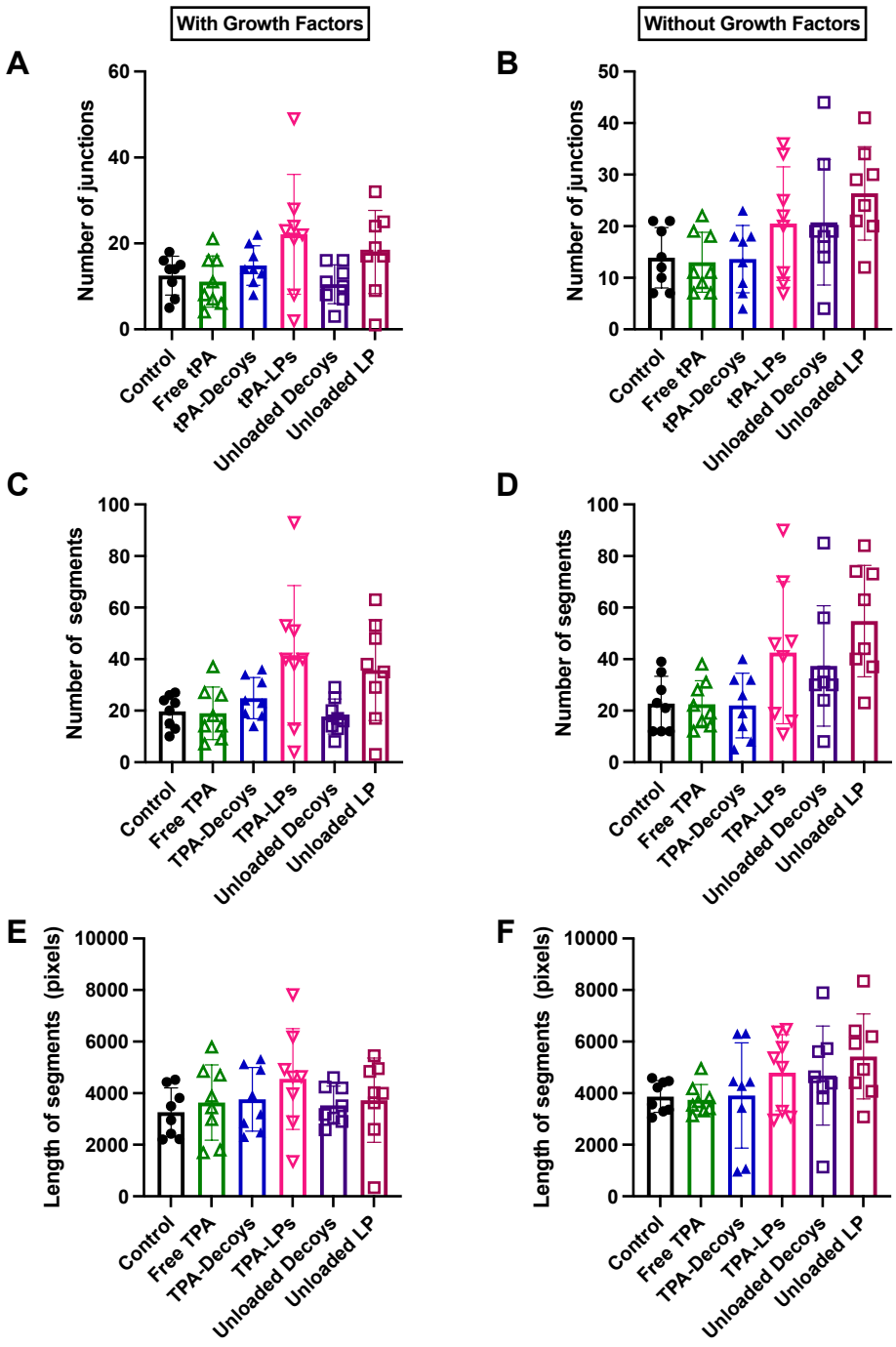

Figure 14: *Effect of the Fibrinolytic Platelet Systems on Angiogenesis Determined using a HUVEC Tube Formation Assay*. (A, B) The junction formation, (C, D) segment formation and (E,F) segment length after 12 hrs with various fibrinolytic platelet and control treatments was measured in the presence of (A, C, E) growth factors and (B, D, F) without growth factors [n=8]. For all samples with free tPA, tPA-Decoys, or tPA-LPs, a final concentration of 0.1 ug/mL Alteplase was used.

For free tPA, tPA Decoys, and unloaded Decoys, there was no significant angiogenic or anti-angiogenic effect on the HUVEC tube junction formation after a 12-hour incubation in growth factor enriched media (Fig. 14A). The number of junctions formed remained consistent between the untreated control and each tested condition, including the free tPA and both fibrinolytic platelet systems. Likewise, there is no significant effect for junction formation after incubation with growth factor deprived media for these groups (Fig. 14B**)**. This was corroborated with both the analyses of the number of segments formed, as well as segment length, with each treatment condition in growth factor enriched or deprived medium (Fig. 14C-F). Although there was also no significant effect with the tPA-LPs and the LPs. However, there was a consistent pro-angiogenic trend. This trend is visible with growth factor treated cells (Fig. 14A,C,E) and more prominent in the growth factor deprived cells (Fig. 14B,D,F).

4.3.5. *In vitro* Dissociation of Tumor Cell Clusters

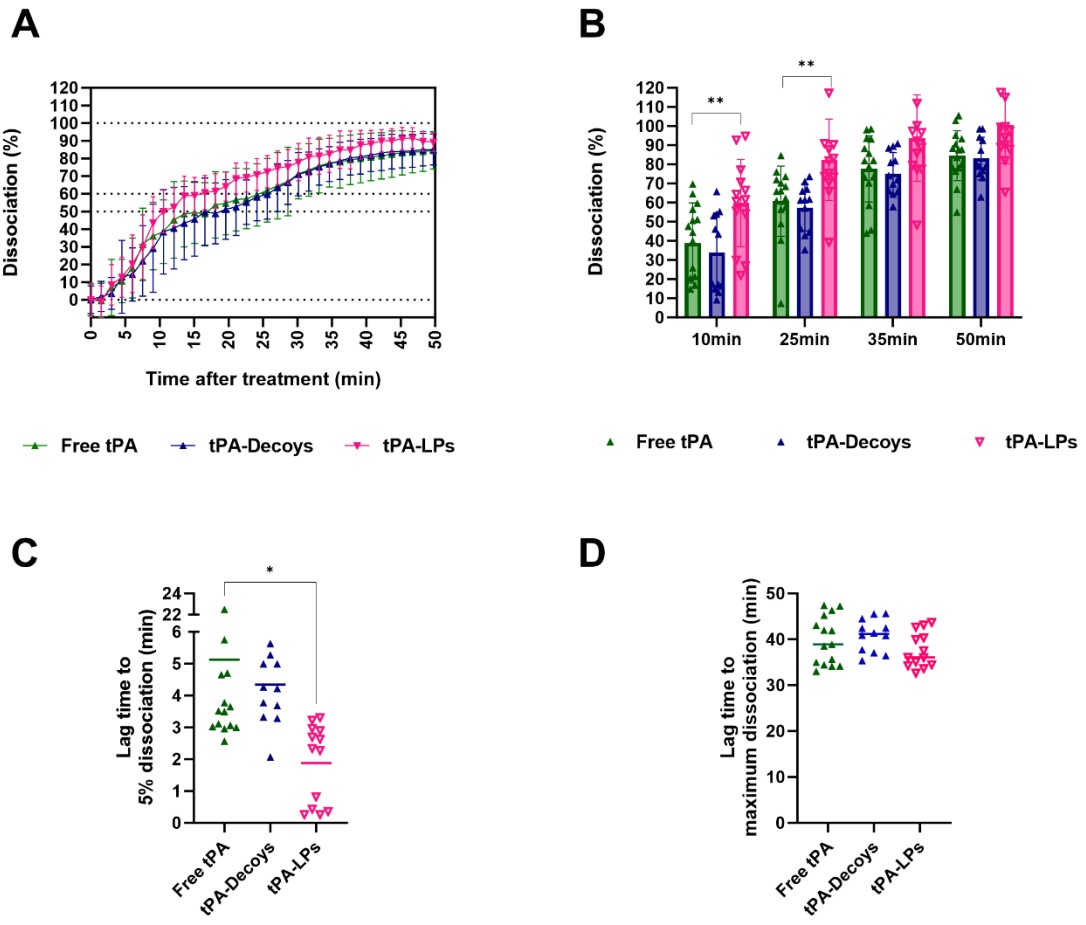

Figure 15: *Characterization of Cancer Cell Disassociation Curves obtained by Light Transmission Aggregometry after Fibrinolytic Platelet Treatment.* MDA-MB-231 cancer cells were allowed to cluster with fibrin and then were treated with either free tPA [n=15], tPA-Decoys [n=12], or tPA-LPs [n=13], all at a concentration of 0.5 ug/mL tPA. (A) Average cancer cell dissociation percentage over time. (B) Cancer cell dissociation at 10 min, 25 min, 35 min, and 50 min after addition of fibrinolytic agent. (C) Lag time between the addition of fibrinolytic agent and the start of cancer cell dissociation as determined by a 5% cancer cell dissociation. (D) Time to maximum recorded dissociation following the addition of fibrinolytic platelets.

Before moving to an *in vivo* mouse model, it was necessary to assess the effectiveness of the fibrinolytic platelet systems for dissociating tumor cell clusters *in vitro*.

As such, the data obtained using the light transmission aggregometry method described above (section 4.2.9) was characterized to determine the dissociation curve, dissociation at specific time points, lag time, and time to maximum recorded dissociation. All tPA conditions successfully dissociate tumor cell clusters over time (Fig. 15A). However, there was a significant difference between the tPA-LPs and the free tPA at 10 min, and 25 min, though the difference decreases as the time increases (Fig. 15B, P=0.0083, P=0.0058). This was supported by the significant difference in lag time between the tPA-loaded LPs and the free tPA treated samples (Fig. 15C, P=0.0292). A similar trend in the lag time was observed with the tPA-loaded Decoys, but this difference was not statistically significant.

4.3.6. Effect of Fibrinolytic Platelets in an Experimental Metastatic Model of Breast Cancer Cell Clusters

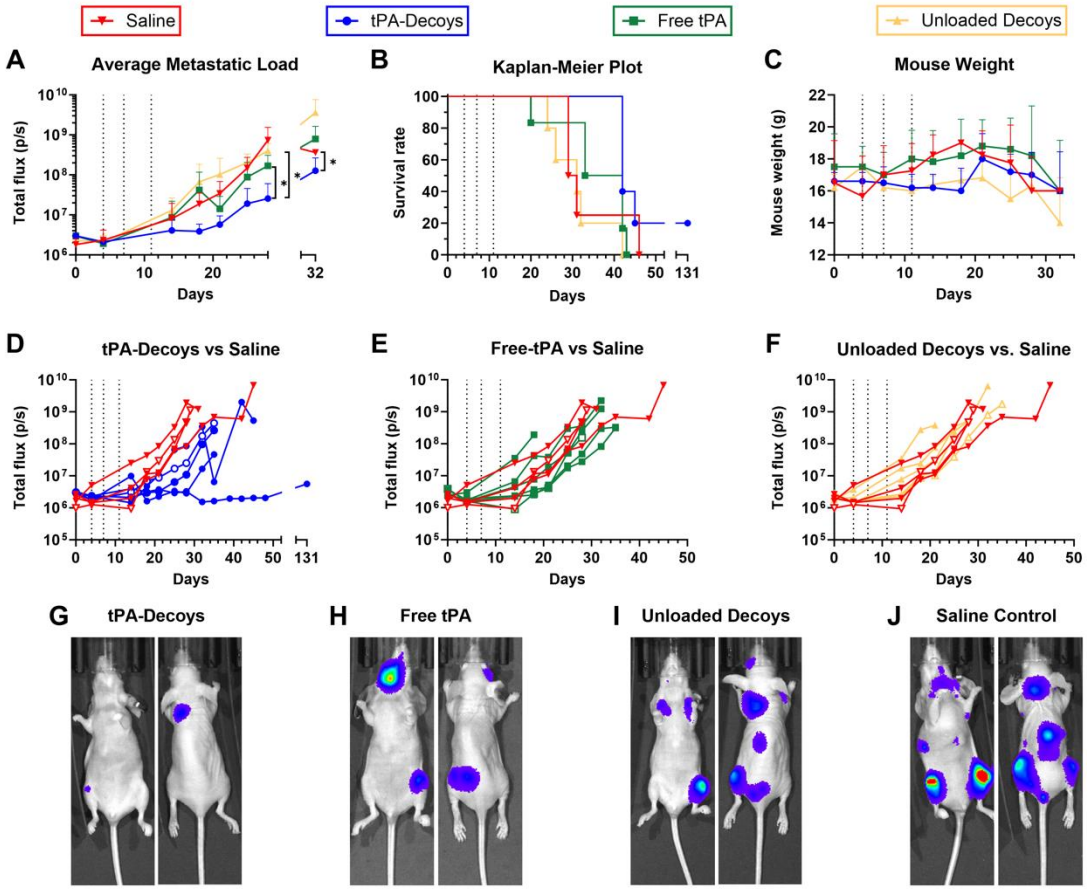

Figure 16: *In Vivo Assessment of Fibrinolytic Platelets Efficiency in Reducing Metastatic Dissemination.* BALB/c mice were injected with 50,000 clustered MDA-MB-231-Luc-D3H2LN and the metastatic load after treatment (saline control: n= 4, tPA-Decoys: n=5, free-tPA: n=6, unloaded-Decoys: n=5) at 0, 4, 7, and 11 days post injection was assessed: (A) total flux determined with the IVIS up to 32 days after the cancer cell cluster injection. Dotted lines are included on each graph to mark the fibrinolytic injection days and significance are shown between groups for the LOCF 2-way ANOVA analysis. (B) Mouse survival and (C) mouse weight over time. During analysis the total metastatic loaded was compared between (D) tPA-Decoys vs. saline, (E) free-tPA vs. saline, and (F) unloaded Decoys vs. saline. Representative IVIS images of the metastatic load at day 28 are also included for mice treated with (G) tPA-Decoys, (H) free-tPA, (I) unloaded Decoys, (J) saline control. (D-F) The total flux curves of mice selected for representative images (G) to (J) are displayed with void symbols.

Finally, the effectiveness of the fibrinolytic platelet Decoys in reducing cancer metastasis was assessed *in vivo*. The mice were injected with clustered tumor cells as described in section 4.2.10, and treated with either tPA-Decoys, free tPA, or unloaded Decoys. The resulting images were analyzed to determine the total flux as a measure of the metastatic load. The data demonstrates a trend for decreased metastatic load for the tPA Decoys compared to all other groups through day 32 (Fig. 16A). A 2-way ANOVA analysis with Last Observation Carried Forward (LOCF) for comparisons withing all groups and withing time points (uncorrected Fisher's LSD) not only highlighted a significantly lower metastatic load for the tPA Decoys compared to the saline-treated control group at day 32 (Fig. 16A, $P = 0.0478$), but also compared to the free tPA and unloaded Decoy groups at day 28 (Fig. 16A**,** $P = 0.0346$ vs. free tPA and $P = 0.0126$ vs. unloaded Decoys). The LOCF method chosen due to its use in clinical trial data and the tendency to conservatively underestimate differences in data(Shao and Zhong, 2003; Jakobsen et al., 2017; van Buuren, 2018). Indeed, the LOCF analysis assumes that the tumor load of the control mice would not increase over time for the imputed data points, despite the previous trend showing increasing flux. As such, it conservatively underestimates differences between treatment and control groups.

In addition, there was no statistical difference between the free tPA, the unloaded Decoys and the saline control group (Fig. 16A, D-F). Interestingly, the tPA-Decoys group is the only group showing significant decrease in initial metastatic dissemination following treatment at day 4 in comparison to day 1 ($P = 0.0022$). Free-tPA treated mice follow the same trend with a near missed significance ($P = 0.0566$), highlighting a clear effect of the fibrinolytic treatments on cancer cell clusters and resulting initial dissemination.

The Kaplan-Meier survival curves indicated a higher survival rate for mice treated with tPA-Decoys (42 days) compared to free tPA (37.5 days), unloaded Decoys (31 days) or saline (30 days) (Fig. 16B). The logrank test did not show significant differences in survival rate (P = 0.0656). However, the tPA-Decoy group included the only mouse to survive beyond the experimental endpoint (day 130) (Fig. 16B). Mouse weights were also collected over time; a 2-way ANOVA with Tukey's multiple comparisons test at each time point showed no significant differences among groups (Fig. 16C).

4.4. Discussion

CTC clusters are associated with poor prognosis in various malignancies including lung (Hou et al., 2012; Murlidhar et al., 2017), breast (Aceto et al., 2014; Jansson et al., 2016; Wang et al., 2017a), prostate (Brandt et al., 1996) and colorectal cancers (Zhang et al., 2017). Thus, it is critical to address this cancer cell population *via* therapeutic approaches, either to delay the metastatic dissemination, or to intercept CTC clusters during surgical tumor resection. The purpose of this study was to develop a fibrinolytic platelet-based therapeutic to target and dissociate CTC clusters and thus reduce metastasis.

To accomplish this, tPA was loaded onto two platelet-based carriers: platelet Decoys and fixed/lyophilized platelets, which are both successfully able to interact with cancer cells (Papa et al., 2019; Schnoor and Papa, 2022). The two systems have dissimilar surface makeup of receptors: for example, Decoys and LPs retain ~ 62% and 33% of GPIIb on their surface, respectively, compared to platelets (Papa et al., 2019; Schnoor and Papa, 2022). 15.8% of LPs display the active conformation of the GPIIb/IIIa receptor, enabling higher affinity for its ligands, while Decoys' GPIIb/IIIa are in resting conformation,

similarly to parent platelets (Papa et al., 2019; Schnoor and Papa, 2022). In contrast, Decoys retain only 20% of platelet GPIb, while LPs retain the majority of them (Papa et al., 2019; Schnoor and Papa, 2022). Our results demonstrate that double the amount of tPA was necessary to load the Decoys to the same level of the LPs, as confirmed by the loading efficiency data. In addition, we identified that tPA binds at, or near, the anti-CD41a binding site of the GPIIb integrin subunit on LPs, while it does not bind to the NMDA-1 receptor on LPs. These results confirm past observations regarding the involvement of GPIIb/IIIa in tPA binding to platelets (Vaughan et al., 1989).

After the tPA was successfully loaded onto the systems, the activity of these fibrinolytic platelets was assessed. Both the tPA-Decoys and the tPA-LPs significantly increased fibrinolytic activity compared to free tPA (Fig. 12), suggesting that the platelet Decoys and the LPs act as a catalyst for tPA. This corresponds well with previous studies that demonstrate tPA displays a strong affinity for the platelet surface (Vaughan et al., 1989), while Miles and Plow suggested that platelets act as a catalyst of the fibrinolytic cascade due to the natural interaction of plasminogen with their surface (Miles and Plow, 1985). Thus, the platelet carriers not only preserve tPA activity, but improve the overall effectiveness of the system.

A key advantage of the platelet-based carriers over synthetic drug delivery systems is their natural bioaffinity for CTCs through receptor interactions (Morris et al., 2022). tPA loading on Decoys and LPs slightly, but significantly, decreased the fibrinolytic carrier interaction with cancer cells. However, over 75% of the MDA-MB-231 breast cancer cells were still decorated with fibrinolytic platelets for each carrier (Fig. 13). We demonstrated that tPA binds near or at the anti-CD41a binding site on platelet GPIIb. In addition, we

have shown in past studies that the interaction between Decoys and MDA-MB-231 is significantly, however not completely, compromised when Decoys' GPIIb/IIIa is blocked using a CD41a antibody prior to their interaction with cancer cells (Papa et al., 2019). These observations altogether further confirm that tPA interacts with GPIIb/IIIa integrin, which could explain the decrease in interactions between tPA-platelet carriers and cancer cells.

Further, the normalized fluorescence of cancer cells interacting with tPA-Decoys was significantly higher compared to fresh platelets (Fig. 13). Since the fluorescence was normalized based on the individual platelet or decoy, this data indicated that there are more tPA-Decoys interacting with each decorated cancer cell on average. The tPA-LP interacting cancer cells have a similar average normalized fluorescence, and thus a similar number of interacting platelets, compared to the cells interacting with fresh platelets. As such, both systems at least maintain significant interactions with the cancer cells, demonstrating that these fibrinolytic platelet systems can effectively interact with circulating tumor cells. It is also important to note that there is not a significant difference between the cell interactions with the tPA-LPs and with the tPA-Decoys (Fig. 13), despite the differences in surface receptor availability and activation (Papa et al., 2019; Schnoor and Papa, 2022). Due to the importance of the GPIIb/IIIa receptor in cancer cell-platelet interactions (Morris et al., 2022), the differences in receptor availability between the Decoys and LPs could have led to a disparity in cancer cell interactions. However, there are several additional platelet-cancer cell interactions to compensate for any decrease in one receptor availability or activation (Morris et al., 2022).

In our experimental setting, tPA loading did not saturate the GPIIb/IIIa receptors on LPs as a significant level of anti-CD41a was detected following the loading of LPs with tPA (Fig. 11D), thus leaving available GPIIb/IIIa receptors for interaction with cancer cells. In addition, the significantly greater loading efficiency (nearly double) of tPA on LPs, versus Decoys, could be correlated with the fact that 15.8% of LPs display active GPIIb/IIIa conformation (Schnoor and Papa, 2022), enabling significantly higher interaction with its ligands, such as tPA, compared to the resting conformation of the integrin. This would explain that even though LPs have less GPIIb/IIIs on their surface than Decoys (i.e. $GPIIb_{LPs} \sim 33\%$; $GPIIb_{Decoys} \sim 62\%$; $GPIIb_{Platelets} = 100\%$), they are still able to load more tPA because a significant fraction of the LP population is activated for ligand binding (Schnoor and Papa, 2022).

Given the systemic circulation of this system and the importance of angiogenesis in tumor development, the fibrinolytic platelets were investigated for potentially influencing angiogenesis. Indeed, tPA has been shown to have both anti-angiogenic effect in combination with captopril (Merchan et al., 2003) and pro-angiogenic effects by promoting VEGF and MMP-9 activity (Ismail et al., 2021). However, the fibrinolytic platelets did not have a significant effect on the formations of tubes in a HUVEC cell culture when measured for number of junctions, number of segments, or segment length (Fig. 14). As such, neither the tPA-Decoy nor the tPA-LP treatment had a significant pro-angiogenic or anti-angiogenic effect, and thus either fibrinolytic platelet system can be utilized without promoting angiogenesis in tumors.

When assessed *in vitro*, our fibrinolytic platelet systems both successfully dissociated tumor cell clusters with a lower lag time trend compared to free tPA (Fig. 15).

This corresponds well to the increased fibrinolytic activity for the fibrinolytic platelets compared to free tPA (Fig. 12). Though, the trend was only significant for the tPA-LPs compared to the free tPA (Fig. 15). The increase in effectiveness for the tPA-LPs could be related to the increased expression of surface receptors or the partial activation of the GPIIb/IIIa receptor on the LP carrier (Schnoor and Papa, 2022). Since the GPIIb/IIIa receptor has a higher affinity when activated and is known to interact with tumor cells (Morris et al., 2022), the partial activation could contribute to faster interaction with cancer cells. However, both of the fibrinolytic platelets do successfully disperse the tumor cell clusters, correlating well to the similar amount of tPA loaded (Fig. 11), the similar catalyzation of tPA activity (Fig. 12), and the similar interaction with cancer cells (Fig. 13) for both circulating tumor cells.

Moreover, only mice treated with tPA-decoys demonstrated a reduced tumor load compared to controls, indicating that the fibrinolytic Decoys are able to disperse the tumor cell clusters more effectively than the unloaded drug (Fig. 16). This conclusion correlates with the increased fibrinolytic activity for the fibrinolytic Decoys compared to the free drug (Fig. 12) and with the interaction of tPA-Decoys with tumor cells *in vitro* (Fig. 13). This analysis is also supported by the initial decrease in metastatic load after tPA-Decoy treatment on day 4 compared to day 1, and the increased survival over time for tPA-Decoy treated mice (Fig. 16A,B). Of note, the tPA-Decoys were chosen as the fibrinolytic platelet system because the tPA-LPs quickly induced sudden animal death in our model shortly after injection. Sudden animal death in this fashion was only observed with tPA-LPs precluding further assessment in the setting of acute toxicity. The fatal adverse event could be due to the hemostatic nature of the LPs (Fitzpatrick et al., 2013) which in a pro-coagulant

cancerous microenvironment could catalyze acute thrombosis. Interestingly, no decrease in tumor load was observed for the unloaded Decoys, even though prior work has shown that platelet Decoys have an inhibitory effect on metastasis for individual tumor cells (Papa et al., 2019). However, the animal model selected here was for appropriate assessment of cancer metastasis associated with clustering of cancer cells rather than individual tumor cells. This highlights that while platelet decoys have an inhibitory effect on individual cells, that by themselves, they are unable to dissociate cancer cell clusters which are already known as a major metastatic driver. The effectiveness of the tPA-Decoy system was further reinforced by the ANOVA analysis with LOCF imputation method, which demonstrated a significant decrease in metastatic load of tPA-Decoy treated mice compared to the saline control group (Fig. 16). With the context of the increased survival and trend for lower metastatic load for the tPA-decoy treated mice, the data indicates that the fibrinolytic platelets are able to reduce cancer cell metastasis and tumor progression.

4.5. Conclusion

In this study, we have successfully developed a fibrinolytic platelet system by loading tPA onto a platelet Decoy and LP carrier system. These systems have increased fibrinolytic activity compared to free tPA, are able to interact with cancer cells, and can disperse tumor cell clusters *in vitro*. Analyzing the *in vivo* metastatic load and survival data in combination with the *in vitro* assessment indicates that the tPA-Decoys can effectively target and disperse tumor cell clusters, leading to reduced cancer cell metastasis and tumor progression. This data demonstrates the viability of this fibrinolytic platelet approach to target circulating tumor cell clusters. This approach could lead to improved patient

outcomes by delaying the progression of the disease and allowing an increased period for effective treatment. Additionally, these fibrinolytic platelets would prevent more serious complications through the targeted delivery of the agent. Further expansion of this approach could be used to target the delivery of tPA for other applications such of pulmonary embolism or stroke. Moreover, this system could be expanded to incorporate additional treatment modalities to further reduce cancer cell metastasis and improve patient outcomes.

Chapter 5: Development and *in vitro* Assessment of Fibrinolytic Platelet Carriers for Thrombosis

After developing our fibrinolytic platelet system for the reduction of cancer metastasis, we expanded the utility of this system by leveraging the modified decoy platelet carrier approach for other critical medical challenges such as thrombosis. One of the primary uses for fibrinolytic agents is the treatment of stroke or acute pulmonary embolisms (PE). Tissue plasminogen activator (tPA) is the first line treatment regimen in the context of stroke and is recommended for high-risk patients with massive PEs. However, tPA significantly increases the risk of hemorrhage, presenting a life-threatening complication and limiting the use of the agent. Activated platelet decoys though have the receptors necessary to interact with thrombi, allowing for their targeting. This represents a significant modification from previous decoy formulations which did not have active GPIIb/IIIa receptors and did not adhere to collagen. When activated, these receptors have a high affinity for platelets adhered onto thrombogenic surfaces, allowing the modified platelet decoys to adhere to the thrombi and more efficiently deliver the fibrinolytic agent. Moreover, the platelet decoys have a catalytic effect on fibrinolysis which, when combined with the increased targeting efficiency, can result in more rapid and effective fibrinolysis of the thrombi. As such, we have expanded upon our prior work by modifying our procedure to produce partially activated platelet decoys. These partially activated decoys (aDecoys) were then characterized to determine their activation, the availability of critical receptors, and their tPA loading. Subsequently, the ability of these aDecoys to adhere to a thrombogenic surface of collagen-adhered platelets was assessed *in vitro* using a microfluidic channel. These results demonstrate of the tPA-aDecoy system to firmly adhere

to a thrombogenic surface, delivering a targeted dose of tPA, and to more efficiently lyse fibrin *in vitro*. Thus, the tPA-aDecoys represent a promising new approach to address the challenge of pulmonary embolisms, and they illustrate the viability of the modified platelet decoys for a variety of drug delivery applications when modified for a specific application.

5.1 Introduction

Acute massive pulmonary embolisms (PEs) present a significant medical challenge with an in-hospital mortality rate of 22% (O'Malley et al., 2020), which has not significantly improved over the last 20 years (Kasper et al., 1997). Moreover, the large majority of PE related fatalities occur within the first 2 hours after presentation of symptoms (Bělohlávek et al., 2013), indicating the importance of rapid treatment options. The current recommended treatment for patients with acute, massive PE is the administration of fibrinolytics such as tissue plasminogen activator (tPA) (Stevens et al., 2021). However, this treatment regimen significantly increases the risk of life-threatening hemorrhage, and is thus not recommended to less critical patients (Stevens et al., 2021). As such, there is a critical need to develop a system that can rapidly deliver a fibrinolytic agent to the site of a pulmonary embolism while limiting the off-target side effects. By increasing the effective dose and limiting the risk of complications such as hemorrhage (Stewart and Kline, 2020), this new strategy could potentially increase the population of patients eligible for tPA-based fibrinolysis.

To address this challenge, we have developed partially activated platelet decoys (aDecoys) capable of delivering tPA to the thrombi. Pulmonary embolisms primarily result from thrombi that migrate to the lungs, causing an obstruction. These embolisms are thus

composed mainly of platelets and fibrin. Our prior work developing fibrinolytic platelet decoys presented a promising approach to this challenge, since tPA can be effectively loaded onto the platelet-decoy carriers (Fig. 11) without loss of tPA activity (Fig. 12). In fact, these platelet decoys act as a catalyst, increasing tPA activity (Fig. 12). This results in more rapid thrombolysis, which is critical in the treatment of acute pulmonary embolism. However, these previously developed platelet decoys were not suitable for this application since they lack the ability to directly target thrombi. Although the platelet decoys developed previously maintain some of the GPIIb/IIIa receptors, these receptors are not in the active conformation required for platelet arrest (Papa et al., 2019). Therefore, the procedure was modified to generate partially activated platelet decoys (aDecoys) *via* an ADP-based activation method during the production of the decoys. Activated GPIIb/IIIa receptors have a much higher affinity for thrombogenic surfaces leading to increased platelets arrest and interaction with thrombi (Michelson, 2013). Utilizing this new procedure, we produced and characterized aDecoys capable of adhering to a thrombogenic surface *in vitro*. Furthermore, aDecoys are capable of delivering tPA to disperse fibrin and platelet thrombi.

The tPA-aDecoy approach offers a method to improve the treatment for PEs by targeting the thrombi and catalyzing the fibrinolytic interaction, improving the efficiency and effectiveness of the tPA treatment. This presents the possibility of improving outcomes for high-risk patients while limiting the risk of hemorrhage. Moreover, increasing the targeting and efficacy of tPA at lower dosages could increase the applicability of the treatment for lower risk patients who currently not eligible due to the considerable risk of hemorrhage at effective dosages of the free drug. Both of these developments could

represent a considerable advancement in the treatment of pulmonary embolism, potentially resulting in lower mortality rates. Furthermore, the tPA-aDecoy approach demonstrates the viability of the platelet decoys for a variety of drug delivery applications.

5.2 Materials and Methods

5.2.1 Materials

The human whole blood was purchased from BioIVT, following approval from the Institutional Biosafety Committee at the George Washington University, and drawn with 3.8% sodium citrate. Commercial blood was collected as late as possible in the day and shipped overnight before being processed in our experiments. The untreated platelets were obtained in platelet rich plasma (PRP) *via* centrifugation at 150 g from the whole blood from healthy donors. Platelet poor plasma (PPP) was obtained *via* centrifugation of the remaining blood fraction after the PRP had been removed. If more PPP was required than could be obtained with this method, addition PPP was produced by centrifuging a portion of PRP at 2,000 g.

The adenosine diphosphate (ADP) utilized for platelet activation was obtained from Chrono Log (cat# 384). The dye-conjugated antibodies were purchased from BD Biosciences: APC mouse anti-human CD41a (cat# 559777), APC mouse IgG, κ isotype control (cat# 555751), FITC mouse anti-human PAC-1 (cat# 340507), FITC mouse IgM, κ isotype control (cat# 551448), Alexa Fluor 647-conjugated fibrinogen was obtained from Thermo-Fisher Scientific (cat# F35200). Calcein AM was purchased from ThermoFisher (cat# C3099). The fibrillar collagen was purchased from Chrono-Log (cat# 385) and the microfluidic glass bottom channels were obtained from Ibidi (cat# 80167).

Sodium chloride (cat# S7653), magnesium chloride (cat# M8266), sucrose (cat# S7903), HEPES (cat# H3537), potassium chloride (cat# P9333), and glucose (cat # D9434) were obtained from Sigma-Aldrich. Sodium citrate (cat# 7228-16) was obtained from Ricca Chemical. Triton X-100 solution (CAS# 9002-93-1) was purchased from ACROS Organics and the protease inhibitor cocktail tablets (cat# 04 693 116 001) were purchased from Roche. Alprostadil (PGE-1) (cat# 1620) was obtained from Tocris. CellMask™ plasma membrane stains (cat# C10046) was procured from Invitrogen. The tPA inhibitor Leupeptin (cat# AS-72160, component E) was obtained from Anaspec, and collagenase (cat# 17018-029) was obtained from Gibco.

Finally, the tissue plasminogen activator conjugated with fluorescein isothiocyanate (tPA-FITC) was obtained from Cell Sciences (cat# CRT172B). The clinical grade tissue plasminogen activator, Alteplase, was procured *via* a material transfer agreement with Genentech.

5.2.2 Partially Activated Decoy Formation

The aDecoys were produced using a modified version of the method described in "Decoy Platelet Preparation" (4.2.3) above. In short, Alprostadil (PGE_1) was added at 50 ng/mL in platelet rich plasma (PRP) obtained by centrifugation at 290 g for 20 min with no braking deceleration. After 15 min, the PRP was then centrifuged at 1,000 g to pellet the platelets. The platelets were then resuspended in 2 mL of platelet poor plasma (PPP) without any additional PGE-1. The sample was then recalcified to a final concentration of 1 mM $CaCl_2$. Then ADP was added at a final concentration of 20 uM before inverting the tubes twice to gently mix the sample. The platelets were incubated with the ADP for 10

min to allow for partial platelet activation. Then 80 uL of 250x concentration of complete protease inhibitor was added to the sample and incubated for 30 min after gently inverting again twice. Next, 2.5 mL of extraction buffer (0.01 M HEPES, 0.05 M NaCl, 2.5 mM $MgCl_2$, and 0.3 M sucrose) was added along with 0.5 mL of 1% Triton X-100. The sample was gently mixed by inversion twice and then centrifuged at 1,000 g for 10 min. The aDecoys were then washed by resuspending in the decoy wash buffer (140 mM NaCl, 5 mM KCl, 12 mM sodium citrate, and 10 mM glucose) and centrifuging twice more. After the second wash, the aDecoys were resuspended in Tyrode buffer.

After the aDecoys were prepared, flow cytometry was used to confirm the expression of activated GPIIb/IIIa receptors on the surface of the system. The aDecoys at a concentration of 10,000 aDecoys/uL (10 uL total volume) were incubated with a mouse anti-human FITC-PAC-1 antibody (12.5 ug/mL) specific to the activated GPIIb/IIIa receptor in Tyrode buffer for 20 min. The aDecoy samples were then analyzed using the Novocyte flow cytometer with excitation by the 488 nm laser and the FITC detection filter. A FITC-conjugated IgM isotype was used as a control.

5.2.3 tPA Loading and Characterization of tPA-aDecoys

The tPA was loaded onto the aDecoys using the same procedure described in under "tPA Loading on Platelet Carriers" (section 4.2.4). In brief, the aDecoys were resuspended in Tyrode at concentration of 250,000 aDecoys/uL in 1500 uL total volume. Then the sample was incubated with 20 ug/mL tPA at 4 °C for 1 h under mixing using an orbital shaker. The tPA-aDecoy suspension was then centrifuged at 15,000 g for 1 h at 4 °C to pellet the decoys. For the assessment of the tPA loading and loading efficiency, a FITC-

conjugated tPA was used. The fluorescence of each sample was measured using a Spectramax ID5 and compared against a standard curve of known tPA concentrations to determine the amount of the fibrinolytic agent loaded onto the decoys and the efficiency of the loading procedure. The fluorescence was measured at an excitation of 488 nm and an emission of 528/45 nm. Alteplase, a clinical grade tPA, was used in all other experiments.

5.2.4 Determining of Receptor Availability for aDecoys and tPA-aDecoys

Flow cytometry was utilized to determine the availability of the GPIIb/IIIa receptor in both inactive and activated conformations on the tPA-aDecoys. After loading the aDecoys *via* the procedure described above (section 5.2.3), the tPA-aDecoys at a concentration of 10,000 aDecoys/uL (10 uL total volume) were incubated with a mouse anti human APC-CD41a antibody (2.5 ug/mL) specific to the GPIIb/IIIa receptor and a mouse anti human FITC-PAC-1 (12.5 ug/mL) specific to the activated conformation GPIIb/IIIa receptor for 20 min. The fluorescence of the stained tPA-aDecoys was then determined using flow cytometry with a 488 nm and 640 nm excitation laser with appropriate filters for each fluorophore to determine the percent of tPA-aDecoys expressing each receptor. For comparison, this same analysis was conducted on unloaded tPA-aDecoys and on unaltered platelets.

5.2.5 Assessing the Ability of Activated Platelet Decoys to Adhere onto Platelets Immobilized on Collagen under Flow

In order to assess the ability of the aDecoys to adhere to a thrombogenic surface, the microfluidic channels were first prepared by adding 0.1 mg/mL Type 1 fibrillar collagen in PBS and incubating for 1 hour to allow the collagen to adhere. Then, 2 mL of human whole blood with 3.8% sodium citrate was perfused through the channel at a rate of 1,800 µL/min. These conditions will achieve a shear stress of approximately 6.2 dynes/cm^2 which is within typical range for veinous blood flow (Papaioannou and Stefanadis, 2005). The channel was then rinsed by perfusing 2 mL of PBS solution through the microfluidic chip. The coating of the channel surface with platelets and collagen was confirmed *via* phase microscopy.

While the channel is being prepared, samples of tPA-aDecoys, unloaded aDecoys, and Decoys (Decoys control prepared without activation) were formulated. The fibrinolytic agent for the tPA-aDecoys were prepared using the method described above under "tPA Loading and Characterization of tPA-aDecoys" (section 5.2.3). The tPA-aDecoys, as well as the unloaded aDecoys and the un-activated Decoys, were then stained using the CellMask™ deep red membrane stain, which was added at a 1,000x total dilution from the manufacturer stock. Each sample was incubated for 1 hour at 37 °C before being centrifuged at 15,000 g for 1 h to remove the excess dye and then washed by resuspending in 500 uL of Tyrode and centrifuging again under the same conditions. After resuspending the tPA-aDecoys, unloaded aDecoys, and Decoys respectively in Tyrode buffer, each sample was added at a concentration of 200,000 carriers/uL to a 1 mL sample of human whole blood with 3.8% sodium citrate. Additionally, for the samples with tPA-aDecoys, a

Leupeptin, a tPA-inhibitor, was added at a concentration of 0.1 mM to prevent the system from disrupting the thrombogenic surface. Each suspension was then perfused through a prepared microfluidic channel 3 times in the same direction at a rate of 1,800 µL/min. Then the channel was rinsed using 4 mL of PBS solution perfused at 1,800 uL/min to remove any of the carriers not firmly adhered to the thrombogenic surface.

After rinsing, the channel was incubated with 100 U/mL collagenase in Tyrode buffer for 1 hour at 37°C to break down the collagen layer and release the adhered tPA-aDecoys, aDecoys, and Decoys, respectively. Then each microfluidic chip was thoroughly rinsed with 250 µL of Tyrode buffer and the fluorescence of CellMask™ deep red stain in each collected sample was then measured (Ex/Em = 494 nm / 517 nm). This fluorescence was then compared against a standard curve created for each condition to determine the number of tPA-aDecoys, aDecoys, and Decoys that had adhered.

5.2.6 Assessing Effectiveness of Activated Fibrinolytic Platelet Decoys in Lysing Fibrin *in vitro*

The ability of the activated fibrinolytic system to lyse fibrin was then assessed *in vitro* utilizing a fluorescently conjugated fibrin layer. First Alexa Fluor 647 (AF647) conjugated fibrinogen at a concentration of 5 ug/mL was incubated in a 96 well plate for 45 min at a temperature of 37 °C to allow a layer of the protein to adhere. This incubation was done with 100 uL total in each well. Each well was then gently rinsed using 100 uL PBS solution. Subsequently thrombin was added at a concentration of 0.1 U/mL to convert the fibrinogen layer into fibrin. After 5 min of incubation each well was then rinsed again with 100 uL of PBS to remove any remaining thrombin and any non-adhered fibrin. Then

each well was treated with either tPA-aDecoys, unloaded a-Decoys, or free tPA in either a Tyrode solution or in whole blood. For the tPA-aDecoys and the free tPA conditions, the tPA was assessed at a concentration of 11.25 ug/mL and the same number of aDecoys was used for the unloaded and tPA loaded aDecoy conditions. Finally, controls without treatments were included: Tyrode control and whole blood. After 20 min of incubation, the supernatant was removed from the wells and the well were rinsed with 100uL of Tyrode to collect any remaining lysed fibrin. The fluorescence of the lysed fibrin for each sample was then measured using a Spectramax ID5 fluorescent plate reader with excitation at 635 nm and emission of 675 nm. These measurements were then normalized compared to the average fluorescence obtained from the control samples with no treatment in Tyrode and whole blood, respectively.

5.2.7 Statistical Analysis

All graphical representations and statistical analyses of the data were developed using the Prism software from GraphPad. For the tPA-loading characterization (section 5.3.1) an unpaired t-test analysis with Welch's correction was used to determine statistical significance, and for the receptor availability analysis (section 5.3.2), a paired t-test analysis was used. The significance between experimental groups for the adherence of the decoy systems (section 5.3.3) and the efficacy of the decoy systems in lysing fibrin *in vitro* (section 5.3.4) was determined using an analysis of variance (ANOVA) method with Tukey's correction was utilized. (*$P \leq 0.05$, **$P \leq 0.01$, ***$P \leq 0.001$, and ****$P \leq 0.0001$) for all analyses.

5.3 Results

5.3.1 Loading and Characterization of tPA-aDecoys

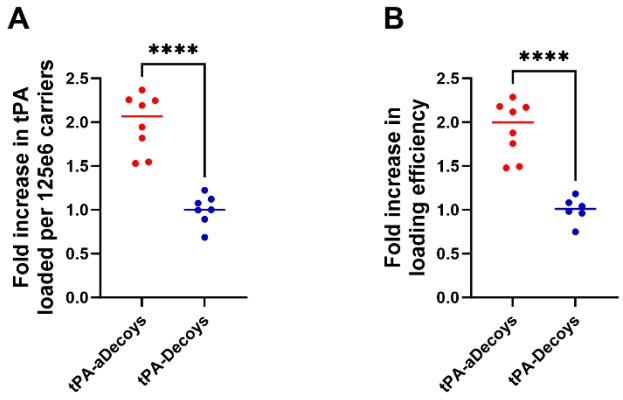

Figure 17: *Characterization of tPA-Loading on aDecoys compared to Decoys.* After loading FITC-conjugated tPA onto the aDecoys, the fluorescence of the tPA-loaded system was measured using a plate reader to determine (A) the amount of tPA loaded onto a sample of 125 million aDecoys normalized compared to decoys, and (B) the loading efficiency of the procedure for aDecoys normalized compared to decoys. [tPA-aDecoys: n=8, tPA-Decoys: (A) n=7 and (B) n= 7, 2 donors]

After the successful creation of the partially activated platelet decoys, the tPA-loading onto this aDecoy system needed to be assessed. An average of 4.17 ug of tPA was loaded per 125 million aDecoys (Fig. 17A). Considering that 10 ug of tPA was used in the procedure for each 125 million aDecoys, this results in an average loading efficiency of 41.7%. When compared to the loading characterization for the platelet decoys without activation, the tPA-aDecoys demonstrate significant increases in both the amount of tPA loaded onto the aDecoys (Fig. 17A, $P<0.0001$) and the tPA loading efficiency (Fig. 17B, $P<0.0001$). The tPA-aDecoys have an average of 1.99 times the amount of tPA loaded per 125 million aDecoys compared to the decoys prepared without activation (Fig. 17A). Similarly, the loading efficiency for the tPA-aDecoys is an average of 1.92 times greater than that of the non-activated decoys.

5.3.2 Receptor Availability for aDecoys and tPA-aDecoys

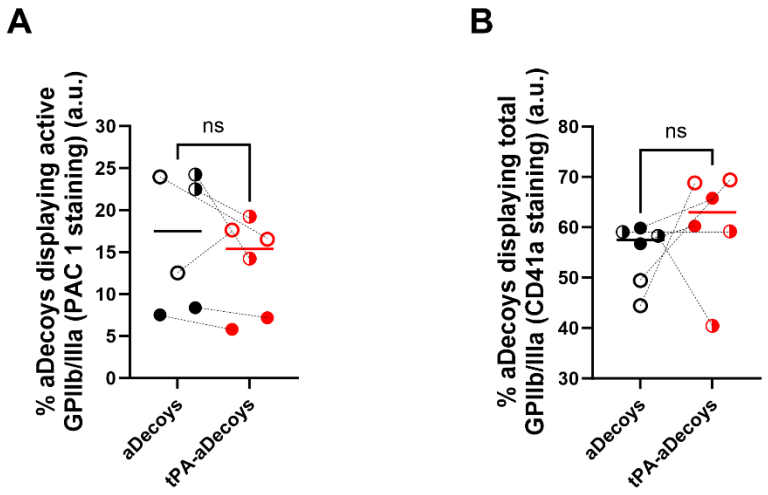

Figure 18: *Flow Cytometry Analysis for Receptors on aDecoys and tPA-aDecoys.* For aDecoy samples before and after tPA-loading, a flow cytometry analysis using fluorescent antibodies was conducted to determine the percentage of aDecoys displaying the GPIIb/IIIa receptor in (A) the active conformation using a PAC-1 antibody and (B) in any conformation using a CD41a antibody. Specimens of aDecoys and tPA-aDecoys produced from the same donor have the same symbol with either the filled circle, circle outline, or half-filled circle. [aDecoys: n=6, tPA-Decoys: n=6; 3 donors for all conditions]

In the previous chapter, GPIIb/IIIa was identified as the (or one of the) receptor(s) binding to tPA (Fig. 11D). Platelet GPIIb/IIIa is also a key receptor involved in both platelet aggregation and the consolidation of platelet adhesion on a thrombogenic surface. Both these processes are essential to platelet integrating with (targeting) a growing thrombus. Thus, it was essential to determine whether some GPIIb/IIIa receptors were still available for thrombus targeting following tPA loading on the activated Decoys. Using flow cytometry analysis, the percent of the aDecoy population displaying the active GPIIb/IIIa antibody before tPA loading was determined to be an average of 16.5% (Fig. 18A). After loading the aDecoys with tPA there was small decrease in the percentage

positive for active GPIIb/IIIa to an average of 13.4%; however, this decrease was not statistically significant (Fig. 18A, P=0.2112). Similarly, there is no significant difference in percentage of aDecoys positive for either resting or active GPIIb/IIIa receptors after tPA loading (Fig. 18B, P=0.3767), with the average being 54.6% for the unloaded aDecoys and 60.6% for the tPA-aDecoys (Fig. 18B).

5.3.3 Adhesion of tPA-aDecoys to Platelets Immobilized on Collagen under Flow

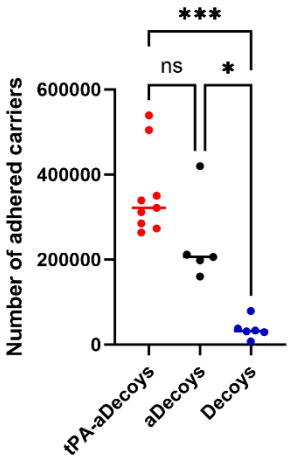

Figure 19: Preliminary data: *Adhesion of tPA-aDecoys, aDecoys, and Decoys to a Thrombogenic Surface under Flow.* For each platelet decoy carrier, the (A) number of carriers adhered to the surface was determined. [tPA-aDecoys: n=9, aDecoys: n=5, Decoys: n=6, 2 donors for each formulation]

For the system to successfully deliver the fibrinolytic to the thrombus or embolism, the aDecoys must be able to adhere to a thrombogenic surface. Thus, the ability of the system to adhere to a surface coated by platelets adhered onto collagen was assessed for the tPA-aDecoys and compared with the unloaded aDecoys, as well as the decoy formulation without activation. The tPA-aDecoys and the aDecoys both show significant

increases in carrier adherence compared with the decoy formulation (Fig. 19, P=0.0009 for tPA-aDecoys, P=0.0176 for aDecoys). With an average of 354,399 carriers adhered onto the thrombogenic surface, this would indicate an average effective delivery of 11.9 ng of tPA based on the average loading. In contrast only an average of 36,378 decoys prepared without activation were able to adhere to the platelet coated surface. When combined with the lower loading of non-activated decoys, this represents a significantly lower ability to deliver tPA to the thrombogenic surface. This data is preliminary as further controls will be added to account for non-specific staining.

5.3.4 Effectiveness of tPA-aDecoys in Lysing Fibrin *in vitro*

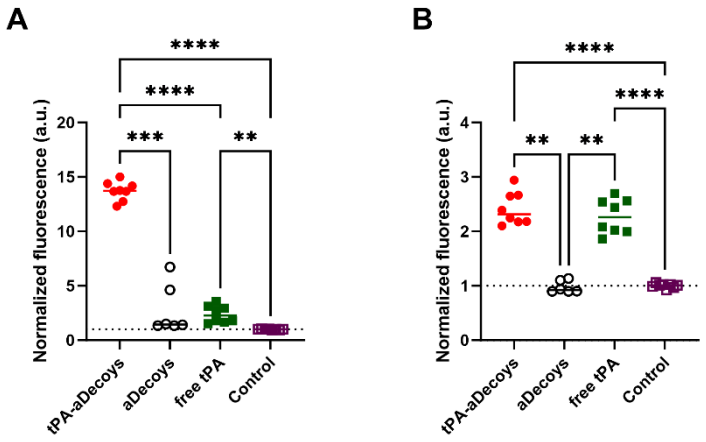

Figure 20: *Effectiveness of tPA-aDecoys in Lysing Adhered Fibrin in vitro.* The fluorescence of fibrin-AF647 released from an adhered layer after incubation with tPA-aDecoys, aDecoys, or free tPA in either (A) Tyrode or (B) whole blood was determined. The fluorescence is then normalized in comparison to the fluorescence released by the control without treatment [tPA-aDecoys: n=8, aDecoys: n=6, Free tPA: n=8, Control: n=8, 2 donors for all conditions]

The ability of the system to lyse fibrin is essential for the effective treatment of thrombotic conditions. As such, the efficacy of the system for lysing fibrin adhered in a

layer was assessed and compared against the same concentration of tPA in both Tyrode solution and whole blood. A non-treatment control and an unloaded aDecoy control were also assessed. When incubated in Tyrode, the free tPA was able to lyse a significant amount of fibrin with a 2.4-fold increase compared to the control (Fig. 20A, P=0.0067). The tPA-aDecoys were able to also significantly lyse the fibrin layer with a 13.7-fold increase in the measured fluorescence compared to the control (Fig. 20A, P<0.0001), which also represents a significant increase compared to the free tPA condition (Fig. 20A, P<0.0001).

Likewise, when incubated in whole blood, both the tPA-aDecoys and the free tPA are able to significantly lyse the fibrin layer with a 2.4-fold and 2.3-fold increase in fluorescence respectively (Fig. 20B, P<0.0001 for both). Although there is a small trend for increased fluorescence with the tPA-aDecoys compared to the free tPA, similar to that seen in the Tyrode conditions, this trend is not significant when the agents are incubated in whole blood (Fig. 20B, P=0.145).

For both the Tyrode and whole blood conditions, there is also no significant increase in fluorescence for the unloaded aDecoys compared to the control (Fig. 20A P=0.2775, Fig. 20B P=0.972).

5.4 Discussion

To address the challenges of treating thrombotic conditions such as PEs, we have developed a new activated decoy carrier approach for delivering tPA. Although, our previous work has shown the feasibility of a fibrinolytic platelet decoy system for reducing metastasis (Schnoor et al., in revisions), the decoys formulated for that application do not adhere to thrombogenic surfaces (Papa et al., 2019). In contrast, lyophilized platelets are

able to adhere to a collagen surface at much higher levels (Schnoor et al., in revisions) and have been used as hemostatic agents (Fitzpatrick et al., 2013; Cellphire Therapeutics, Inc., 2019, 2020, 2021). This difference in effect likely stems from the partial activation observed *via* flow cytometry with the lyophilized platelets (Valeri et al., 2004; Milford and Reade, 2016; Schnoor et al., in revisions). The activation of platelets, and the corresponding expression of activated GPIIb/IIIa receptors, is a key component of platelets ability to adhere to a thrombogenic surface and incorporate into growing thrombi (Hantgan et al., 1990; Khurana et al., 1997; Michelson, 2013). As such, it was critical to develop a decoy system that included a significant percentage of decoys with activated GPIIb/IIIa receptors. The success of this approach was demonstrated *via* the flow cytometry with PAC-1 antibodies (Fig. 18A).

The modification of decoys to include a population with activated GPIIb/IIIa also has significant effects on the loading of tPA. The aDecoys displayed significantly higher tPA loading and loading efficiency compared to the previously formulated decoys with approximately a 2-fold increase in both measures (Fig. 17). This improvement in the tPA loading for aDecoys is consistent with the data indicating that tPA binds to the GPIIb/IIIa receptor on platelets (Schnoor et al., in revisions). Given that the active conformation of GPIIb/IIIa has a higher binding affinity, the activated Decoys would logically have an increased ability to bind the tPA through these receptors. This increased tPA loading provides several key benefits, such as having less wasted tPA in the formulation process (i.e. a higher loading efficiency), and a higher amount of tPA delivered for each adhered carrier. Additionally, the same dose of tPA can be achieved with lower numbers of aDecoys compared to the decoys formulated previously. Moreover, the difference in tPA loading

introduces the opportunity to modulate the loading affinity of the carrier based on the application. For applications where a sustained lower dose would be ideal, such as for reducing cancer metastasis by dispersing fibrin bound CTC clusters, a lower tPA loading system can be selected. However, for an application such as the treatment of PE where an immediate high dose is optimal, then the higher loading affinity carrier can be chosen. With further characterization and refinement of the formulation procedure, the loading affinity may be tuned to the application.

With the successful tPA-loading onto the aDecoy carrier, it was essential to also characterize the receptor expression for GPIIb/IIIa in both active and inactive conformations. Since GPIIb/IIIa has been identified as a key receptor in platelet interactions with tPA (Schnoor et al., in revisions), there was possibility that the increased tPA loading for the aDecoys could lead to a decrease in accessible GPIIb/IIIa receptors. These receptors are also critical for the adhesion of the aDecoys on thrombogenic surfaces and the interaction of platelets with thrombi (Hantgan et al., 1990; Michelson, 2013). As such, the tPA-aDecoys must retain a significant population of aDecoys expressing the active conformation of GPIIb/IIIa in order to leverage the increased binding affinity. Indeed, despite the increased tPA-loading, there is no significant decrease in the percentage of the aDecoy population expressing activated GPIIb/IIIa receptors after tPA is loaded onto the carrier (Fig. 18A). Though, there is a slight decreasing trend after tPA-loading, which is consistent with the role of the GPIIb/IIIa receptor in tPA binding (Fig. 18A). Furthermore, there is no significant change in the percentage of decoys with expressed GPIIb/IIIa when analyzed for both conformations (Fig. 18B). Because the percentage of aDecoys expressing these key receptors is maintained, the loading of tPA does not inhibit

the utility of these receptors for interacting with thrombi.

The activated GPIIb/IIIa receptors can be leveraged for the aDecoys to adhere to thrombogenic surfaces. Active conformation GPIIb/IIIa receptors are able to interact with fibrinogen and von Willebrand factor with a high affinity, allowing activated platelets to adhere more firmly on a thrombogenic surface and interact with other platelets (Varga-Szabo et al., 2008). As such, the aDecoys can more effectively adhere to thrombotic surfaces such as collagen. This is supported by the dramatic increase in aDecoy adherence compared to the non-active decoy formulation. Though, it is important to note that these aDecoys are still inactive, and thus do not have the signaling pathways to undergo the full firm adhesion and consolidation that a native platelet would (Varga-Szabo et al., 2008; Michelson, 2013). Nonetheless, the aDecoys are still able to significantly adhere onto the surface even under physiological flow and shear stress conditions. The increased aDecoy adhesion allows for more effective local delivery of the tPA to the thrombosis, with an average of 11.9 ng of tPA delivered to the surface (Fig. 19). This adhesion of the aDecoys also has another benefit. Our previous work demonstrated that the platelet decoys can catalyze tPA activity (Schnoor et al., in revisions). Therefore, this aDecoy system both increases localization and persistence of the tPA at the thrombotic site and provides a catalytic surface to further enhance the effectiveness of the agent. Furthermore, the adherence of these tPA-aDecoys reduces the circulation of tPA to non-target areas, thus theoretically limiting the off-target side effects. Given the high risk of complications such as hemorrhage with fibrinolytics such as tPA (Stewart and Kline, 2020), there is a significant advantage to reducing the associated off-target adverse events.

The advantages of this aDecoy system are further reinforced with the ability of the

tPA loaded system to lyse fibrin *in vitro*. When examined in Tyrode, the tPA-aDecoys demonstrate a significantly increased effectiveness in lysing fibrin compared to the same concentration of free tPA (Fig. 20A). This correlates well to the prior data indicating that platelets can act as catalysts for fibrinolysis as they provide a surface for the colocalization of plasminogen and plasminogen activator (Miles and Plow, 1985). This increase in activity compared to the free tPA diminished when examined in whole blood (Fig. 20B). This effect is likely due to the addition of platelets, which have been shown to bind to both plasminogen activator and plasminogen, thus providing a catalytic surface for the fibrinolysis (Miles and Plow, 1985; Vaughan et al., 1989). For both the Tyrode and the whole blood conditions, the tPA-decoys were at least as effective as free tPA in lysing fibrin. Combined with the ability of the tPA-aDecoys to adhere to a platelet-coated thrombogenic surface (Fig. 19), this indicates that the tPA-aDecoys are able to deliver increased tPA amounts with at least as much fibrinolytic activity along with adhered carriers that can have a catalytic effect.

These results support the feasibility of these aDecoy carriers to efficiently load tPA and adhere to thrombotic surfaces *via* activated receptors in order to deliver tPA to thrombi to effectively lyse the fibrin network. Moreover, the development of these aDecoys demonstrate the potential of optimizing platelet decoys for a variety of applications. By modulating the activation of platelets during the decoy formulation procedure, the carriers were optimized to load tPA and adhere to thrombogenic surfaces. For other applications however, where longer circulation times or different biodistributions are preferred, the adherence of the aDecoys may be a hindrance and thus non-activated decoys may be preferred. Through modulating the formulation of platelet-decoys, such drug delivery

carriers could be fine-tuned and optimized for the specific application.

5.5 Conclusions

Through this project, we have successfully developed a partially activated fibrinolytic decoy platelet system for the lysis of thrombi. With this formulation there is a notable portion of the aDecoys expressing activated GPIIb/IIIa receptors, which is maintained after loading. These aDecoys have increased tPA-loading compared to non-activated decoys and are able to adhere to thrombogenic surfaces under flow conditions, allowing for increased delivery of tPA to the thrombotic area. Moreover, this tPA is at least as effective as free tPA in lysing fibrin at the same concentration. As such, these results demonstrate the feasibility of the aDecoy system to effectively deliver tPA to thrombi for the fibrinolytic treatment of embolisms and other thrombotic disorders. This approach could reduce the risk of hemorrhagic complications with fibrinolytic treatment by increasing the effective dose at the thrombotic site and therefore reducing off target effects. This could also expand the availability of this treatment method to higher risk or less severe patients, improving outcomes for thrombotic conditions overall.

Chapter 6: Conclusions

The objective of this project is to develop a fibrinolytic platelet system that can leverage platelet receptors to target the delivery of tissue plasminogen activator. Through this approach, we aim to reduce cancer cell metastasis by disassociating tumor cell clusters in circulation, and more effectively treat pulmonary embolisms with reduced complications.

In order to accomplish these tasks, we first characterized lyophilized platelets and their effect on unaltered platelet functioning. Before these LPs could be explored as a carrier for the fibrinolytic system, we needed to determine the receptor expression and understand their interactions with native platelets. Through this analysis we found that the LPs maintained key surface receptors, and had significant phosphatidylserine exposure associated with increased fibrinogen adhesion. These factors indicated that LPs could be effectively utilized as a platelet-based carrier to leverage the platelet-CTC receptor interactions. Beyond the immediate applications of the characterized LPs, the contrary pro-adhesion and anti-aggregation effects provides for possible future research and drug delivery approaches.

After characterization, these LPs were investigated along with platelet-decoys components in developing the fibrinolytic platelet system to reduce cancer metastasis. These platelet-based carriers were selected because they retained the receptors necessary to target CTC clusters while remaining inert to eliminate any pro-oncogenic signal pathways. The tPA required to dissociate CTC clusters was successfully loaded onto both carrier systems without impairing the fibrinolytic activity or impeding the platelet-CTC interactions. In fact, the platelet-based carriers enhance fibrinolytic activity by catalyzing

the reaction. The fibrinolytic platelet systems are also able to effectively dissociate tumor cell clusters *in vitro*, indicating the viability of this approach. The efficacy of the fibrinolytic platelet decoy system was then demonstrated *in vivo* by reducing the spread of metastasis in a mouse model. The success of this system in targeting and dissociating tumor cell clusters *in vivo* illustrates the significant advantages of this system and could presents the opportunity for a new treatment approach.

Once the utility of the fibrinolytic platelet system was validated for reducing tumor metastasis, we leveraged this system to address the challenges of treating thrombosis. The enhanced fibrinolytic activity and the receptor targeted delivery provided by the tPA-decoys made our fibrinolytic platelets a promising approach to improve the treatment of thrombosis. However, the previously developed decoys designed to target circulating tumor cells were not engineered to adhere to collagen or thrombogenic surfaces. Thus, we modified the decoy preparation to develop activated platelet decoys (aDecoys), featuring active conformation GPIIb/IIIa receptors with a significantly increased binding efficiency. In order to assess the viability of this approach, we first characterized the activation of these new aDecoys and assessed the tPA loading for this system, demonstrating an increased tPA loading compared to decoys while maintaining significant active conformation GPIIb/IIIa receptor availability. Furthermore, this tPA-aDecoy system was able to adhere to a collagen and platelet coated surface under flow. The viability of this approach was also supported by the efficacy of the system in lysing fibrin *in vitro*.

The development of these platelet-based carriers and the fibrinolytic platelets provides an effective new approach to key medical challenges such as the reduction of cancer metastasis and the lysing of fibrin in thrombotic conditions

References

Aceto, N. (2023). Alone you go faster, together you go farther. *Molecular Oncology*, 1878–0261.13549. doi: 10.1002/1878-0261.13549

Aceto, N., Bardia, A., Miyamoto, D. T., Donaldson, M. C., Wittner, B. S., Spencer, J. A., et al. (2014). Circulating Tumor Cell Clusters Are Oligoclonal Precursors of Breast Cancer Metastasis. *Cell* 158, 1110–1122. doi: 10.1016/j.cell.2014.07.013

Al Mahmasani, L., Hodroj, M. H., Finianos, A., and Taher, A. (2021). COVID-19 pandemic and transfusion medicine: the worldwide challenge and its implications. *Ann Hematol* 100, 1115–1122. doi: 10.1007/s00277-021-04441-y

Al-Amer, O. M. (2022). The role of thrombin in haemostasis. *Blood Coagulation & Fibrinolysis* 33, 145. doi: 10.1097/MBC.0000000000001130

Alemany, M., Hernandez, M. R., Bozzo, J., Galan, A. M., Reverter, J. C., Mazzara, R., et al. (1997). In vitro Evaluation of the Hemostatic Effectiveness of Non Viable Platelet Preparations: Studies with Frozen-Thawed, Sonicated or Lyophilized Platelets. *Vox Sanguinis* 73, 36–42. doi: 10.1046/j.1423-0410.1997.7310036.x

Bambace, N. M., and Holmes, C. E. (2011). The platelet contribution to cancer progression. *J Thromb Haemost* 9, 237–249. doi: 10.1111/j.1538-7836.2010.04131.x

Barroso, J., Osborne, B., Teramura, G., Pellham, E., Fitzpatrick, M., Biehl, R., et al. (2018). Safety evaluation of a lyophilized platelet-derived hemostatic product. *Transfusion* 58, 2969–2977. doi: 10.1111/trf.14972

Bělohlávek, J., Dytrych, V., and Linhart, A. (2013). Pulmonary embolism, part I: Epidemiology, risk factors and risk stratification, pathophysiology, clinical presentation, diagnosis and nonthrombotic pulmonary embolism. *Exp Clin Cardiol* 18, 129–138.

Bode, A. P., Read, M. S., and Reddick, R. L. (1999). Activation and adherence of lyophilized human platelets on canine vessel strips in the Baumgartner perfusion chamber. *Journal of Laboratory and Clinical Medicine* 133, 200–211. doi: 10.1016/S0022-2143(99)90013-6

Brandt, B., Junker, R., Griwatz, C., Heidl, S., Brinkmann, O., Semjonow, A., et al. (1996). Isolation of prostate-derived single cells and cell clusters from human peripheral blood. *Cancer Res* 56, 4556–4561.

Bynum, J. A., Meledeo, M. A., Peltier, G. C., McIntosh, C. S., Taylor, A. S., Montgomery, R. K., et al. (2019). Evaluation of a lyophilized platelet-derived hemostatic product. *Transfusion* 59, 1490–1498. doi: 10.1111/trf.15167

Carpentier, G., Berndt, S., Ferratge, S., Rasband, W., Cuendet, M., Uzan, G., et al. (2020). Angiogenesis Analyzer for ImageJ — A comparative morphometric analysis of "Endothelial Tube Formation Assay" and "Fibrin Bead Assay." *Sci Rep* 10, 11568. doi: 10.1038/s41598-020-67289-8

Cellphire Therapeutics, Inc. (2017). Evaluation of the Safety and Immunogenicity of Autologous Thrombosomes® in Healthy Human Subjects; A Microdose Escalation Study (Cohorts 1 - 4) and Repeat Microdose Immunogenicity Study (Cohort 5). clinicaltrials.gov. Available at: https://clinicaltrials.gov/ct2/show/NCT02223117 (Accessed February 20, 2021).

Cellphire Therapeutics, Inc. (2019). A Phase I, Multi-Center, Open-Label, Dose Escalation Study of Thrombosomes® in Bleeding Thrombocytopenic Patients in Three Cohorts. clinicaltrials.gov. Available at: https://clinicaltrials.gov/ct2/show/NCT03394755 (Accessed February 20, 2021).

Cellphire Therapeutics, Inc. (2020). Thrombosomes for Expanded Access Use. clinicaltrials.gov. Available at: https://clinicaltrials.gov/ct2/show/NCT04619108 (Accessed February 20, 2021).

Cellphire Therapeutics, Inc. (2021). A Prospective, Multicenter, Randomized, Open-Label Phase 2, Parallel, Dose Ranging Multidose Study of Thrombosomes® vs Liquid Stored Platelets (LSP) in Bleeding Thrombocytopenic Patients. clinicaltrials.gov. Available at: https://clinicaltrials.gov/ct2/show/NCT04631211 (Accessed February 20, 2021).

Cellphire Therapeutics, Inc. (2022). Randomized Controlled Trial Comparing Dimethyl Sulfoxide Cryopreserved Platelets to Liquid Stored Platelets in Patients Undergoing Cardiopulmonary Bypass Surgery (CRYPTICS). clinicaltrials.gov. Available at: https://clinicaltrials.gov/ct2/show/NCT04709705 (Accessed March 9, 2022).

Cesarman-Maus, G., and Hajjar, K. A. (2005). Molecular mechanisms of fibrinolysis. *British Journal of Haematology* 129, 307–321. doi: 10.1111/j.1365-2141.2005.05444.x

Chapin, J. C., and Hajjar, K. A. (2015). Fibrinolysis and the control of blood coagulation. *Blood Rev* 29, 17–24. doi: 10.1016/j.blre.2014.09.003

Chen, W., Hoffmann, A. D., Liu, H., and Liu, X. (2018). Organotropism: new insights into molecular mechanisms of breast cancer metastasis. *npj Precision Onc* 2, 1–12. doi: 10.1038/s41698-018-0047-0

Choi, J. W., Kim, J. K., Yang, Y. J., Kim, P., Yoon, K.-H., and Yun, S. H. (2015). Urokinase exerts antimetastatic effects by dissociating clusters of circulating tumor cells. *Cancer Res* 75, 4474–4482. doi: 10.1158/0008-5472.CAN-15-0684

Chung, T., Connor, D., Joseph, J., Emmett, L., Mansberg, R., Peters, M., et al. (2007). Platelet activation in acute pulmonary embolism. *Journal of Thrombosis and Haemostasis* 5, 918–924. doi: 10.1111/j.1538-7836.2007.02461.x

Collen, D. (1987). Molecular mechanism of action of newer thrombolytic agents. *Journal of the American College of Cardiology* 10, 11B-15B. doi: 10.1016/S0735-1097(87)80422-9

Cummings, M. C., Simpson, P. T., Reid, L. E., Jayanthan, J., Skerman, J., Song, S., et al. (2014). Metastatic progression of breast cancer: insights from 50 years of autopsies. *The Journal of Pathology* 232, 23–31. doi: 10.1002/path.4288

Dang, Y., and Guan, J. (2020). Nanoparticle-based drug delivery systems for cancer therapy. *Smart Materials in Medicine* 1, 10–19. doi: 10.1016/j.smaim.2020.04.001

Eriksson, O., Mohlin, C., Nilsson, B., and Ekdahl, K. N. (2019). The Human Platelet as an Innate Immune Cell: Interactions Between Activated Platelets and the Complement System. *Front. Immunol.* 10. doi: 10.3389/fimmu.2019.01590

Félez, J., Miles, L. A., Fabregas, P., Jardi, M., Plow, E. F., and Lijnen, R. H. (1996). Characterization of Cellular Binding Sites and Interactive Regions within Reactants Required for Enhancement of Plasminogen Activation by tPA on the Surface of Leukocytic Cells. *Thromb Haemost* 76, 577–584. doi: 10.1055/s-0038-1650625

Fischer, T. H., Merricks, E. P., Bode, A. P., Bellinger, D. A., Russell, K., Reddick, R., et al. (2002). Thrombus Formation with Rehydrated, Lyophilized Platelets. *Hematology* 7, 359–369. doi: 10.1080/1024533021000047954

Fischer, T., Merricks, E., Bellinger, D., Hayes, P., Smith, R., Raymer, R., et al. (2001). Splenic Clearance Mechanisms of Rehydrated, Lyophilized Platelets. *Artificial Cells, Blood Substitutes, & Immobilization Biotechnology* 29, 439. doi: 10.1081/BIO-100108549

FitzGerald, G. A. (1991). Mechanisms of platelet activation: Thromboxane A2 as an amplifying signal for other agonists. *The American Journal of Cardiology* 68, B11–B15. doi: 10.1016/0002-9149(91)90379-Y

Fitzpatrick, G. M., Cliff, R., and Tandon, N. (2013). Thrombosomes: a platelet-derived hemostatic agent for control of noncompressible hemorrhage. *Transfusion* 53, 100S-106S. doi: 10.1111/trf.12043

Food and Drug Administration (2020). Bacterial Risk Control Strategies for Blood Collection Establishments and Transfusion Services to Enhance the Safety and Availability of Platelets for Transfusion; Guidance for Industry. 21.

Gay, L. J., and Felding-Habermann, B. (2011a). Contribution of Platelets to Tumor Metastasis. *Nat Rev Cancer* 11, 123–134. doi: 10.1038/nrc3004

Gay, L. J., and Felding-Habermann, B. (2011b). Contribution of platelets to tumour metastasis. *Nat Rev Cancer* 11, 123–134. doi: 10.1038/nrc3004

Gousset, K., Tsvetkova, N. M., Crowe, J. H., and Tablin, F. (2004). Important role of raft aggregation in the signaling events of cold-induced platelet activation. *Biochimica et Biophysica Acta (BBA) - Biomembranes* 1660, 7–15. doi: 10.1016/j.bbamem.2003.09.009

Hantgan, R., Hindriks, G., Taylor, R., Sixma, J., and de Groot, P. (1990). Glycoprotein Ib, von Willebrand factor, and glycoprotein IIb:IIIa are all involved in platelet adhesion to fibrin in flowing whole blood. *Blood* 76, 345–353. doi: 10.1182/blood.V76.2.345.345

Harrison, P., and Cramer, E. M. (1993). Platelet alpha-granules. *Blood Rev* 7, 52–62. doi: 10.1016/0268-960x(93)90024-x

Hearn, J. I., Green, T. N., Hisey, C. L., Bender, M., Josefsson, E. C., Knowlton, N., et al. (2022). Deletion of Grin1 in mouse megakaryocytes reveals NMDA receptor role in platelet function and proplatelet formation. *Blood* 139, 2673–2690. doi: 10.1182/blood.2021014000

Hou, J.-M., Krebs, M. G., Lancashire, L., Sloane, R., Backen, A., Swain, R. K., et al. (2012). Clinical Significance and Molecular Characteristics of Circulating Tumor Cells and Circulating Tumor Microemboli in Patients With Small-Cell Lung Cancer. *JCO* 30, 525–532. doi: 10.1200/JCO.2010.33.3716

Ismail, A. A., Shaker, B. T., and Bajou, K. (2021). The Plasminogen–Activator Plasmin System in Physiological and Pathophysiological Angiogenesis. *Int J Mol Sci* 23, 337. doi: 10.3390/ijms23010337

Jackson, D. P., Sorensen, D. K., Cronkite, E. P., Bond, V. P., and Fliedner, T. M. (1959). EFFECTIVENESS OF TRANSFUSIONS OF FRESH AND LYOPHILIZED PLATELETS IN CONTROLLING BLEEDING DUE TO THROMBOCYTOPENIA*. *J Clin Invest* 38, 1689–1697.

Jakobsen, J. C., Gluud, C., Wetterslev, J., and Winkel, P. (2017). When and how should multiple imputation be used for handling missing data in randomised clinical trials – a practical guide with flowcharts. *BMC Medical Research Methodology* 17, 162. doi: 10.1186/s12874-017-0442-1

Jansson, S., Bendahl, P.-O., Larsson, A.-M., Aaltonen, K. E., and Rydén, L. (2016). Prognostic impact of circulating tumor cell apoptosis and clusters in serial blood samples from patients with metastatic breast cancer in a prospective observational cohort. *BMC Cancer* 16, 433. doi: 10.1186/s12885-016-2406-y

Jung, S. M., and Moroi, M. (2000). Signal-transducing Mechanisms Involved in Activation of the Platelet Collagen Receptor Integrin α2β1*. *Journal of Biological Chemistry* 275, 8016–8026. doi: 10.1074/jbc.275.11.8016

Kailashiya, J., Gupta, V., and Dash, D. (2019). Engineered human platelet-derived microparticles as natural vectors for targeted drug delivery. *Oncotarget* 10, 5835–5846. doi: 10.18632/oncotarget.27223

Karpatkin, S., and Pearlstein, E. (1981). Role of Platelets in Tumor Cell Metastases. *Ann Intern Med* 95, 636–641. doi: 10.7326/0003-4819-95-5-636

Kasper, W., Konstantinides, S., Geibel, A., Olschewski, M., Heinrich, F., Grosser, K. D., et al. (1997). Management Strategies and Determinants of Outcome in Acute Major Pulmonary Embolism: Results of a Multicenter Registry. *Journal of the American College of Cardiology* 30, 1165–1171. doi: 10.1016/S0735-1097(97)00319-7

Khurana, S., Mattson, J. C., Westley, S., O'neill, W. W., Timmis, G. C., and Safian, R. D. (1997). Monitoring platelet glycoprotein IIb/IIIa—fibrin interaction with tissue factor—activated thromboelastography. *Journal of Laboratory and Clinical Medicine* 130, 401–411. doi: 10.1016/S0022-2143(97)90040-8

Kooistra, T., Schrauwen, Y., Arts, J., and Emeis, J. J. (1994). Regulation of endothelial cell t-PA synthesis and release. *Int J Hematol* 59, 233–255.

Kottana, R. K., Schnoor, B., and Papa, A.-L. (2024, accepted). A Method to Quantitatively Characterize the Formation and Dissociation of Tumor Cell Clusters Using Light Transmission Aggregometer. *Molecular Oncology*.

Kumar, A., Mhaskar, R., Grossman, B. J., Kaufman, R. M., Tobian, A. A. R., Kleinman, S., et al. (2015). Platelet transfusion: a systematic review of the clinical evidence. *Transfusion* 55, 1116–1127. doi: 10.1111/trf.12943

Labelle, M., Begum, S., and Hynes, R. O. (2011). Direct Signaling between Platelets and Cancer Cells Induces an Epithelial-Mesenchymal-Like Transition and Promotes Metastasis. *Cancer Cell* 20, 576–590. doi: 10.1016/j.ccr.2011.09.009

Lesept, F., Chevilley, A., Jezequel, J., Ladépêche, L., Macrez, R., Aimable, M., et al. (2016). Tissue-type plasminogen activator controls neuronal death by raising surface dynamics of extrasynaptic NMDA receptors. *Cell Death Dis* 7, e2466–e2466. doi: 10.1038/cddis.2016.279

Li, J., Sharkey, C. C., Wun, B., Liesveld, J. L., and King, M. R. (2016). Genetic engineering of platelets to neutralize circulating tumor cells. *Journal of Controlled Release* 228, 38–47. doi: 10.1016/j.jconrel.2016.02.036

Li, X., Zhang, G., and Cao, X. (2023). The Function and Regulation of Platelet P2Y12 Receptor. *Cardiovasc Drugs Ther* 37, 199–216. doi: 10.1007/s10557-021-07229-4

Liu, Q., Shi, K., Wang, Y., and Shi, F.-D. (2023). Neurovascular Inflammation and Complications of Thrombolysis Therapy in Stroke. *Stroke* 54, 2688–2697. doi: 10.1161/STROKEAHA.123.044123

Macko, A. R., Crossland, R. F., Cap, A. P., Fryer, D. M., Mitchell, T. A., Pusateri, A. E., et al. (2016). Control of severe intra-abdominal hemorrhage with an infusible platelet-derived hemostatic agent in a nonhuman primate (rhesus macaque) model: *Journal of Trauma and Acute Care Surgery* 80, 617–624. doi: 10.1097/TA.0000000000000964

Malek, A. M., Alper, S. L., and Izumo, S. (1999). Hemodynamic Shear Stress and Its Role in Atherosclerosis. *JAMA* 282, 2035–2042. doi: 10.1001/jama.282.21.2035

Manzari, M. T., Shamay, Y., Kiguchi, H., Rosen, N., Scaltriti, M., and Heller, D. A. (2021). Targeted drug delivery strategies for precision medicines. *Nat Rev Mater* 6, 351–370. doi: 10.1038/s41578-020-00269-6

McNicol, A., and Israels, S. J. (1999). Platelet Dense Granules: Structure, Function and Implications for Haemostasis. *Thrombosis Research* 95, 1–18. doi: 10.1016/S0049-3848(99)00015-8

Merchan, J. R., Chan, B., Kale, S., Schnipper, L. E., and Sukhatme, V. P. (2003). In vitro and in vivo induction of antiangiogenic activity by plasminogen activators and captopril. *J Natl Cancer Inst* 95, 388–399. doi: 10.1093/jnci/95.5.388

Michelson, A. D. ed. (2013). *Platelets*., 3rd ed. London ; Waltham, MA: Academic Press.

Miles, L. A., and Plow, E. F. (1985). Binding and activation of plasminogen on the platelet surface. *J Biol Chem* 260, 4303–4311.

Milford, E. M., and Reade, M. C. (2016). Comprehensive review of platelet storage methods for use in the treatment of active hemorrhage. *Transfusion* 56, S140–S148. doi: 10.1111/trf.13504

Morris, K., Schnoor, B., and Papa, A.-L. (2022). Platelet cancer cell interplay as a new therapeutic target. *Biochimica et Biophysica Acta (BBA) - Reviews on Cancer* 1877, 188770. doi: 10.1016/j.bbcan.2022.188770

Murlidhar, V., Reddy, R. M., Fouladdel, S., Zhao, L., Ishikawa, M. K., Grabauskiene, S., et al. (2017). Poor Prognosis Indicated by Venous Circulating Tumor Cell Clusters in Early-Stage Lung Cancers. *Cancer Research* 77, 5194–5206. doi: 10.1158/0008-5472.CAN-16-2072

Ohana, O. M., Ozer, J., Prinsloo, I., Benharroch, D., and Gopas, J. (2015). Hodgkin lymphoma cell lines bind to platelets. Incubation with platelets induces CD15 and P-selectin dependent adhesion of the cell lines to Human Umbilical Vein Endothelial cells (HUVEC). *Cancer Biol Ther* 16, 1651–1659. doi: 10.1080/15384047.2015.1095411

Ohanian, M., Cancelas, J. A., Davenport, R., Pullarkat, V., Hervig, T., Broome, C., et al. (2022). Freeze-dried platelets are a promising alternative in bleeding thrombocytopenic patients with hematological malignancies. *American Journal of Hematology* 97, 256–266. doi: 10.1002/ajh.26403

O'Malley, T. J., Choi, J. H., Maynes, E. J., Wood, C. T., D'Antonio, N. D., Mellado, M., et al. (2020). Outcomes of extracorporeal life support for the treatment of acute massive pulmonary embolism: A systematic review. *Resuscitation* 146, 132–137. doi: 10.1016/j.resuscitation.2019.11.018

Ortiz-Otero, N., Marshall, J. R., Lash, B. W., and King, M. R. (2020). Platelet mediated TRAIL delivery for efficiently targeting circulating tumor cells. *Nanoscale Adv.* 2, 3942–3953. doi: 10.1039/D0NA00271B

Palumbo, J. S., Talmage, K. E., Massari, J. V., La Jeunesse, C. M., Flick, M. J., Kombrinck, K. W., et al. (2005). Platelets and fibrin(ogen) increase metastatic potential by impeding natural killer cell-mediated elimination of tumor cells. *Blood* 105, 178–185. doi: 10.1182/blood-2004-06-2272

Papa, A.-L., Jiang, A., Korin, N., Chen, M. B., Langan, E. T., Waterhouse, A., et al. (2019). Platelet decoys inhibit thrombosis and prevent metastatic tumor formation in preclinical models. *Sci. Transl. Med.* 11, eaau5898. doi: 10.1126/scitranslmed.aau5898

Papaioannou, T. G., and Stefanadis, C. (2005). Vascular wall shear stress: basic principles and methods. *Hellenic J Cardiol* 46, 9–15.

Park, S., Harker, L. A., Marzec, U. M., and Levin, E. G. (1989). Demonstration of single chain urokinase-type plasminogen activator on human platelet membrane. *Blood* 73, 1421–1425.

Pearson, G. W. (2019). Control of Invasion by Epithelial-to-Mesenchymal Transition Programs during Metastasis. *Journal of Clinical Medicine* 8, 646. doi: 10.3390/jcm8050646

Rayes, J., Watson, S. P., and Nieswandt, B. (2019). Functional significance of the platelet immune receptors GPVI and CLEC-2. *J Clin Invest* 129, 12–23. doi: 10.1172/JCI122955

Reddy, E. C., and Rand, M. L. (2020). Procoagulant Phosphatidylserine-Exposing Platelets in vitro and in vivo. *Frontiers in Cardiovascular Medicine* 7, 15. doi: 10.3389/fcvm.2020.00015

Reed, M., Kerndt, C. C., and Nicolas, D. (2023). “Alteplase,” in *StatPearls*, (Treasure Island (FL): StatPearls Publishing). Available at: http://www.ncbi.nlm.nih.gov/books/NBK499977/ (Accessed September 5, 2023).

Rendu, F., and Brohard-Bohn, B. (2001). The platelet release reaction: granules’ constituents, secretion and functions. *Platelets* 12, 261–273. doi: 10.1080/09537100120068170

Roberts, D. E., McNicol, A., and Bose, R. (2004). Mechanism of Collagen Activation in Human Platelets *. *Journal of Biological Chemistry* 279, 19421–19430. doi: 10.1074/jbc.M308864200

Rumbaut, R. E., and Thiagarajan, P. (2010). “Platelet Aggregation,” in *Platelet-Vessel Wall Interactions in Hemostasis and Thrombosis*, (Morgan & Claypool Life Sciences). Available at: https://www.ncbi.nlm.nih.gov/books/NBK53449/ (Accessed March 22, 2024).

Savage, B., Almus-Jacobs, F., and Ruggeri, Z. M. (1998). Specific Synergy of Multiple Substrate–Receptor Interactions in Platelet Thrombus Formation under Flow. *Cell* 94, 657–666. doi: 10.1016/S0092-8674(00)81607-4

Schnoor, B., Morris, K., Kottana, R. K., and Papa, A.-L. (in revisions). Fibrinolytic Platelet Decoys Reduce Cancer Metastasis by Dissociating Circulating Tumor Cell Clusters. *Adv Healthcare Mat*.

Schnoor, B., and Papa, A.-L. (2022). Lyophilized platelets inhibit platelet aggregation with simultaneous paradoxical promotion of platelet adhesion. *Frontiers in Bioengineering and Biotechnology* 10. Available at: https://www.frontiersin.org/articles/10.3389/fbioe.2022.941817 (Accessed August 31, 2023).

Shao, J., and Zhong, B. (2003). Last observation carry-forward and last observation analysis. *Statistics in Medicine* 22, 2429–2441. doi: 10.1002/sim.1519

Shattil, S. J., Hoxie, J. A., Cunningham, M., and Brass, L. F. (1985). Changes in the platelet membrane glycoprotein IIb.IIIa complex during platelet activation. *Journal of Biological Chemistry* 260, 11107–11114. doi: 10.1016/S0021-9258(17)39154-8

Siddiqui, F. A., Desai, H., Amirkhosravi, A., Amaya, M., and Francis, J. L. (2002). The presence and release of tissue factor from human platelets. *Platelets* 13, 247–253. doi: 10.1080/09537100220146398

Sierko, E., and Wojtukiewicz, M. Z. (2004). Platelets and Angiogenesis in Malignancy. *Semin Thromb Hemost* 30, 95–108. doi: 10.1055/s-2004-822974

Soff, G. A., Wang, H., Cundiff, D. L., Jiang, K., Martone, B., Rademaker, A. W., et al. (2005). In vivo generation of angiostatin isoforms by administration of a

plasminogen activator and a free sulfhydryl donor: a phase I study of an angiostatic cocktail of tissue plasminogen activator and mesna. *Clin Cancer Res* 11, 6218–6225. doi: 10.1158/1078-0432.CCR-04-1514

Stevens, S. M., Woller, S. C., Kreuziger, L. B., Bounameaux, H., Doerschug, K., Geersing, G.-J., et al. (2021). Antithrombotic Therapy for VTE Disease: Second Update of the CHEST Guideline and Expert Panel Report. *CHEST* 160, e545–e608. doi: 10.1016/j.chest.2021.07.055

Stewart, L. K., and Kline, J. A. (2020). Fibrinolytics for the treatment of pulmonary embolism. *Translational Research* 225, 82–94. doi: 10.1016/j.trsl.2020.05.003

Stolla, M., Refaai, M. A., Heal, J. M., Spinelli, S. L., Garraud, O., Phipps, R. P., et al. (2015). Platelet Transfusion – The New Immunology of an Old Therapy. *Frontiers in Immunology* 6. Available at: https://www.frontiersin.org/article/10.3389/fimmu.2015.00028 (Accessed June 5, 2022).

Stone, R. L., Nick, A. M., McNeish, I. A., Balkwill, F., Han, H. D., Bottsford-Miller, J., et al. (2012). Paraneoplastic Thrombocytosis in Ovarian Cancer. *New England Journal of Medicine* 366, 610–618. doi: 10.1056/NEJMoa1110352

Stroncek, D. F., and Rebulla, P. (2007). Transfusion Medicine 2: Platelet transfusions. *The Lancet* 370, 427–438.

Takagi, S., Tsukamoto, S., Park, J., Johnson, K. E., Kawano, Y., Moschetta, M., et al. (2018). Platelets Enhance Multiple Myeloma Progression via IL-1β Upregulation. *Clin Cancer Res* 24, 2430–2439. doi: 10.1158/1078-0432.CCR-17-2003

Tang, S., Zhang, F., Gong, H., Wei, F., Zhuang, J., Karshalev, E., et al. (2020). Enzyme-powered Janus platelet cell robots for active and targeted drug delivery. *Science Robotics* 5. doi: 10.1126/scirobotics.aba6137

Valeri, C. R., Macgregor, H., Barnard, M. R., Summaria, L., Michelson, A. D., and Ragno, G. (2004). In vitro testing of fresh and lyophilized reconstituted human and baboon platelets. *Transfusion* 44, 1505–1512. doi: 10.1111/j.1537-2995.2004.04135.x

van Buuren, S. (2018). *Flexible Imputation of Missing Data, Second Edition*. Milton, UNITED KINGDOM: CRC Press LLC. Available at: http://ebookcentral.proquest.com/lib/gwu/detail.action?docID=5455460 (Accessed November 14, 2023).

Varga-Szabo, D., Pleines, I., and Nieswandt, B. (2008). Cell adhesion mechanisms in platelets. *Arterioscler Thromb Vasc Biol* 28, 403–412. doi: 10.1161/ATVBAHA.107.150474

Vaughan, D. E., Mendelsohn, M. E., Declerck, P. J., Van Houtte, E., Collen, D., and Loscalzo, J. (1989). Characterization of the binding of human tissue-type plasminogen activator to platelets. *J Biol Chem* 264, 15869–15874.

Wang, C., Mu, Z., Chervoneva, I., Austin, L., Ye, Z., Rossi, G., et al. (2017a). Longitudinally collected CTCs and CTC-clusters and clinical outcomes of metastatic breast cancer. *Breast Cancer Res Treat* 161, 83–94. doi: 10.1007/s10549-016-4026-2

Wang, C., Sun, W., Ye, Y., Hu, Q., Bomba, H. N., and Gu, Z. (2017b). In situ activation of platelets with checkpoint inhibitors for post-surgical cancer immunotherapy. *Nature Biomedical Engineering* 1, 1–10. doi: 10.1038/s41551-016-0011

Xu, P., Zuo, H., Chen, B., Wang, R., Ahmed, A., Hu, Y., et al. (2017). Doxorubicin-loaded platelets as a smart drug delivery system: An improved therapy for lymphoma. *Scientific Reports* 7, 42632. doi: 10.1038/srep42632

Young, J. S., and Simmons, J. W. (2017). Chemotherapeutic Medications and Their Emergent Complications. *Hematology/Oncology Clinics of North America* 31, 995–1010. doi: 10.1016/j.hoc.2017.08.005

Yun, S.-H., Sim, E.-H., Goh, R.-Y., Park, J.-I., and Han, J.-Y. (2016). Platelet Activation: The Mechanisms and Potential Biomarkers. *Biomed Res Int* 2016, 9060143. doi: 10.1155/2016/9060143

Zhang, D., Zhao, L., Zhou, P., Ma, H., Huang, F., Jin, M., et al. (2017). Circulating tumor microemboli (CTM) and vimentin+ circulating tumor cells (CTCs) detected by a size-based platform predict worse prognosis in advanced colorectal cancer patients during chemotherapy. *Cancer Cell Int* 17, 6. doi: 10.1186/s12935-016-0373-7

Appendix I: List of Manuscripts, Conference Proceedings and Local Presentations

(*co-first author)

Published Manuscripts:

1. **Schnoor, B**. & Papa, A.-L. (2022). Lyophilized platelets inhibit platelet aggregation with simultaneous paradoxical promotion of platelet adhesion. *Frontiers in Bioengineering and Biotechnology*, 10:941817. https://doi.org/10.3389/fbioe.2022.941817

2. Morris*, K., **Schnoor*, B.,** Papa, A.-L. (2022). Platelet cancer cell interplay as a new therapeutic target. *Biochimica et Biophysica Acta (BBA) - Reviews on Cancer*, *1877*(5), 188770. https://doi.org/10.1016/j.bbcan.2022.188770

3. Kottana, R. K., Maurizi, L., **Schnoor, B.**, Morris, K., Webb, J. A., Massiah, M. A., N. Millot, N., Papa A.-L. (2021). Anti-Platelet Effect Induced by Iron Oxide Nanoparticles: Correlation with Conformational Change in Fibrinogen. *Small* 17, 2004945. doi: 10.1002/smll.202004945.

Manuscripts In Progress:

1. Kottana*, R.K., **Schnoor*, B.,** Papa, A.-L. (accepted, 2024). A method to quantitatively characterize the formation and dissociation of tumor cell clusters using Light Transmission Aggregometer. *Molecular Oncology.*

2. **Schnoor**, **B.,** Morris, K., Kottana, R.K., Papa, A.-L. (in revisions) Fibrinolytic platelet decoys target circulating tumor cells and decrease their metastatic potential. *Advanced Healthcare Materials.*

3. **Schnoor*, B.**, Morris*, K., Papa, A.-L. (in preparation). Engineering Approaches to Platelet Based Drug Delivery Systems.

4. **Schnoor*, B.,** Papa, A.-L. (in preparation) Development of Fibrinolytic Platelet Carriers for the Targeting of Thrombosis.

Conference Presentations:

1. Barron, J., Muldoon, R., **Schnoor**, **B.,** Papa, A.-L., **"***In vitro* analysis of fibrinolytic dissociation of tumor cell clusters", Fifteenth Annual Virginia-North Carolina Louis Stokes Alliance for Minority Participation Undergraduate Research Symposium, Charlottesville, Virginia, April 3-4, 2024 (oral presentation).

2. **Schnoor**, **B.,** Kottana, R. K., Papa, A.-L., "Light Transmission Aggregometry Method to Measure Tumor Cell Cluster Dissociation", TechConnect World Innovation Conference, Washington, DC, June 19-21, 2023 (oral presentation).

3. **Schnoor, B.**, Morris, K., Papa, A.-L, "Platelet decoys in cancer and cancer-associated thrombosis", American Society of Hematology's Workshop on Interplay between Coagulation and Malignancy, New Orleans, Louisiana, December 9, 2022 (Invited speaker)

4. Morris, K., **Schnoor**, **B.,** Papa, A.-L. "The Role of Calcium in Metastasis", AACR Special Conference on Cancer Metastasis, Portland, Oregon, November 14-17, 2022 (poster).

5. **Schnoor**, **B.,** Papa, A.-L., **"**Development of fibrinolytic platelet systems to dissociate circulating tumor cell clusters", AACR Special Conference on Cancer Metastasis, Portland, Oregon, November 14-17, 2022 (poster).

6. **Schnoor, B.,** & Papa, A.-L. "Lyophilized Platelet Interactions with Native Platelets", TechConnect World Innovation Conference, Washington, DC, Oct. 18-20, 2021 (oral presentation).

7. Kottana, R. K., Maurizi, L., **Schnoor**, **B.,** Morris, K., N. Millot, N., Papa, A.-L. "Superparamagnetic Iron oxides modulate platelet functions", MRS 2020 Spring/Fall Meeting and Exhibit, virtual, November 27 – December 4, 2020 (oral presentation).

8. **Schnoor, B.,** & Papa, A.-L. "Development of Platelet-Based Drug Delivery System", MRS 2020 Spring/Fall Meeting and Exhibit, virtual, November 27 – December 4, 2020 (oral presentation).

GWU Presentations:

1. Barron, J., Muldoon, R., **Schnoor**, **B.,** Papa, A.-L., **"***In vitro* analysis of the fibrinolytic dissociation of tumor cell clusters", Undergraduate Research Poster Session - SPARC and Chem "Green" Programs, August 03, 2023 (poster).

2. **Schnoor**, B., Kottana, R. K., Papa, A.-L. **"**Light Transmission Aggregometry Method to Study Tumor Cell Clusters", 2023 SEAS R&D Showcase, April 28, 2023 (poster).

3. Ronning-Arnesen, G., Kottana, R. K., **Schnoor**, **B.,** Papa, A.-L. **"**Nanoplastics are in our blood. What Now? How Nanoplastics are Impacting Platelet Function", BME Day - November 14, 2022 (oral presentation).

4. **Schnoor, B.** & Papa, A.-L. "Development of Modified Platelet Carrier Systems to Target CTC Clusters", BME student award presentation (winner), October 19, 2022 (oral presentation).

5. **Schnoor, B.** & Papa, A.-L. "Development of Fibrinolytic Platelet System to Reduce Metastasis by Disassociating Circulating Tumor Cell Clusters", GW Research Showcase, Washington, DC. April 11-15, 2022 (poster).

6. **Schnoor, B.** & Papa, A.-L. "*In Vitro* Characterization of Interactions between Lyophilized Platelets and Human Platelets", GW Research Showcase, Washington, DC. April 12-16, 2021 (poster).

7. Kottana, R.K., Maurizi, L., **Schnoor**, **B.,** K. Morris, K. , Webb, J.A., Massiah, M. A., Millot, N., Papa, A.-L., "Iron Oxide Nanoparticle-Induced Conformational Change in Fibrinogen and Implications on Platelet Response", GW Research Showcase, Washington, DC. April 12-16, 2021 (poster).

8. **Schnoor, B.** & Papa, A.-L. "A Cellular Engineering Approach to Target Cancer Cell Clusters", SEAS R&D Showcase, Washington, DC, October 25, 2019 (poster).

Appendix II: Permissions

Permission was obtained from Elsevier using Rightslink under the author rights policy for the use of text from the article:

K. Morris*, B. Schnoor*, A.L. Papa, Platelet cancer cell interplay as a new therapeutic target. *Biochimica et Biophysica Acta (BBA) - Reviews on Cancer, 1877*(5), 188770 (2022). *co-first authors

Permission was obtained from Frontiers Journals under Creative Commons CC-BY license for the use of text and figures from the article:

B. Schnoor, A.L. Papa, Lyophilized platelets inhibit platelet aggregation with simultaneous paradoxical promotion of platelet adhesion. *Frontiers in Bioengineering and Biotechnology,* 10:941817 (2022).

Permission for the use of figure 3, taken from the article cited below, was obtained using Rightslink from Wolters Kluwer Health, Inc. and Copyright Clearance Center under license 5754990010514 on March 23, 2024.

Varga-Szabo, D., Pleines, I., and Nieswandt, B. (2008). Cell adhesion mechanisms in platelets. *Arterioscler Thromb Vasc Biol* 28, 403–412. doi: 10.1161/ATVBAHA.107.150474

Documentation for all permissions and copyright policies is available in supplementary materials.